An x-ray diffraction study of the nerve myelin sheath(Dissertation_全文)

AUTHOR(S):

Inouye, Hideyo

CITATION:

Inouye, Hideyo. An x-ray diffraction study of the nerve myelin sheath. 京都大学, 1979, 薬学博士

ISSUE DATE:

1979-07-23

URL:

https://doi.org/10.14989/doctor.k2249

AN X-RAY DIFFRACTION STUDY OF THE NERVE MYELIN SHEATH

a thesis submitted to the Faculty of Pharmaceutical Sciences of Kyoto University.

by

Hideyo Inouye

in fulfilment of the requirements for the degree of Doctor of Pharmaceutical Sciences.

1979

Preface

In 1953 Watson and Crick proposed the striking hypothesis of DNA reproduction (DNA structure and function), which was the origin of the development of Molecular Biology and was the first step towards the essential understanding of life. Their success was due to an alliance of two schools, a structural school and an informative school.

Since then, our approach to life has been inevitably based at the molecular level and correlation with DNA sequence. Today we are in the process of elucidating the structure of complex organizations at the molecular level, where unsolved phenomena emerge, such as motility, recognition of the external environment, adaptation, sensitivity and so on.

Biological membrane is mainly composed of proteins and lipids which are integrated in a complex organization in an unknown way and are capable of sophisticated functions not directly related to that of the composing units. The special function involved in biological membrane is obviously based on its situation as a boundary between outer space and inner space. Interest in membrane structure and function lies in the mechanism by which lipids and proteins form a more highly organized entity which is called " *Membrane* " in the special boundary condition.

Technically we have developed the tools for the purpose of elucidating the highly organized structure, such as x-ray diffraction , neutron diffraction, electron microscopy and so on.

As a specimen, nerve myelin historically made a great contribution to the understanding of biomembranes for its naturally occurring multilamellared liquid crystalline structure.

My research is aimed at the clarification of the mechanism by which individual components integrate themselves to form nerve myelin sheath as it appears to us.

Acknowledgements

I should like to express my sincere gratitude to Professor Kenji Osaki of Kyoto University, Faculty of Pharmaceutical Sciences, for his invaluable guidence, generous suggestions and constant encouragement throughout the course of this graduate work.

I am deeply grateful to Dr. Norio Masaki of Kyoto University , Faculty of Pharmaceutical Sciences, who directly supervised me to carry out this graduate work and inspired me of the interests in the x-ray diffraction study of the nerve myelin sheath.

I owe Dr. Robert Freeman of European Molecular Biology Laboratory, for his kind advice especially on the experimental technique during his stay in Kyoto University, Faculty of Pharmacertical Sciences.

I am greatly indebted to Professor Hiroshi Takagi of Kyoto University, Faculty of Pharmaceutical Sciences, Professor Yoshimi Misu of Yokohama City University, Faculty of Medicine, and Dr. Masamichi Satoh of Kyoto University, Faculty of Pharmaceutical Sciences, for their kind supply and manipulation of animals used in this study and for useful advice on the electron microscopy.

Acknowledgements are also made to Professor Jutaro Okada of Kyoto University, Faculty of Pharmaceutical Sciences, for his kind help for instrumentation.

I should like to thank Professor Ikuo Yamashina and Dr. Kyozo Hayashi of Kyoto University, Faculty of Pharmaceutical Sciences, for their helpful suggestions about biochemical manipulation of nerves and for the centrifuge.

I also thank Professor Toyozo Uno, Dr. Katsunosuke Machida and Dr. Terumichi Nakagawa of Kyoto University, Faculty of Pharmaceutical Sciences, for their advice on the chemical and instrumental analysis of reagent.

I am indebted to Professor Tamotsu Iwai of Kyoto University, Faculty of Agriculture, for his kind suggestion on the treatment of fishes.

Acknowledgements are also made to Professor Shun-ichi Ohnishi and Dr. Toyozo Maeda of Kyoto University, Faculty of Science, for their valuable discussions and kind help for the biophysical and biochemical experiments.

I was particularly grateful to Dr. Hisao Iizuka of The Tokyo Metropolitan Institute of Medical Science, for the computer programs.

Thanks are due to many members of Faculty of Pharmaceutical Sciences, especially to all members of Department of Inorganic Chemistry. During the graduate course I was continuously

encouraged throuth the discussions with Dr. Tooru Taga, Dr. Tsuneyuki Higashi, Mr. Ichiro Fujisao and other members of this laboratory.

Without them these studies would not have been completed.

CONTENTS

CHAPTER 1

GENERAL INTRODUCTION

History of biomembrane study

Since Geren's postulation (1954) on the mechanism of myelination the structure of the nerve myelin sheath has been paid attention not only for its neurological importance but also as a structural model for the biological membrane.

In 1925 Gorter and Grendel for the first time proposed a lipid bilayer model for the structure of the red cell membrane, which was deduced from the experimental results that the surface area of the monomolecular layer of lipids extracted from erythrocyte was almost twice that of the whole cell. Thereafter many models of biological membrane were put forward. They can be classified in two types, one of which is the unit membrane model (Danielli and Davson,1956) (Robertson,1959) and the other is the repeating unit model (Green and Perdue,1966) (Benson,1966) (Vanderkooi and Green,1970).

The unit membrane model referred to as Davson-Danielli-Robertson model insists on the existence of the lipid bilayer framework interacting ionically with protein layer at the hydrophillic space, whereas the repeating unit model mainly presented by Green and Benson shows the existence of the repeating subunit with the hydrophobic interaction between lipid and protein.

The course of the discussion between them in 1960's are described by Stoeckenius and Engelman (1969).

In 1970 Frye and Edidin demonstrated that different antigens on the surfaces of nucleated mouse cells and human cells rapidly intermix when the cells are fused by inactivated Sendai virus, hence it has been widely accepted that proteins in the plasma membrane have considerable mobility.

In 1972 Singer and Nicolson proposed a new model referred to as the fluid mosaic model which had the basis on the points, 1) thermodynamic stability, 2) heterogeneity of the integral membrane proteins, 3) proteins in a variety of intact membranes showing appreciable amount of α-helical conformation, 4) membrane thickness from 75Å to 90Å, 5) the bilayer character of membrane lipids shown on the intact mycoplasma membrane. This model assumes that the integral proteins are heterogeneous set of globular molecules, which are partially embedded in a matrix of phospholipid, which is organized as a discontinuous fluid bilayer. In this model quite different from the former models, there are involved new concepts, those are 1) intrinsic and peripheral protein, 2) fluidity and 3) a small fraction of the lipid specifically interacting with membrane proteins.

At that same period, ESR (Hubbell and McConell,1968), x-ray (Engelman,1970), freeze fracture electromicroscopy (Branton,1971), SDS acrylamide electrophoresis (Shapiro et al.

,1967), calorimetry (Steim et al.,1970) (Melchoir et al.,1970), NMR and other techniques were beginning to be applied to the membrane study.

As to the character of fluidity, Kornberg and McConnell (1971a,b) measured for the first time the rates of lateral diffusion and of flip-flop of lipid component in the membrane, which showed that the passage of a phospholipid molecule from one side of a bilayer to the other is much slower than that of lateral diffusion. X-ray study (Engelman,1970) and calorimetric study also detected the fluidity of lipid molecule in the physiological state.

The other main property to be considered for the membrane structure was provided from the biochemical study on erythrocyte membrane using sodium dodecyl sulfate (SDS) polyacrylamide gels. Berg (1969), Bretcher (1971) and other biochemists clarified the presence and asymmetric location of the membrane bound protein and ascertained the structure and function of the membrane.

In 1973 Edelman et al. suggested the function of cytoplasmic microtubules in controlling the movement and distribution of membrane protein. It was also shown that microfilaments are likely to be associated with them. Singer and Nicolson's fluid mosaic model lays too much stress on the fluidity and randomness of membrane particles, even though the ordered structure can be detected in purple membrane or gap junction.

At present we have the most probable model of biomembrane

structure, reviewed by Nicolson (1976), which has the framework of Singer's fluid mosaic structure added with some glycoprotein components anchored by a microfilament and microtubule cytoskeletal assemblage.

Thus it can be said that today the most intense interest in biomembrane study lies in the points, 1) how are the asymmetric distribution or location of the membrane components realized in the biological system, 2) how is the membrane fluidity controlled. These points have been also cited to be important by Bretscher (1971a,1971b and 1975), Rothman and Lenard (1977) and Blobel et al. (1975).

History of nerve myelin study

In developing the model of membrane structure described above, studies on the nerve myelin sheath played a great role. The reviews by Worthington (1971), Mokrasch, Bear and Schmitt (1971), Norton (1975) and Kirshner (1977) give light on the background of the current structural study.

In 1931 Boem observed a meridionally accentuated ring at 4.7Å by x-ray diffraction from nerve. This wide angle pattern was explained by Schmitt, Bear and Clark in 1935 from the hydrocarbon chain lying in radial directions. In 1935 they showed for the first time a low angle x-ray diffraction pattern from frog sciatic nerve (2nd, 3rd, 4th and 5th order reflections

of 171Å period structure). In the subsequent work (Schmitt et al. ,1941) they reported the x-ray diffraction patterns from frog sciatic nerve (1st, 2nd, 3rd, 4th and 5th order reflections with 171Å period structure), dog and cat spinal roots (184Å period) and the corresponding air dried nerve.

In 1949 Sjostrand confirmed the laminar structures in nerve tissue by electromicroscopic study using ultra thin section and osmium fixed material, then in 1953 showed the myelin periodicity (Sjostrand,1953), which was almost two thirds of the value observed in fresh nerve by x-ray diffraction method.

In 1954 Geren postulated that compact myelin in peripheral nervous system (PNS) was formed by satellite cell (Schwann cell), spirally winding around the axon. Her observation confirmed that the periodical unit observed in x-ray diffraction pattern contained two triple layered membrane units and that the periodical unit is centrosymmetric. In the case of myelin from the central nervous system (CNS) Peters (1960) and Maturana (1960) independently demonstrated the same mode of myelination formed by oligo-dendroglia cell.

In 1957 Finean and Millington discovered the swelling phenomenon in the frog sciatic nerve myelin treated by diluted Ringer's solution. Robertson (1958) demonstrated that swelling takes place at the intra-period line, hereby it was confirmed that swelling takes place in the external (extracellular) space.

Hereafter using the swelling technique Finean and Burge in 1963 for the first time determined the phases of the observed reflections up to 5th order and calculated the electron density distribution, which showed the existence of the lipid bilayer in nerve myelin.

Since then in the x-ray diffraction study on the nerve myelin, the rigorous structure analysis has been carried out, which was mainly facilitated by the advent of the new camera (Franks,1955) (Elliot,1965) and the strong x-ray generator. At present there are two types of absolute scale electron density distribution profiles for nerve myelin, one of which was presented by Caspar and Kirshner (1971) at 10Å resolution and the other was by Worthington and McIntosh (1974) at 7Å resolution. The difference between them is due to different selection of the phase, plus or minus in higher order reflections, especially in the 11th order reflection. Caspar and Kirshner's model shows the bump in the space of lipid bilayer at the external side, which was interpreted to be asymmetrically located cholesterol. In neither models, however, a certain explanation was given as to the location of proteins.

On the other hand Pinto da Silva and Miller (1975) demonstrated the presence of integral particles in the myelin sheath by using freeze fracture electron microscopy. At the same period there were reported the existence of specialized paranodal

and inter-paranodal glial-axonal junctions (Schnapp and Mugnaini, 1975) (Livingston et al.,1973). These were striking demonstrations in contrast with the widely accepted view that nerve myelin was an exceptionally inactive membrane and it could not be a structural model of the cell membrane (Green and Perdue,1966). Today in the study of nerve myelin structure it is essential to think of the common features, such as protein asymmetric distribution, cytoskeletal control and so on, that other active membranes are expressing.

In fact the chemical analysis of nerve myelin shows the presence of the peripheral and intrinsic protein including glycoprotein after the definition given by Singer (1974), as well as the presence of myelin specific enzymes. For CNS myelin proteins it is at present generally agreed that there are three major proteins in myelin, 30% to 50% intrinsic proteolipid protein, 30% to 35% peripheral basic protein and a lower percentage of a higher molecular weight protein (Wolfgram protein), whereas for PNS myelin it was reported that there are intrinsic P_0 (J-protein, X-protein) protein, basic P_1 and P_2 proteins. In addition several enzymes specific to myelin were reported, namely 2',3'-cyclic nucleotide-3'-phosphohydrolase, cholesterol ester hydrolase and protein kinase.

Before the application of the technique of polyacrylamide gel electrophoresis, biochemical analysis on nerve myelin was

limited to lipid study. It was due to this historical situation that Finean (1957), Robertson (1960), Vanderheuvel (1963), Caspar et al. (1971) and Worthington et al. (1974) discussed only lipid distribution on the myelin structural model they proposed.

In that context, now it is extremely needed to determine the location or distribution of membranous proteins and lipids. The most recent structural model of nerve myelin was given by Crang and Rumsby (1977), taking consideration of the recent information about protein. They showed the one to one complex of globular shaped proteolipid and elongated shaped basic protein residing at cytoplasmic site. They proposed that the cytoplasmic apposition is made by the ionic interaction between basic protein and minus charged polar head groups of acidic lipids. Their model was the first to describe the similarity of the myelin structure to that of other active membrane.

Neurological interests in myelin

As to the neurological interests in nerve myelin, it appears well established that the main role of myelin is to permit much higher conduction velocities than can be attained in a comparably sized unmyelinated fiber (Tasaki,1953).
Stressing the value on the nerve network system, which is the basis of the essential problem in the central nervous system,

nerve myelin is reported to be intimately involved in the formation of the nerve network (Tsukada,1977). On the other hand there are reported some demyelinating deseases, such as multiple sclerosis and so on, which has been assumed to be a result of the selective myelin lesion. In addition Schnapp et al. (1975) speculated that the tight junction at the internal mesaxon , at the paranodal loop and at the paranodal axoglial junction might contribute to the induction of the saltatory conduction and preventing the production of auto-antibodies to myelin.

In these regards it is quite important to study the mechanism of myelination or demyelination, which is consequently based on the structural stability of nerve myelin to preserve the highly organized structure.

In this dissertation the author presents some information on the structural stability of nerve myelin in situ system by using x-ray diffraction method with special attention on nervous system and species.

For studying the physico-chemical property involved in forming the planar membrane system, the author set up the following idealized experimental system in situ, that is he aimed to correlate the x-ray diffraction patterns with the artificial external conditions, through which he deduced the interaction, component to component, leading to the organized stability. Response to the

external perturbation assumingly reflects the internal physico-chemical interaction. So far similar experiments were fully carried out, beginning with the pioneering x-ray works by Schmitt et al.. They demonstrated the x-ray diffraction pattern from dried nerve. In 1950's Finean studied the effects of drying, heating, freezing, high salt solution and solvent action in comparison with the electron microscopic study. In 1975 Kirshner and Caspar observed the x-ray diffraction pattern from nerve myelin treated by dimethyl sulfoxide (DMSO).

In this dissertation the author describes the modification of myelin structure by the treatment with DMSO, acetone and glutaraldehyde for rabbit nerve myelin and carp nerve myelin.

In chapter 2 experimental procedure is generally described and the accuracy of spacing of nerve myelin is discussed.

In chapter 3 is shown the structural modification of rabbit nerve myelin by DMSO, acetone and glutaraldehyde.

In chapter 4 is shown the structural study on carp nerve myelin, which was reported to show the curious diffraction pattern.

In chapter 5 is shown the correlation of x-ray diffraction patterns of central and peripheral nerve myelin modified by DMSO, acetone and glutaraldehyde. Concludingly general discussions are made on the structural stability of nerve myelin and structural correlation between central and peripheral nerve

myelin.

In appendix is given the general description of nerve myelin with respect to morphology and chemical components.

CHAPTER 2

GENERAL EXPERIMENTAL DESCRIPTION AND STUDY ON THE ACCURACY OF REPEAT PERIOD OF NERVE MYELIN DETERMINED BY X-RAY DIFFRACTION METHOD

2-1 Introduction

Nerve myelin is naturally occurring multilamellared structure. For example in rabbit sciatic nerve myelinated axon is from 2 to 20 μm in diameter and the myelin sheath in thickness is from about 0.2 to 2μ, which approximately corresponds to 10 to 100 as a number of bilayers. When rabbit sciatic nerve measuring about 1mm in diameter is used from consideration of the x-ray absorption coefficient, there are about 10^4 myelinated filaments per mm^2 cross sectional area of the nerve (Caspar and Phillips,1976). Thus nerve myelin sheath gives quite intense x-ray reflections at low angle up to $\theta = 4.2 \cdot 10^{-3}$ rad (184Å) for rabbit sciatic nerve and $\theta = 4.8 \cdot 10^{-3}$ rad (160Å) for rabbit optic nerve, when Cu Kα ($\lambda = 1.542$ Å) x-ray radiation is used.

X-ray diffraction method gives the information about the fresh state structure and uniquely determines the repeat period. On the other hand electron microscopy also provides direct structural information, however it unavoidablly estimates the artifacts introduced during several step preparation of the specimen, such as fixing, staining, dehydrating, embedding and so on. In fact

it is familiar that periodicity observed in electron microscopy is almost two thirds of that from x-ray diffraction pattern in the case of nerve myelin. In this context x-ray diffraction technique is the only tool to study directly the structure of intact nerve myelin.

Descriptions in this chapter are focused on the experimental technique and procedure for studying nerve myelin to obtain reliable data and lay the basis on which the experiments described in the following chapters are performed.

In subsection 2-2, the camera optics or geometry, which is related to the resolution and intensity, are described.

In subsection 2-3, the errors inherent in the geometry of the x-ray camera constant and its effect on the determination of spacing are discussed.

In subsection 2-4, the determination of standard reflection at low angle is studied.

In subsection 2-5, the determination of the repeat period of nerve myelin is described as an example.

2-2 Low angle x-ray camera

For the study of low angle x-ray diffraction pattern four different types of camera have been constructed. In the first type (Bear,1942) (Boluduan and Bear,1949), narrow slit or pinhole systems are used. The pioneering x-ray diffraction studies on nerve myelin were carried out with this type. In the second type (Guinier,1939), the beam is focused and monochromatized by reflection from one or more curved crystals. In the third type (Franks,1955 and 1958) (Elliot,1965), x-ray beam is reflected from a plane or curved polished surface. For the study of the membrane structure this type is mostly used. There are now two types of this focusing system commercially available, one of which is Franks camera and the other is Elliot type toroid camera. In Franks camera the focusing is accomplished by the total reflection either by one elastically bent optical flat to form a line focus, or by two flats at right angles to form a point focus. In Elliot type toroid camera, x-ray is focused by a gold coated toroidal or ellipsoidal mirror. In the fourth type (Huxley and Brown,1967), Huxley-Holms type, x-rays are focused by the combination of mirror and monochromator.

Throughout the experiments in this work, Franks single mirror camera and toroid camera are used for recording low angle diffraction and wide angle diffraction, respectively.

A. The geometry of Franks single mirror camera

Fig. 2-1 shows the schematic plan of the single mirror Franks camera. Ideally the reflector should be part of a cylinder having elliptical cross section with F and F' as the foci of the ellipse. When x-rays are emitted from F' (x-ray tube focus) at a glancing angle α , they reunite at the point, F. Diffracted x-rays are focused on the focal circle and the scattered radiation or parasitic radiation, is removed in part by setting the guard slit just before the specimen. The region from L_1 to L_2 on the flat film is covered by scattered radiation. In the experiment to record low angle reflection with maximum resolving power, the flat film is to be replaced by a curved film along the focal circle. At higher diffraction angle, the reflection broadening, shown as $B(\theta)$, is produced. Parasitic radiation and broadening of the diffracted radiation are inevitably produced due to the geometry depicted in Fig. 2-1.

B. Resolution of the single mirror Franks camera

As to the resolution obtained with a small angle camera there are two quantities to be considered, the first order visibility and the higher order resolving power. The former shows the largest observable periodicity and the latter gives a measure of distinguishing successive reflections as two signals.

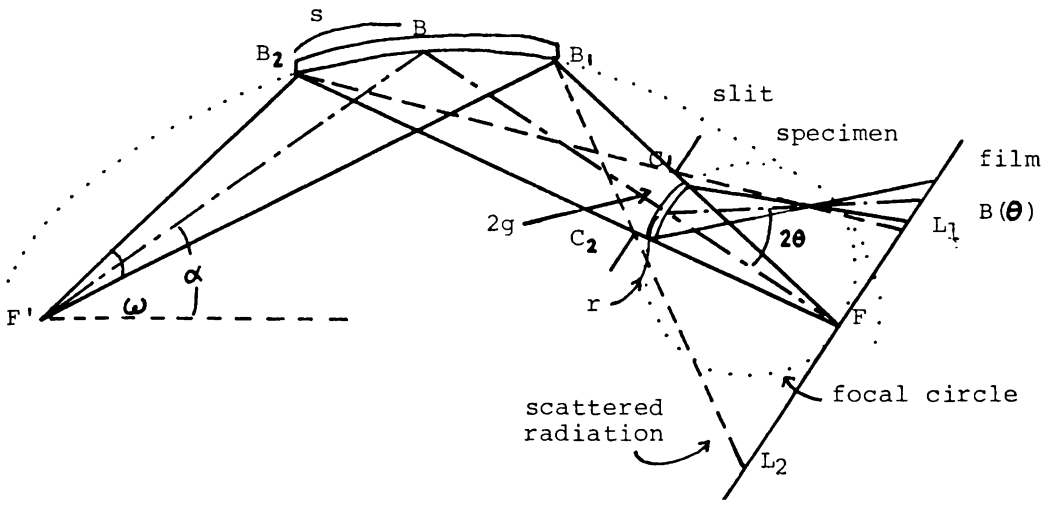

Fig. 2-1 Schematic plan of the single mirror Franks camera $\overline{FB} = \overline{F'B} = f$, $\overline{B_1BB_2} = 2s$, $\langle FF'B = \alpha$, $\overline{C_1C_2} = 2g$, $\overline{L_1F} = L_1$, $\overline{L_2F} = L_2$, $L_1 + L_2 = L$, R is the specimen-to-film distance.

The first order visibility

Defining each quantity as shown in Fig. 2-1, the region covered by parasitically scattered x-rays is given in the following way.

Let L_1 and L_2 are the distances from the direct beam image on the flat film to the scattered beam, then

$$L_1 = \frac{2g\cdot(f + s)}{s + f - R} \quad \text{and} \quad L_2 = \frac{2g\cdot(f - s)}{- s + f - R}$$

where $\cos\alpha = 1$ is used.

Then the observable largest spacing is given by

$$d = \frac{\lambda \cdot R}{L_1} = \frac{\lambda\cdot R\cdot(s + f - R)}{2g\cdot(f + s)}$$

if $R = \dfrac{s + f}{2}$ d gives the maximum value

$$d_{max} = \frac{\lambda \cdot R}{4g}$$

Resolving power

If reflection to reflection distance on the film is larger than $2B(\theta)$, half width of each reflection, two successive reflections are identified as two peaks. Setting the flat film shown in Fig. 2-1 and ignoring the effects regarding the film thickness

and grain size and densitometry (aperture size, scanning speed and etc.), $B(\theta)$ may be estimated as,

$$B(\theta) = \frac{r \cdot (1 - \cos^2 2\theta)}{\cos^2 2\theta} + a$$

where r is the exposed width of specimen to x-rays and a is the half width of the focused beam.

The distance between successive reflections on both sides of the film is calculated to be

$$\Delta L = \frac{4R \cdot \tan\theta \cdot \Delta d}{(\cos 2\theta)^2 \cdot d}$$

Assuming $\tan\theta = \theta$ and $\cos 2\theta = 1$, the minimum Δd is given as

$$\Delta d_{min} = \frac{a \cdot \lambda}{2 \cdot R \cdot \theta^2}$$

where the successive reflections, d and $d + \Delta d_{min}$, can be identified as two peaks.

C. The intensity per unit area, I , of the focused beam at the film

Setting the geometry as depicted in Fig. 2-1 where h is the diameter of focus at F' and F, B is the brilliancy, and f is the distance from focus to reflection, the average intensity at the film may be estimated as follows.

The total x-ray energy per sec. reflected from the reflector at an angle α is proportional to the total power of the x-ray source and to ω, divided by the distance f, so that

$$\frac{B \cdot h^2 \cdot \omega}{f}$$

A constant fraction of this energy is dispersed over the circle, $R \cdot \tan 2\theta$ in radius, at the film by specimen diffraction, then I is proportional to

$$\frac{B \cdot h^2 \cdot \omega}{f \cdot R \cdot \Delta L}$$

where ΔL is the width of the diffracted x-rays at the film.

Assuming that ΔL is equal to h, finally I is calculated as

$$I \propto \frac{B \cdot h \cdot \omega}{f \cdot R}$$

Above estimation on the resolution and intensity involved in the setting of the Franks single mirror camera shows that the demand for high resolution and high intensity are conflicting, so the allignment of the camera is to be made according to the exper-

iment being planned, considering what is more important in attaining the aim.

2-3 Errors inherent in the geometry of Franks camera and its effect on the determination of repeat period of the nerve myelin

In determining the precise lattice constant of a single crystal, the standard method is to extrapolate the observed points to $\theta = \pi/2$ and eliminate the systematic as well as random errors as far as possible (Ekstein,1949) (Klug et al.,1974). In the case of nerve myelin, whereas, the above method is not applicable because the reflections appear only at low angle region. Hence it is critical to minimize the effect of the systematic error. In this section systematic errors involved in the geometry of the single mirror Franks camera will be discussed.

A. Random error

From Bragg equation, $2d\sin\theta = \lambda$, the ambiguity in spacing is given as

$$|\Delta d| / d = \cot\theta |\Delta\theta|$$

Fig. 2-2 (Parrish and Wilson,1968) shows the percentage precision of the spacing as a function of the diffraction angles for various errors in diffraction angle. This is the minimum error caused by the limited accuracy with which the reflection angle can be measured. From the geometry depicted in Fig. 2-1,

$L = 2 \cdot R \cdot \tan 2\theta$ is given.

With the range of the diffraction angle where $\cos\theta$ and $\sin\theta$ are approximated to 1 and θ respectively, the precision of the diffraction angle can be estimated as is described in the following.

$$\left(\Delta\theta/\theta \right)^2 = \left(\Delta R/R \right)^2 + \left(\Delta L/L \right)^2$$

where R is the specimen to film distance and $L/2$ is the distance from direct beam to diffracted beam on the film.

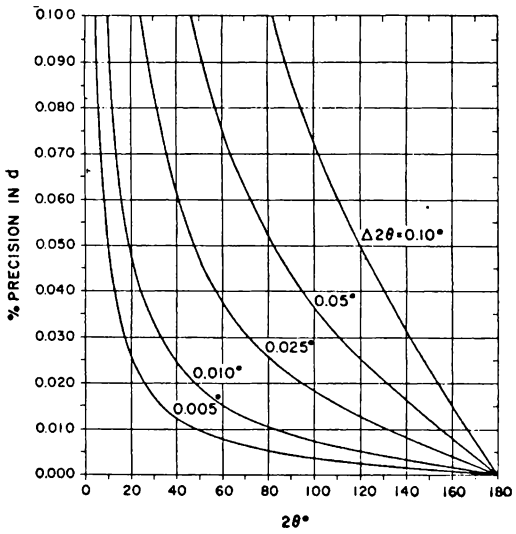

Fig. 2-2 Percentage precision of d(spacing measurement) as a function of reflection angles for various errors $\Delta 2\theta$. ($|\Delta d|/d = \cot\theta |\Delta\theta|$.) (Parrish and Wilson,1968)

B. Systematic error

Three systematic errors, 1) radius error and film shrinkage, 2) displacement of the specimen from the focal circle and absorption of the x-ray beam by the specimen, 3) displacement of the film from the focal circle, are taken into consideration in the single mirror Franks camera.

1) Radius error and film shrinkage

From the geometry of the single mirror Franks camera shown in Fig. 2-1, $\tan 2\theta = L/(2 \cdot R)$.

On differentiation it gives

$$\Delta\theta = \frac{\sin 4\theta}{4} \left(\frac{\Delta L}{L} - \frac{\Delta R}{R} \right) .$$

When $\Delta R=0$ the above equation gives the contribution of L to $\Delta\theta$.

$$\Delta\theta = \frac{\sin 4\theta}{4} \cdot \frac{\Delta L}{L}$$

2) Displacement of the specimen and absorption effect

If the specimen is displaced from its ideal position in the way shown in Fig. 2-3, the apparent L is given as,

$$L^{app} = L - 2\Delta\varepsilon \cdot \tan 2\theta$$

If the specimen is displaced in its own plane the apparent L is equal to L , although the exposed region of specimen is smaller.

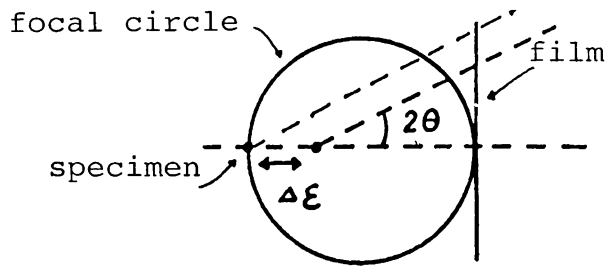

Fig. 2-3 Schematic drawing of the geometry for the specimen displacement.

3) Film displacement

Assuming the film is displaced from the focal circle as shown in Fig. 2-4 the apparent L is given as,

$$L^{app} = R \cdot \tan 2\theta \cdot \cos 2\theta \cdot \left(\frac{1}{\cos(2\theta + \phi)} + \frac{1}{\cos(2\theta - \phi)} \right)$$

$$= (L/2) \cdot \cos 2\theta \cdot \left(\frac{1}{\cos(2\theta + \phi)} + \frac{1}{\cos(2\theta - \phi)} \right)$$

when $\phi \simeq 0$

$$\simeq (L/2) \cdot \cos 2\theta \cdot \left(\frac{1 + \phi \tan 2\theta}{\cos 2\theta} + \frac{1 - \phi \tan 2\theta}{\cos 2\theta} \right)$$

$$+ (\text{ quantities of the order } \phi^2)$$

$$\simeq L$$

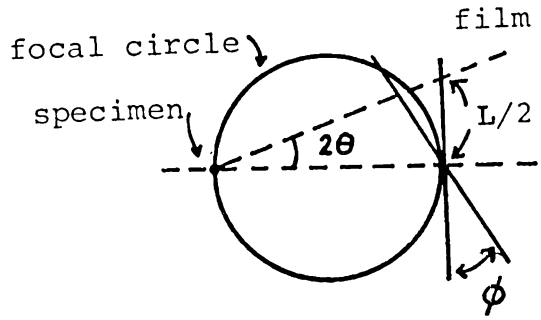

Fig. 2-4 Schematic drawing of the geometry for the film displacement.

From *1) 2) 3)*

$$\frac{\Delta d}{d} = -\frac{\Delta L}{L} + \frac{\Delta R}{R} - \frac{4\Delta\varepsilon \cdot \theta}{L}$$

$$= \frac{1}{R}\left(-\frac{\Delta L}{4} + \Delta R - \Delta\varepsilon \right)$$

The systematic errors, ΔL, ΔR and $\Delta\varepsilon$ can be estimated by using the standard substance giving clear reflections at low angle wherein above equation is valid.

2-4 On the determination of standard reflection at low angle

As was discussed in the former subsection 2-3, standard substance giving x-ray diffraction at small angle is needed to determine the spacing exactly. So far, in the study of nerve myelin several standard substances were used, that is sodium stearate (Chandross et al.,1978), sodium myristate (Fruya et al., 1976) and cholesterol (Freeman,1975). In the present study cholesterol and sodium myristate are used. Both of them show the polymorphic nature which depends on the external condition (Vold et al.,1952) (Skoulios et al.,1959), so that reliable lattice constant has not been reported. For cholesterol, for example, Finean reported 34.5Å as the largest periodical distance (Finean,1961), ASTM gives 33.6Å , recently Craven (1977) gives 33.89Å for anhydrous cholesterol and Shieh gives 33.95Å for monohydrate cholesterol.

In this subsection, therefore, the precise spacings for standard low angle reflections, were determined for powdered cholesterol and sodium myristate respectively, by using Guinier camera. In this camera low and wide angle x-ray reflections are simultaniously recorded using the cylindrical film holder.

A. Experimental procedure

Commercially available cholesterol (Nakarai, K,K) is dissolved in acetone (Nakarai, K,K no further purification), re-

crystallized, ground into powder and applied to the sample holder (500μ in thickness). Cholesterol and sodium myristate without further purification are prepared in the similar way. As four kinds of different specimens can be exposed at the same time in this Guinier camera, the following combination was taken, cholesterol or sodium myristate, cholesterol or sodium myristate mixed with standard powder (sodium chloride or aluminum) and standard powder only. The standard lattice spacings are 2.338Å for aluminum (Swanson and Tatge,1953) and 3.258Å, 2.821Å and 1.994Å for sodium chloride (Swanson and Fuyat,1953).

X-ray diffraction patterns were obtained from specimens at room temperature using monochromator focused Guinier-DeWolff camera No II (DeWolff,1948a and 1948b), $K\alpha_1$ and $K\alpha_2$ of Cu radiation from the Toshiba x-ray sealed tube, with effective focus of 0.1mm•10mm, operated at 35KV, 15mA.

The distance from direct beam to diffracted beam on the film (Kodak, XR-5) was measured on the optical density chart against diffraction angle, which was an output of ten times multiple scanning with 0.0219cm each step by using Syntex AD-1 Auto Densitometer with 0.0109cm • 0.0219cm aperture. As to the multiple scanning technique (Golay,1963) (Savitzky,1964) (Saeki,1972) for x-ray diffraction study, Iizuka (1977) related the signal to noise ratio to the grain size of the film and demonstrated the utility of the multiple scanning to attain the satisfactory

intensity values of the weak reflections.

In Fig. 2-5 is depicted the schematic plan of the Guinier camera. X-rays from the tube focus reunite at the other focus on the film by appropriately bending the focusing monochromator crystal which is a quartz slab cut at an angle of 4.5 degree from the (1 0 $\bar{1}$ 1) net plane. To register the diffracted x-rays the film is cylindrically positioned following the focal circle on which the diffracted x-rays are focused at every diffraction angle.

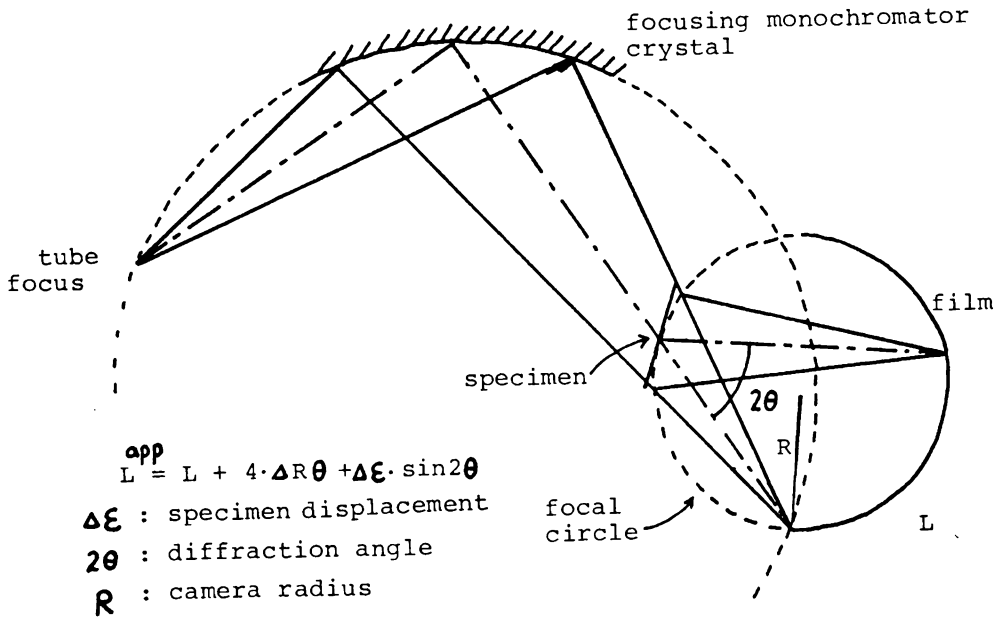

Fig. 2-5 Schematic plan of the Guinier camera.

B. Calculation of the lattice constant of cholesterol and sodium myristate

There are several systematic errors to be considered in the case of Guinier camera. Among them 1) radius errors and film shrinkage, 2) displacement of the specimen from an ideal position and absorption of the x-ray beam by the specimen are estimated in the following.

Defining camera radius R, diffraction angle θ, specimen displacement $\Delta\varepsilon$, true distance from direct beam L, and apparent value L^{app}, L^{app} is given as

$$L^{app} = L + 4 \cdot \Delta R \cdot \theta + \Delta\varepsilon \sin 2\theta$$

Applying the several kinds of standard diffraction angle for sodium chloride or aluminum and observed value of L^{app} to the above equation ΔR and $\Delta\varepsilon$ will be calculated.

C. Results

Table 2-1 shows the L^{app} values for sodium chloride and aluminum, from which ΔR and $\Delta\varepsilon$ are calculated using the above equation, as 0.480cm and - 0.918cm respectively. These values are too large to be considered reasonable. In fact a plausible size of the systematic errors ΔR and $\Delta\varepsilon$ are of the order of 10^{-2} cm, judging from the experimental set up in Guinier camera. These

Table 2-1. Observed distances on the film between the standard reflections and the direct beam.

d_s(Å)	L_s^{app}(cm)	ΔL_s^{app}(cm)	trial
3.258(NaCl)	5.5118	0.0061	3
2.821(NaCl)	6.393	0.011	3
2.338(Al)	7.7510	0.0057	5
1.994(NaCl)	9.1506	-	1

d_s, spacing of the standard reflection. L_s^{app}, apparent distance. ΔL_s^{app}, deviation in the apparent distance.

discrepancies can be ascribed to the computational error which came from the interdependence of ΔR and $\Delta\varepsilon$. To overcome this difficulty, it was decided to adopt only ΔR as the independent variable, making use of the very similarity between $\sin 2\theta$ and 2θ. The value of the systematic error ΔR obtained in this way came out to be + 0.04cm or 0.7% in $\Delta R/R$.

Hence in this experiment, L^{app} is expressed in the following.

$$L^{app} = 4\theta\bullet(R + \Delta R) = 4\theta\bullet 5.768\text{cm}$$

L^{app} values of the reflections whose periodicities are close to 17Å, were measured as 1.03 (0.01) cm for cholesterol and 0.984 (0.003) cm, 1.480 (0.003) cm for sodium myristate. In result

17.3 (0.2)Å for cholesterol and 18.08 (0.07)Å, 12.02 (0.03)Å for sodium myristate were obtained, where the following equation was applied.

$$(\Delta d/d)^2 = (\Delta L^{app}/L^{app})^2 + (\Delta(R+\Delta R)/(R+\Delta R))^2$$

In the mixed sample, cholesterol and aluminum, the diffraction pattern demonstrated a difference from that of non-mixed cholesterol sample, in addition purified cholesterol did not give the same pattern as that of non purified pattern, even though the periodical distances close to 17Å, which were the main problem to be determined, were constant within the uncertainty of deviation. These structural changes by chance provide an interesting subject on the cholesterol structure.

The relative deviation for the cholesterol (1%) is rather larger than expected. If $\Delta\lambda$ is almost zero and $\sin\theta$ or $\cos\theta$ are approximated toθ or 1 respectively, from Bragg equation and Guinier camera geometry, $|\Delta d|$ is equal to $\frac{|\Delta L| \cdot d^2}{11.5 \cdot \lambda}$. In the densitometer profile by smoothing the curve it is possible to measure the location of the peak within the accuracy of 10μ . Appling the 0.2Å and 17.3Å to Δd and d , respectively $|\Delta L|$ becomes 118μ. The large deviation of $|\Delta L|$ is mainly due to the sample preparation and setting of the Guinier camera, for the errors involved in the densitometry and film grain size etc. are negligible in this case.

2-5 The example of the determination of the repeat period of nerve myelin and general description of the experimental procedure

In this subsection an example of the determination of the repeat period for nerve myelin is shown. Fish spinal cord, for example, was reported as giving two structure phases (Blaurock and Worthington,1969), one of which is from 182Å to 183Å and the other is 156Å in period. For the purpose of obtaining the exact repeat period the experimental procedure is carried out in the following way, 1) the allignment of the camera, 2) specimen preparation, 3) photography, 4) densitometry, 5) determination of the repeat period of nerve myelin.

Setting of single mirror Franks camera for carp spinal cord

As shown in subsection 2-2 it is conflicting to demand both the high intensity and high resolution, so according to the purpose of the experiment a certain allignment should be selected considering what is more important. For example in the fish spinal cord, there are reported two structures, one of which is from 182Å to 183Å and the other is 156Å. To obtain a satisfactory photograph the following camera setting was chosen. Referring to Fig. 2-1 shown in subsection 2-2, reflector length s = 2cm, the glancing angle $\alpha = 3 \cdot 10^{-3}$ rad, specimen to film distance R = 15cm, tube focus to reflector distance f = 25cm, slit aperture

$2g = 0.01cm$.

In this condition the largest spacing to be observed is approximately 1000Å and using the resolving power equation, $\Delta d_{min} = a \cdot \lambda/(4 \cdot R \cdot \theta^2)$, the observable reflections, 182Å (1, 2,3, 4, 5, 6 order reflection) and 156Å (1, 2, 3, 4, 5, 6) could be resolved except for the 6th order of 182Å phase and the 5th order of 156Å phase. Above estimation is carried out on the assumption that the breadth of the focused beam is 0.01cm.

After approximate setting of single mirror Franks camera, the exact values of camera constants were determined using standard reflections of cholesterol and sodium myristate. As shown in subsection 2-3, three systematic errors, ΔR, $\Delta\varepsilon$, ΔL are to be considered. Using the equation, $2R\tan 2\theta = L$, specimen to film distance (R) is calculated from the lattice spacing of the standard substance and the observed L value. Using this R value systematic error in d is cancelled. Thus in this experimental condition, systematic errors, (ΔR, ΔL, $\Delta\varepsilon$) cannot be practically taken into consideration.

For example 34.5Å cholesterol reflection gave 1.354cm as L value with the 0.14% accuracy. In result the effective specimen to film distance could be calculated with 1.05% accuracy, where

$$(\Delta R/R)^2 = (\Delta L/L)^2 + (\Delta d/d)^2$$ was used.

The relative deviation of $\Delta L/L$ comes from various random errors, such as in specimen displacement, film deformation, measurement of the position of the diffracted beam and so on.

The specimen preparation

Nerve myelin is known to degenerate on the animals' death, therefore in every experiments the diffraction patterns were observed as time after execution. Especially in fish case, postmortem deterioration was observed in such a way that 155Å phase transforms to 183Å phase. In addition to get the sharp reflection the nerve fibers were forced to be in order by either sealing them into 0.7mm in diameter thin walled glass capillaries or holding them in the specimen chamber under tension. The deviations due to age, species, sex could be removed to some extent by rearing the animals under the same condition. This step needed a lot of experience.

Photography and densitometry

Syntex AD-1 Auto Densitometer was used for measuring the optical density, in the similar way as described in subsection 2-4. Aperture size, 0.0109cm•0.0219cm, was used considering the grain size of the film.

The result on the repeat period for carp spinal cord myelin

The freshly dissected out nerve myelin was sealed in glass capillary tube, 0.7mm in diameter, with Ringer's solution. The nerve specimen was mounted on the same place where standard substance was placed. In this experimental condition, there is no systematic error to be considered. Hence the repeat period for nerve myelin was calculated by the measured value, L , and the effective specimen-to-film distance which was obtained by using standard substance. Thus the accuracy of the repeat period, $\Delta d/d$, is expressed in the following where $\Delta R/R$ is independent of $\Delta L/L$.

$$(\Delta d/d)^2 = (\Delta R/R)^2 + (\Delta L/L)^2$$

Fig. 2-6 shows the repeat period vs. time for carp spinal cord myelin. The vertical line for each point shows the deviation when specimen to film distance is constant. In both structure phases, the repeat periods at each time are randomly distributed, hence it is concluded that the repeat periods are independent on the time after execution. In this case $\Delta L/L$ value was 0.58% for 155Å phase and 0.66% for 183Å phase. After all the repeat periods of each phase were determined as 155Å and 183Å with 1.2% accuracy.

The relative deviation of L comes from the random error in the specimen position, film deformation, the measurement of the

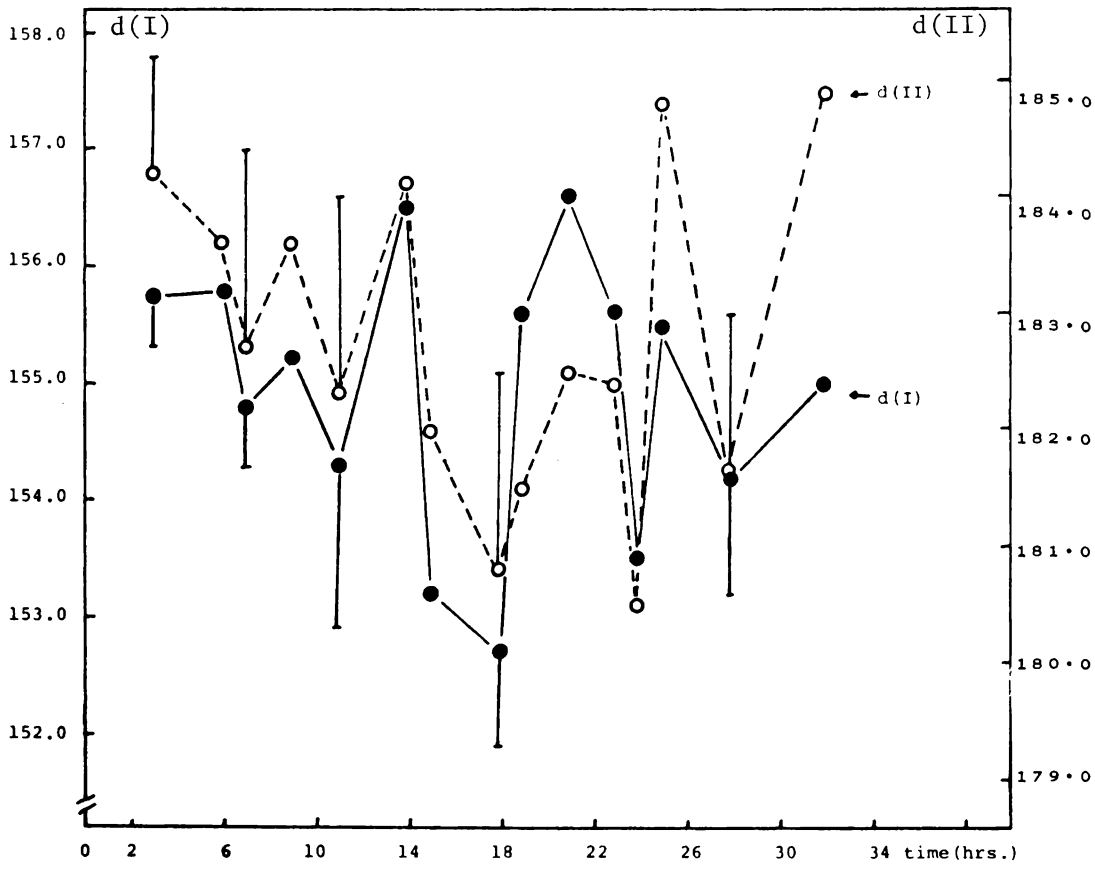

Fig. 2-6 Dependence of the repeat period of the I-phase and of the II-phase on time after execution for carp spinal cord myelin. d(I), repeat period of the I-phase. d(II), repeat period of the II-phase.

position of the diffracted beam and so on. Comparing with the accuracy obtained for standard substance ($\Delta L/L = 0.14\%$), the difference in accuracy is due to the ambiguous effects involved in animal, specimen preparation and specimen itself. However the accuracy in the repeat period, 1.2%, is small enough considering the accuracy of the reported periodicity from nerve myelin (see appendix). This means that even in biological substances careful treatment on the specimen may lead to a rather constant value.

The main factor contributing to the deviation comes from the uncertainty of the spacings of the standard substances. For further accuracy to be attained, it is most important to find some suitable substances, giving clear x-ray diffraction pattern at low angle.

2-6 Summary

In this chapter was described the experimental procedure, which lays the basis on which the following experiments are performed.

Section 2-2 shows relationship between the geometry of the low angle camera and resolution or intensity, whereby it is important to set the camera according with the experiment to be planned.

For the accurate determination of the spacing at low angle,

several factors, both systematic and random, are involved. In section 2-3 systematic error associated with the geometry was discussed and shown to be removed by the use of the standard substance for calibration. For that purpose cholesterol and sodium myristate were used and the spacings of them were determined by Guinier camera.

Practical example for the determination of the repeat period of nerve myelin was given in section 2-5, and it was clarified that the uncertainty in the spacing of the standard substance mostly contributes to the error in result. Furthermore it was shown that the errors due to ambiguous effects in animal could be sufficiently removed by the careful treatment of nerve myelin.

CHAPTER 3

STRUCTURE STUDY OF RABBIT NERVE MYELIN

3-1 Introduction

In an attempt to clarify the structure of nerve myelin the external perturbation has been generally in use, because 1) a highly organized structure is quite difficult to analyze directly and 2) the response to the perturbation may reflect the internal physico-chemical interactions which organize the structure. In the case of x-ray diffraction study of nerve myelin, Schmitt et al. (1935 and 1941) already observed the structural modification in a number of amphibian and mammalian medulated nerves by drying, heating, treating by detergent and calcium ions with comparative studies on extracted lipids, which was correlated with the excitability of nerve axon. From their experiments they concluded that 1) characteristic long spacing equatorial reflections were due to lipid molecules whose long chains were directed radially in sheath and 2) the meridionally accentuated short spacing ring at 4.7Å was due to the interchain distance of the lipids in the tangential direction. Furthermore they proposed four possible models for the packing of lipid and protein in nerve myelin, hereby it was possible for them to estimate the lipid to protein volume ratio as about 5.4 and water content as at least 30% in myelin sheath, which are remarkably close to the values chemically determined afterwards.

Since such a perturbation technique proved to give valuable clues regarding the thickness of the lipid and protein layers and the general arrangement of molecules within these layers, many x-ray diffraction experiments have been carried out similarly (Finean,1961) (Finean et al.,1968), that is drying, freezing, heating, modifying ionic strength, organic solvents, pH, treating by enzymes and so on in combination with electron microscopic study. In 1961 Finean noted that the structural modification due to dehydration of frog sciatic nerve was accomplished by air drying, by treatment with hypertonic solutions, by freezing or by treatment with lipid extracting solvent. The initial state of dehydration caused by partial air drying, by freezing to about 25% water content or by salt solutions of about 2M strength, was characterized by the appearance of a strong reflection in the region of 60Å, which was apparently the second order of a periodicity of 120Å. On replacing the nerve in normal conditions in this case this phase (120Å) which was named collapsed phase completely disappeared and the original myelin pattern was fully restored. In the second stage of modification, which was irreversible, air dried nerve showed a typical strong reflection in the region of 43Å and eventually gave a very sharp reflection at about 34.6Å. With respect to the process of dehydration, striking similarities were shown to exist between nerve myelin and other cell membranes, erythrocyte

membranes, muscle microsomal membranes, whereby it was noted that membranes are fundamentally similar in structure although highly individual in detail (Finean et al.,1968).

Up to now there are proposed two accounts for the explanation of this reversible modification, one of which is the separation of lipid phase from membrane and the other is the contraction of water layer, leaving the bilayers essentially unaltered. Presently no consolidated explanation is given for the mechanism of this reversible phenomenon, for the main problem, whether collapsed phase is lipid phase or lipo-protein phase, remains unclarified. However this reversible-to-irreversible transformation must be an idealized experimental system to give the valuable information about the mechanism of integration into the myelin structure.

Recently Kirshner and Caspar (1975) observed the modification of nerve myelin structure by dimethyl sulfoxide (DMSO) for rabbit sciatic, optic and bull frog sciatic nerves. They considered that the collapsed phase, approximately 120Å with intense 2nd order reflection, was brought about by the dehydrating effect of DMSO. Furthermore the known effect of DMSO as a blocking reagent on nerve conduction was speculated to be correlated with the dehydrating effect on the nerve myelin sheath. The x-ray diffraction patterns demonstrated complete transformation of the myelin structure at concentrations above 40%, at which DMSO had been shown to produce reversible blockage of nerve conduction (Davis

et al.,1967) (Becker et al.,1969).

That was the first experiment to relate the physiological function to the structure of nerve myelin. However, taking account of the unanimously accepted biological membrane model, it seems improbable that the drastic change in diffraction pattern is induced simply by the removal of the water layer residing in extra-cellular surface and in cytoplasmic surface which correspond to the intraperiodline and the major dense line, respectively in the transverse section of electron micrograph. Luzzati (1968) has already established for lipid that significant polymorphism was caused according to the change in concentration and temperature, and moreover it is well known that the phase segregation interpreted as the rearrangement of the membranous particles, could be induced in reconstituted and naturally occurring membrane by subtle perturbation (Cherry,1976).

In this regards it is reasonable to carry out the DMSO experiment to reexamine the structural mechanism of the reversible-to-irreversible transformation in nerve myelin. This study may lead an invaluable insight into the myelin stability. Acetone was also studied in the same way as DMSO, for acetone has the similar chemical structure and similar dehydrating action to the nerve myelin (Elkes and Finean,1953a and 1953b). In addition , glutaraldehyde gives, for its crosslinking and fixing property (Steck,1972) (Sabatini,Bensch and Barrnett,1963) (Moretz,Akers

and Parsons,1961), significant basis to correlate the x-ray diffraction pattern and the chemical composition.

In subsection 3-2, DMSO effect on rabbit sciatic nerve is studied with respects to periodicity, diffracting power, half width of reflection and structure factor.

In the same way modification in rabbit sciatic nerve by acetone is shown in subsection 3-3.

In subsection 3-4, the x-ray study on the glutaraldehyde treated rabbit sciatic nerve is shown.

In subsection 3-5, is shown the cross effect as DMSO or glutaraldehyde effect on acetone treated-and-washed rabbit sciatic nerve.

In subsection 3-6, is shown the cross effect as glutaraldehyde effect on DMSO treated nerve or vice versa.

In subsection 3-7, is shown the drying effect on DMSO treated rabbit sciatic nerve.

To compare the structural relationship between peripheral nervous system and central nervous system in mammalian species, DMSO, acetone and glutaraldehyde are applied to rabbit optic nerve , which is shown in subsection 3-8.

In subsection 3-9, is given the discussion on the myelin stability.

3-2 DMSO effect on rabbit sciatic nerve

A. Experiment

Sciatic nerve of rabbit (above 2.5kg weight, male and one year old) was dissected out immeadiately after the animal was killed. For the purpose of the isolation of DMSO effect from myelin natural degradation, the following two series of experiments were carried out, the first is a short exposure and the second is a long exposure experiment.

In the first series of experiment the single specimen of the same nerve under constant tension in specimen chamber was used throughout the experiment, DMSO treatment for 2 hours and washing in normal mammalian Ringer's solution for 1 hour were carried out in the specimen chamber, keeping the nerve in constant place. Incubation time was determined from the preliminary experiment so that the induced modification attained to the equlibrium. Every exposure lasted one hour.

In the second series of experiment, in order to detect higher order reflections, nerve specimens were incubated in DMSO solution for two hours, then sealed in thin walled glass capillaries and exposed for about 15 hours.

In both series of experiments (short and long exposure) single mirror Franks camera and Cu target x-ray tube operated at 40KV, 18mA, were used for getting low angle reflections, while

for wide angle reflections Elliot toroidal camera was used.

For intensity measurement and determination of periodicities from the x-ray photographs, Syntex AD-1 Autodensitometer was used. For three states, fresh, treated and treated-and-washed, the following values were calculated.

Periodicity, d

Integrated intensity of h-th order reflection, I(h)

Structure factor, $F(h) = \pm\sqrt{hI(h)}$ (Blaurock and Worthington, 1966), where $\sum|F(h)|^2/d$ = constant (Worthington,1969)

Diffracting power, $P = \sum hI(h)/d^2$

Half width of reflection, A

Wide angle reflections were observed for fresh nerve, 20% DMSO treated nerve and 40% DMSO treated nerve by the toroidal camera. For comparison, low angle reflections were also recorded in parallel by Franks camera. Diffraction patterns from fresh nerve were observed for the freshly dissected rabbit sciatic nerve which was sealed in thin walled glass capillary tube. Those from DMSO treated nerves were obtained from the specimen which were treated in incubation medium for 2 hours and sealed in capillary tube with immersion medium. The exposure was 4 hours. Wide angle x-ray diffraction patterns were obtained using the toroid type mirror-focused Cu Kα radiation from the point source arrangement of a Philips fine focus x-ray tube operated at 33KV, 7mA. All

the experimental procedures were carried out at room temperature (20°C).

Mammalian Ringer's solution was prepared from NaCl 860mg, KCl 30mg, $CaCl_2 2H_2O$ 33mg, adding distilled water to the total volume of 100ml. DMSO solution is prepared by the dissolution of DMSO (Guaranteed Reagent of Nakarai Chemicals, LTD., without further purification) in mammalian Ringer's solution.

B. Results

1) Short exposure experiment

Fig. 3-1 shows one series of diffraction pattern from the same rabbit sciatic nerve treated with 20% and 40% DMSO V/V in Ringer's solution. In the fresh and DMSO treated-and-washed (washed state), 2nd, 3rd, 4th and 5th order reflections are observed for one hour exposure, whereas in the treated state the reflection at approximately 60Å is quite intense, which is the characteristic diffraction of the dehydrated state already reported. Comparing the results for 20% and 40% DMSO, the diffraction patterns at first sight are similar, even though in detail they are different.

In the following, periodicity, structure factor, half width and diffraction power measured from these diffraction patterns are described.

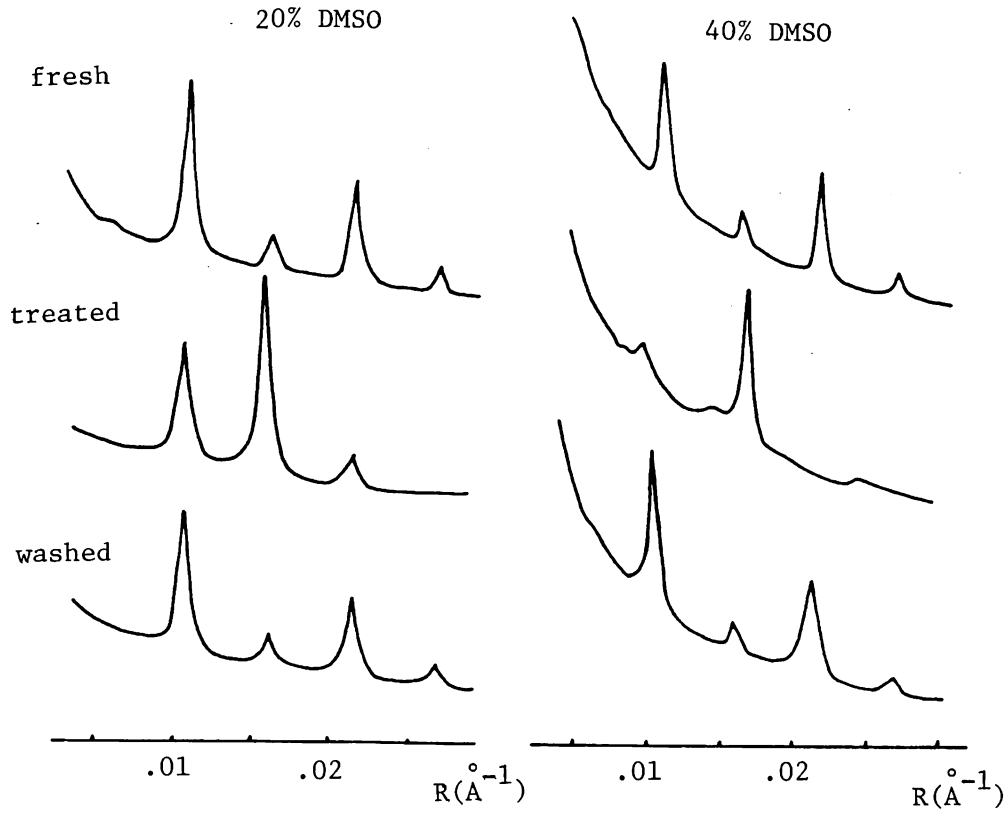

Fig. 3-1 Densitometer tracings vs. diffraction angle for fresh, DMSO treated and DMSO treated-and-washed rabbit sciatic nerve myelin.

Periodicity

Fig. 3-2 and Table 3-1 show the periodicities as the function of DMSO concentration in the treated nerve and treated-and-washed nerve. In the treatment with DMSO above 10%, a new collapsed phase (C phase) and native-like phase (N phase) are observed. The C phase gradually shrinks from 129Å at 10% to 114Å at 70% DMSO solution, while the N phase keeps constant at 184Å until 30%, then

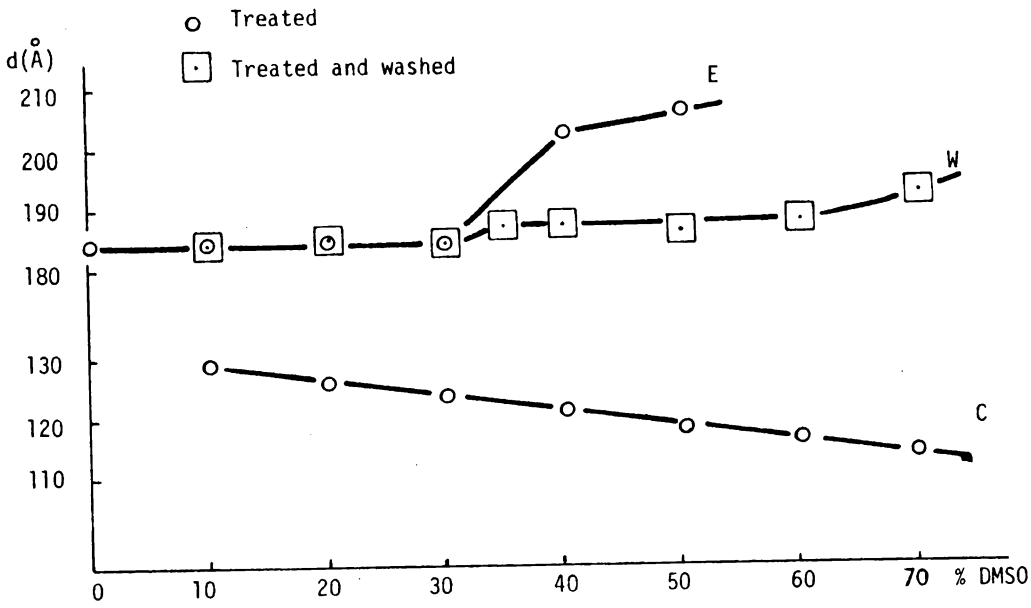

Fig. 3-2 Dependence on DMSO concentration of the periodicity of the native-like phase (N-phase), of the collapsed phase (C-phase) and of the expanded phase (E-phase) in the DMSO treated state (marked in circle) and of the washed phase (W-phase)in DMSO treated -and-washed state (marked in square) for rabbit sciatic nerve.

Table 3-1 Periodicity of rabbit sciatic myelin membrane in the fresh, DMSO treated and DMSO treated-and-washed state.

DMSO(%)	10	20	30	40	50	60	70
Fresh	184.0	184.0	184.0	184.0	184.0	184.0	184.0
Treated	183.6	184.0	183.9	201.7	206.3	-	-
	129.3	126.0	123.8	120.5	117.3	115.6	113.9
Washed	184.0	184.8	183.6	186.7	185.6	187.2	192.2

expands to 202Å at 40% and to 206Å at 50% DMSO solution. The change from N phase to E phase (the expanded phase observed in the treated nerve) takes place between 30% and 40% DMSO.

In the x-ray diffraction pattern from the DMSO treated-and-washed nerve, at the range of concentration from 10% to 30%, C phase and N phase fade away and are replaced by fresh phase at least in periodicity, whose value is 184.0Å, 184.8Å, 183.6Å at 10% , 20%, 30% DMSO, respectively. Above 40% DMSO concentration, however, C phase and E phase are replaced by a new phase which is similar to the fresh phase but is a slightly expanded phase (F' phase). The periodicity of F' phase gradually increases with DMSO concentration, such that 186.7Å, 185.6Å, 187.2Å, 192.2Å are observed at 40%, 50%, 60% and 70%, respectively. Considering that the random error is 1% at most, which is discussed in chapter 2, this expansion in the periodicity is significant.

Thus it is shown that the irreversible change, namely the transformation from F phase to F' phase, is induced at the same DMSO concentration where E phase emerges in the treated state.

Diffracting power of C phase in the treated state

In Fig. 3-3 is shown the dependence of the contribution of the power of the C phase against the total diffracting power of the treated state on DMSO concentration. The value is normalized, so as the total diffracting power equals 1.0 . The contribution of

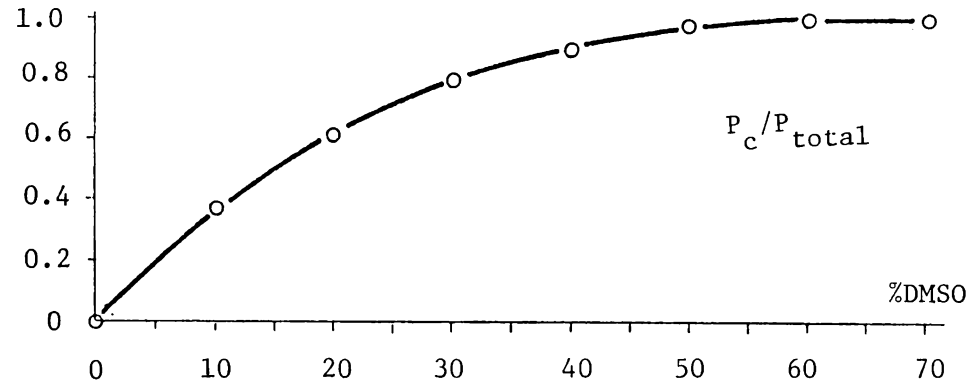

Fig. 3-3 Dependence of the diffracting power of the collapsed phase (P_c) in the DMSO treated state on DMSO concentration for rabbit sciatic nerve myelin. The value is relative to the total diffracting power.

the C phase increases as the concentration of DMSO increases and at 50% DMSO none of the other phases can be detected. At 30% concentration, above which irreversible change begins, the C phase amounts to 81% of the total diffracting power.

Structure factors for DMSO treated-and-washed rabbit sciatic nerve

In Fig. 3-4 is depicted the structure factor of the treated-and-washed state. Below the concentration of 30% DMSO, $|F(h)|$ value for each reflection is constant, while above that point the structure factors of the odd order reflections, 3rd and 5th, decrease and that of 4th order increases. Table 3-2 shows the

structure factors in the treated-and-washed state at various DMSO concentrations.

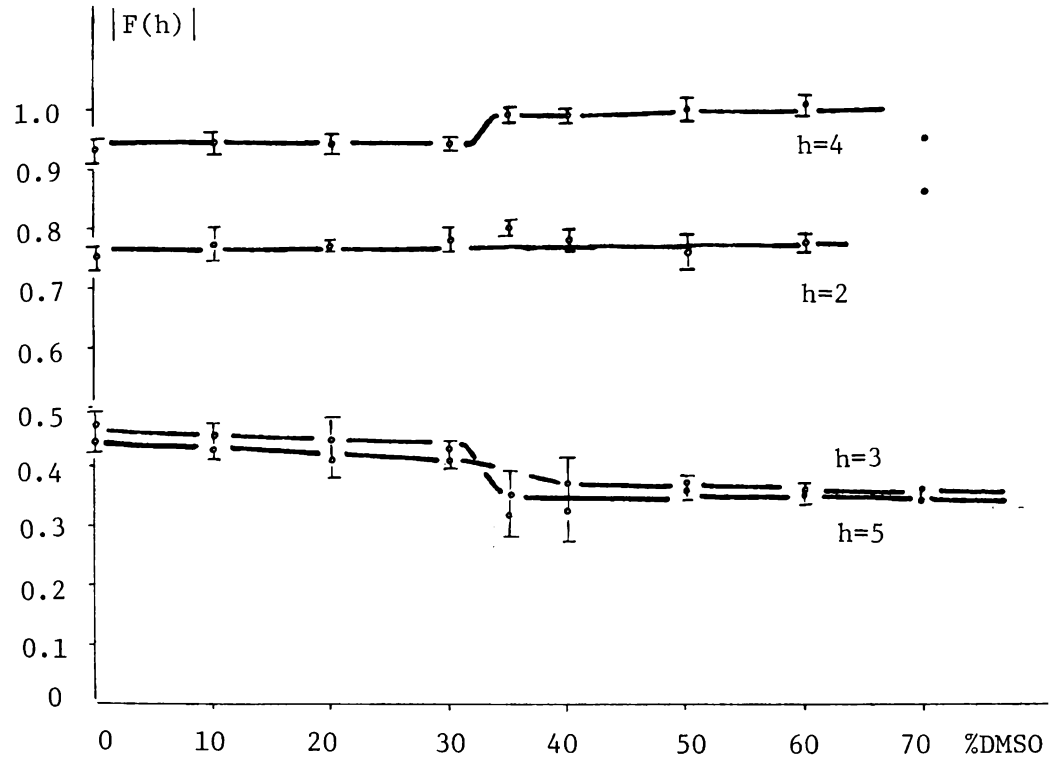

Fig. 3-4 Dependence of the structure factor of the washed phase in the DMSO treated-and-washed state on DMSO concentration for rabbit sciatic nerve myelin. Structure factor is normalized as $\sum|F(h)|^2/d= 0.01$.

Table 3-2 Structure factor of the washed phase in the DMSO treated-and-washed state at different DMSO concentration for rabbit sciatic nerve myelin.

%DMSO	|F(2)|	|F(3)|	|F(4)|	|F(5)|
0	0.75	0.44	0.93	0.47
10	0.74	0.43	0.95	0.45
20	0.77	0.44	0.94	0.41
30	0.78	0.41	0.94	0.43
35	0.80	0.32	0.99	0.35
40	0.78	0.37	0.99	0.36
50	0.76	0.37	1.00	0.36
60	0.78	0.36	1.01	0.35
70	0.86	0.36	0.95	0.34

Half width broadening of the Bragg reflection for the treated-and-washed state in rabbit sciatic nerve

Fig. 3-5 shows the dependence of the half width broadening for each reflection in treated-and-washed state on the DMSO concentration. The value of the half width is obtained in the relative scale to that in the fresh state. For each order of reflection the half width increases above the 30% DMSO, with the trend that the higher order reflection broadens more than that of the lower. Since the broadeness of the reflection is associated with the orderness of the structure and the volume from which x-rays are diffracted, the F' phase observed in the treated-and-

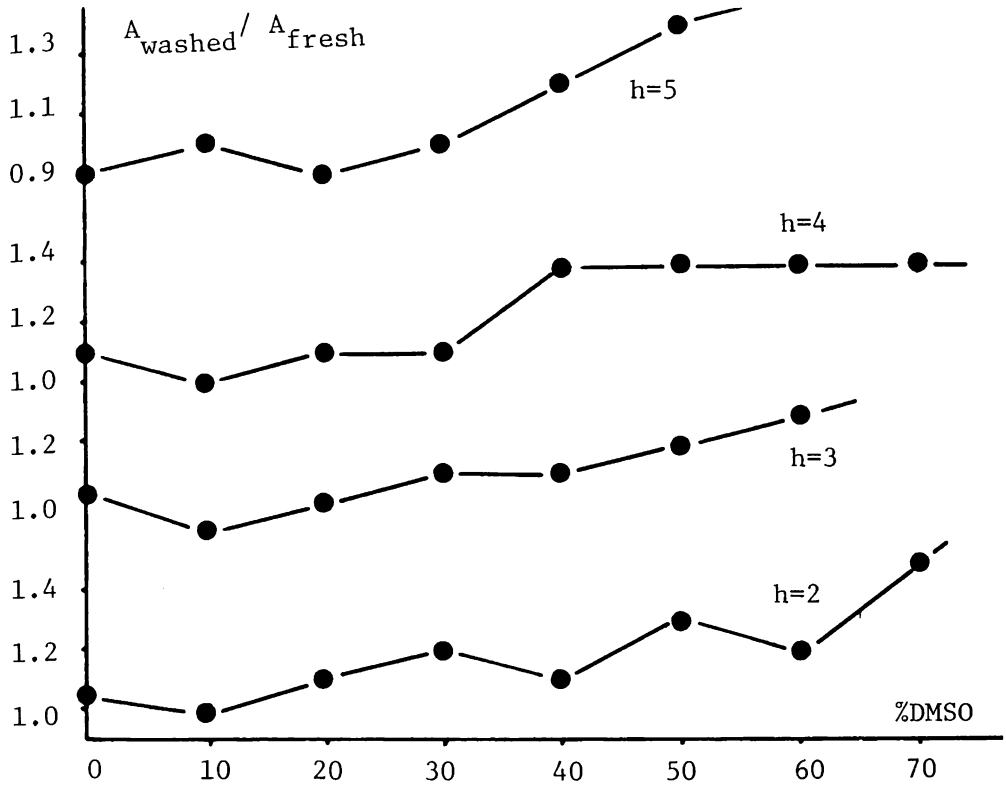

Fig. 3-5 Dependence of the half width of the diffraction spectrum in DMSO treated-and-washed state on DMSO concentration for rabbit sciatic nerve myelin.

washed state above 30% DMSO appears less ordered than the fresh phase.

The above experimental results give the DMSO concentration at which the modification by DMSO becomes irreversible. Below that point, in the treated state the collapsed phase and the native-

like phase which is periodically identical to the fresh phase are observed, and above that concentration a new expanded phase is observed. In an attempt to get the structural correlation among F, N, C and E phases the higher order reflections were recorded by longer exposure.

2) Long exposure experiment

Fig. 3-6 shows the long exposure x-ray diffraction pattern from 20% DMSO treated rabbit sciatic nerve myelin, which was recorded for the nerve sealed in thin walled glass capillary (usually 0.7mm in diameter) with DMSO solution after two hours incubation in bulk DMSO solution at room temperature. Fig. 3-7 shows the diffraction pattern from 40% DMSO treated rabbit sciatic nerve myelin. With 20% DMSO (40% DMSO) solution the collapsed phase showed higher orders up to the 10th (8th) order, in addition to the weak native-like or the expanded phases.

At 20% DMSO concentration, which is within the range of the reversible modification, the collapsed phase with periodicity 125Å occupies 76% of the total diffracting power and the remainder, 24% is the 184Å native-like phase. In contrast, with the 40% DMSO treated nerve the total diffracting power consists of the collapsed phase (119Å, 93%) and the expanded phase (223Å, 7%). Comparison between short and long exposure experiment demonstrates the increase in the amount of the collapsed phase

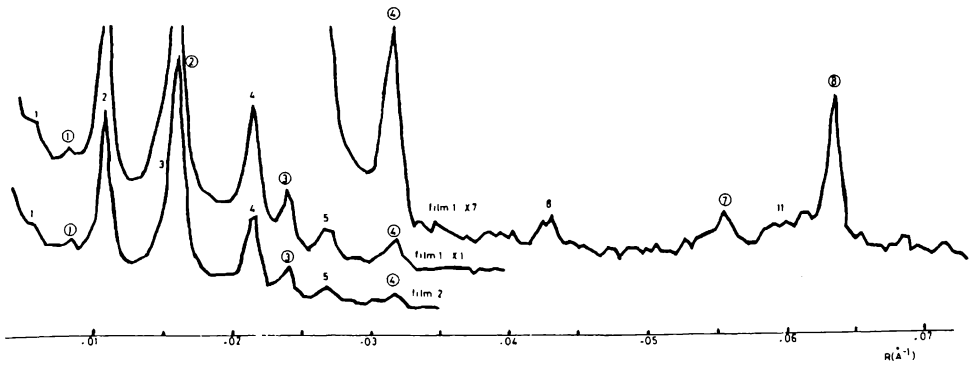

Fig. 3-6 Densitometer tracing vs. diffraction angle for 20% DMSO treated rabbit sciatic nerve myelin.

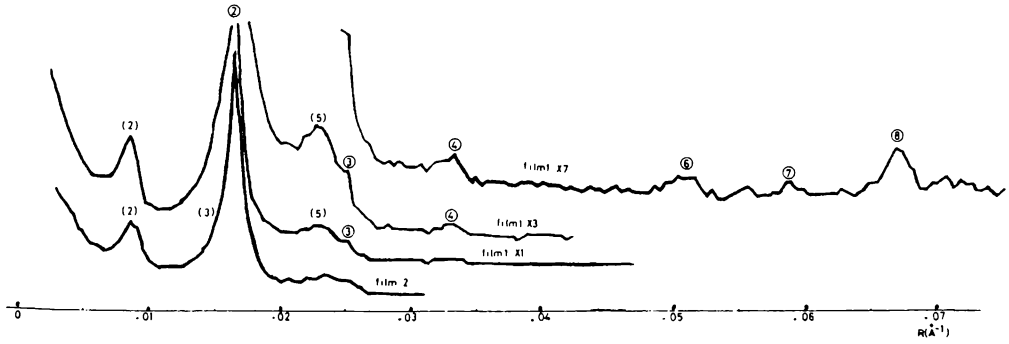

Fig. 3-7 Densitometer tracing vs. diffraction angle for 40% DMSO treated rabbit sciatic nerve myelin.

during the exposure. However no significant change is observed with regard to the periodicities in both phases.

Collapsed phase (C phase)

In Fig. 3-8 (Table 3-3) is depicted the structure factors from the collapsed phase for 20% and 40% DMSO treated nerve myelin against the reciprocal space. They show relatively similar patterns with the exception of the 3rd order reflection which contributes significantly to the electron density distribution. In this comparative study, the structure of the collapsed phase is changed at DMSO concentration where the irreversible modification is introduced, that is, the relative intensity of the odd order reflection in the collapsed phase reduces at 30% DMSO concentration. In the following description the collapsed phase showing stronger odd order reflection is termed C phase and the collapsed phase with weaker odd order reflection is called C' phase.

Native-like phase (N phase)

Fig. 3-9 shows the relative intensity distribution from the native-like phase (N phase) observed below 25% DMSO concentration. At the range from 0% to 25% DMSO, native-like phase shows the constant periodicity (184Å) and occupies from 100% to 15% of the total diffracting power. Because of the superposition of the 3rd

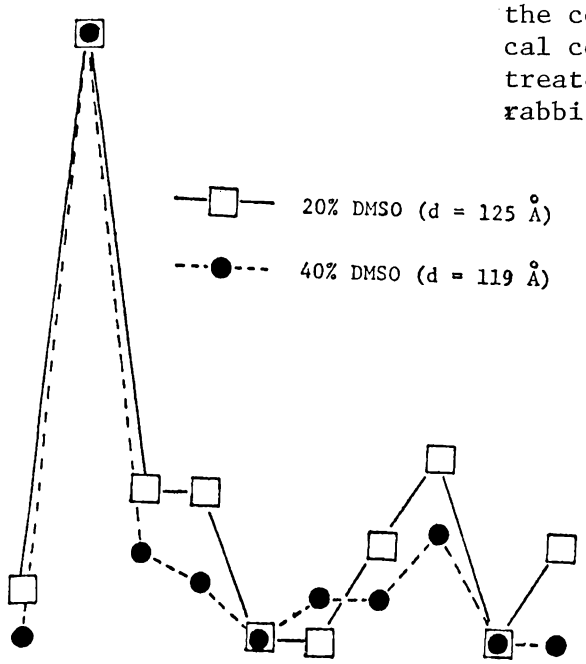

Fig. 3-8 Structure factor of the collapsed phase vs. reciprocal coordinate for 20% DMSO treated and 40% DMSO treated rabbit sciatic nerve myelin.

	20%	40%
d	125Å	119Å
P_c	76%	93%
F(h)		
1	0.08	-
2	1.00	1.06
3	0.24	0.14
4	0.24	0.09
5	-	-
6	-	0.07
7	0.16	0.07
8	0.30	0.18
9	-	-
10	0.16	-

Table 3-3 Periodicity, structure factor and P_c value of the collapsed phase for 20% and for 40% DMSO treated rabbit sciatic nerve myelin.

order of the native-like phase and the 2nd order of the collapsed phase, and of the weakness in intensity of the native-like phase the relative intensities for 2nd, 4th and 5th order reflection are measured as,

$$|F(h)|/\sum|F(h)|$$

where $\sum|F(h)| = |F(2)| + |F(4)| + |F(5)|$ and

$$|F(h)| = \sqrt{I(h)}$$

On increasing DMSO concentration the relative intensity of the 2nd order gradually increases and those of the 4th and 5th order decrease. It is suggested, therefore, that some kind of structural rearrangement should take place in the native-like phase depend on DMSO concentration, with the periodicities being unaltered.

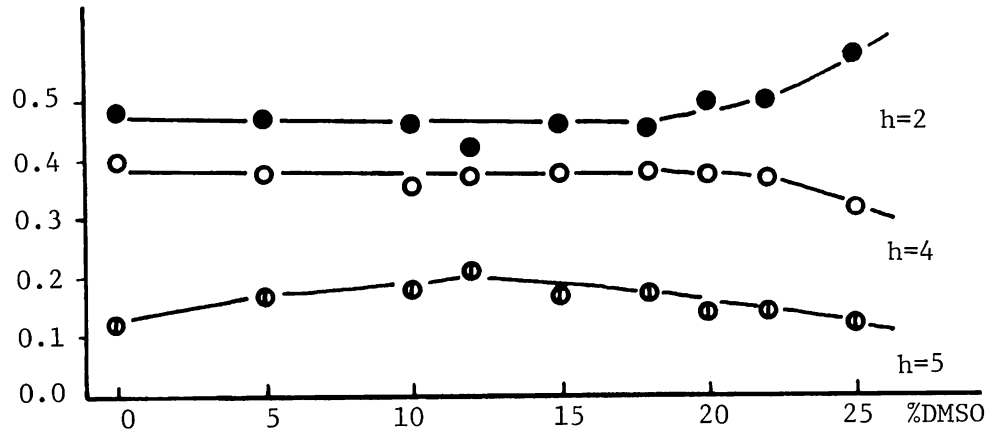

Fig. 3-9 Dependence of the relative intensity of the native-like phase on DMSO concentration for DMSO treated rabbit sciatic nerve myelin.

Expanded phase (E phase)

Above 30% DMSO broad reflections from an expanded phase, 208Å to 224Å, are observed. Long exposure diffraction pattern gives 2nd, 4th and 5th order reflections visibly identified, while the 3rd order reflection is almost superposed by the intense 2nd order reflection of the collapsed phase. At 33% DMSO, the expanded phase (208Å) shows 2nd and 4th order reflection and weak 5th order reflection as I(4)/I(2) is 0.33, on increasing the DMSO concentration 4th order reflection becomes invisible while the 5th order reflection increases, such as, for example at 40% DMSO I(5)/I(2) is 0.19 and I(4)/I(2) is almost zero. Thus the intensity distribution of the reflections from the expanded phase in accordance with the increase of periodicity, is shown to be changed from symmetrical to asymmetrical structure.

3) Wide angle reflection

Fig. 3-10 shows the wide angle reflections from fresh, 20% DMSO treated and 40% DMSO treated nerve. At fresh state the meridionally accentuated broad ring at 4.6Å can be detected and the low angle reflections are visibly identified near the beam stop. At 20% DMSO treated state no vigorous change is observed. At 40% DMSO treated state, however, the broad ring changes to the sharp ring at 4.6Å. Such transformation is associated with the change in the low angle reflections, at 40% DMSO treated state the native phase fades

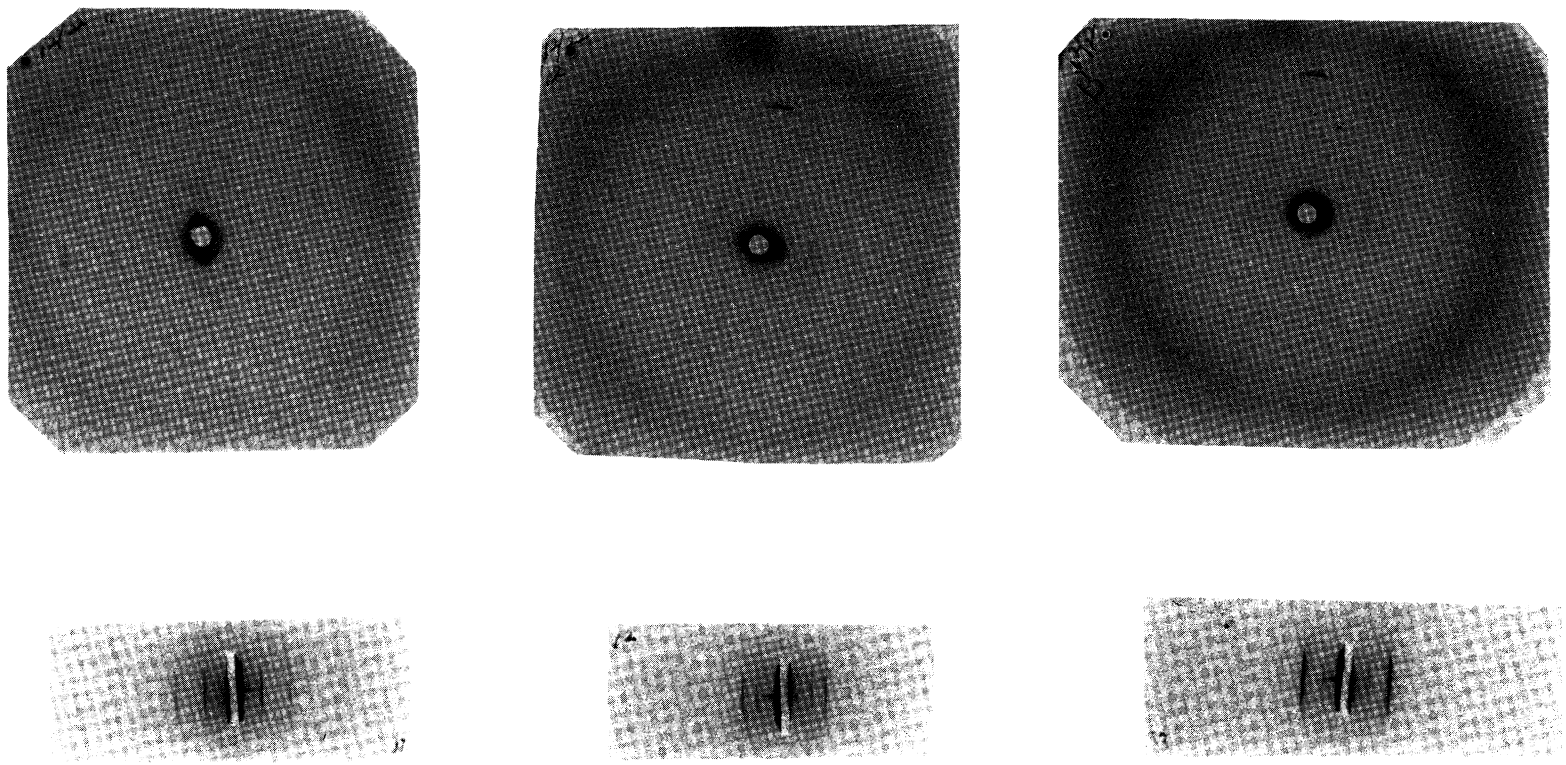

Fresh state 20% DMSO treated state 40% DMSO treated state

Fig. 3-10 Diffraction patterns from the fresh, 20% DMSO treated and 40% DMSO treated rabbit sciatic nerves. Above are given by using Elliot type toroid camera and below by using the single mirror Franks camera.

away and the expanded phase emerges.

These results clearly show the critical rearrangement in the packing of the hydrocarbon chains in membrane at the DMSO concentration where reversible-to-irreversible transformation is induced.

4) Electron density distribution

DMSO treated-and-washed nerve

Because of the quasi fresh pattern given by the washed state , sign relations for the diffraction spectra were assigned so that the density profiles correspond with membrane bilayer profiles of other peripheral nerve myelin, that is + + - - were assigned for 2nd, 3rd, 4th and 5th order reflections. Fig. 3-11 shows the density profiles by applying all combinations of sign relation, for example, in 40% DMSO treated-and-washed state.

Fig. 3-12 shows the low resolution electron density distribution profiles for washed state after 0%, 20%, 40% and 70% DMSO treatment, respectively. Each structure factor was calculated by the intensity data up to the 5th order reflection, recorded in short exposure experiment.

Between 0% and 20% DMSO treated-and-washed pattern there is no significant change in the electron density profiles, while for 40% DMSO treated-and-washed pattern the slight increase in periodicity (3Å) is ascribed to the separation at the cytoplasmic

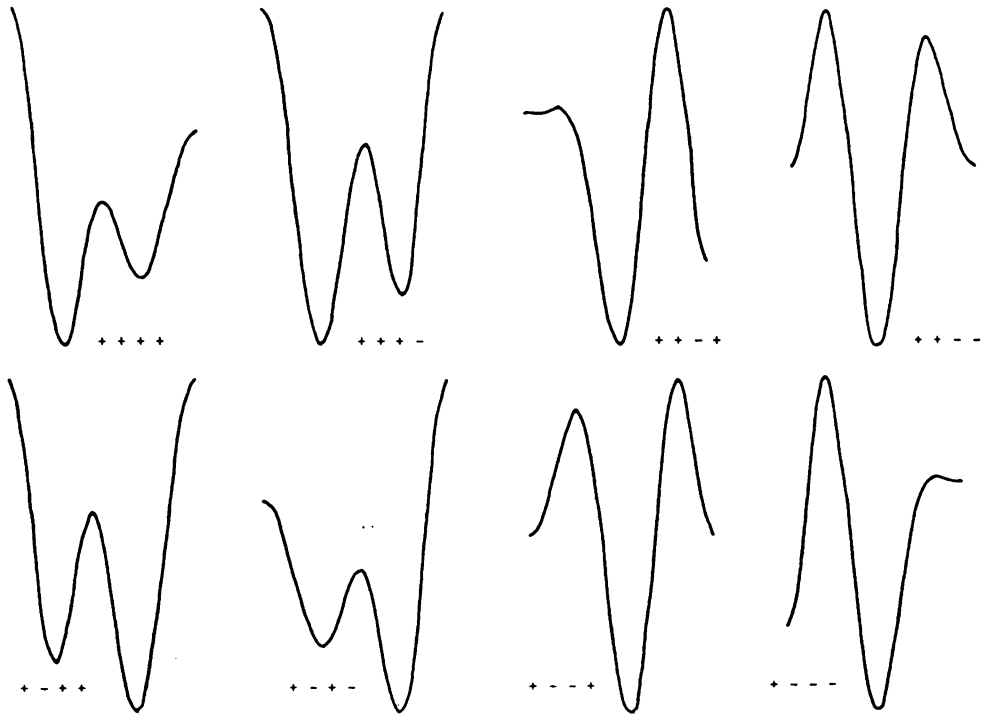

Fig. 3-11 Calculated electron density profiles with all sign relations of myelin membrane unit for 40% DMSO treated-and-washed rabbit sciatic nerve myelin.

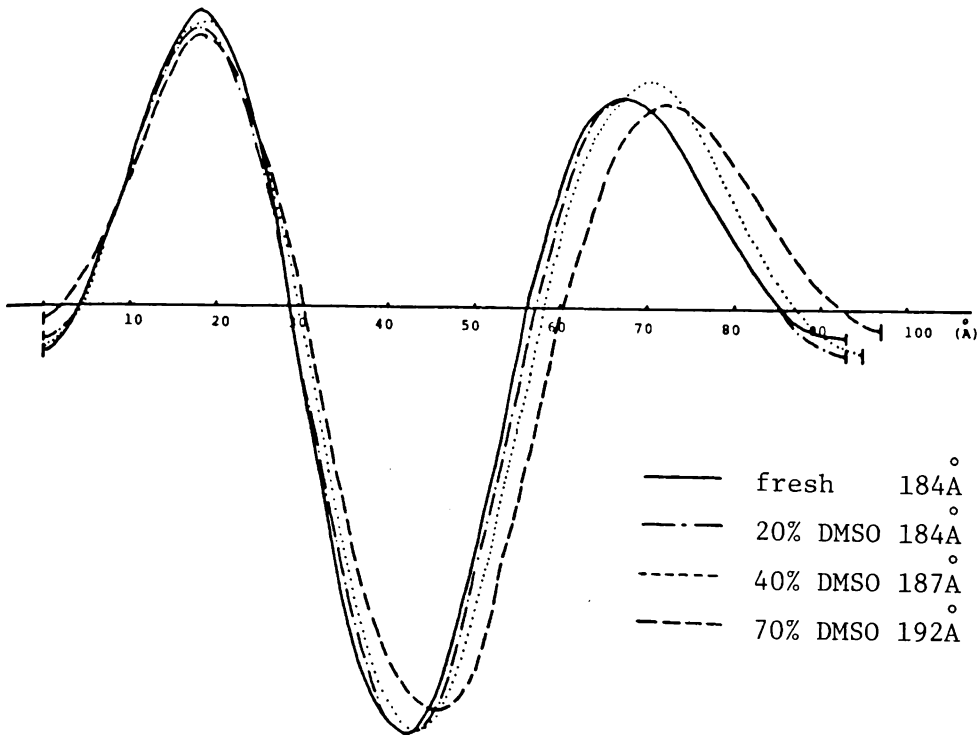

Fig. 3-12 Calculated electron density profiles of myelin membrane units for fresh, 20% DMSO treated-and-washed, 40% DMSO treated-and -washed and 70% DMSO treated-and-washed rabbit sciatic nerve myelin as a function of distance from the cytoplasmic boundary.

boundary and the center to center separation of the high density peaks. On increasing the concentration of the DMSO solution, for 70% treated-and-washed state, which is 192Å in period, this expansion is mainly due to the center to center separation. Moreover the ratio between high density peaks of the electron density at cytoplasmic boundary and at the external boundary is markedly reduced than that for the fresh case, which means the membrane structure becomes symmetric in the washed state after 70% DMSO treatment.

In addition the high density components residing at the cytoplasmic boundary which contributes to the membrane asymmetry could be changed by the DMSO treatment in their conformation or distribution on the membrane surface.

Collapsed phase

The electron density profiles of the collapsed phases in 20 % DMSO and 40% DMSO treated nerve were studied. The sign relations for the diffraction spectra were chosen so that the density profiles show the existence of the lipid bilayer as given in the reported density profiles, that is + + - - were assigned for the 2nd, 3rd, 4th and 8th order reflections. Structure factors were calculated by the intensities of the 2nd, 3rd, 4th and 8th order reflections,which were recorded in the long exposure experiment. Fig. 3-13 shows the density profiles by applying all combina-

Fig. 3-13 Calculated electron density profiles with all sign relations of myelin membrane units for the collapsed phase from the 20% DMSO treated rabbit sciatic nerve myelin.

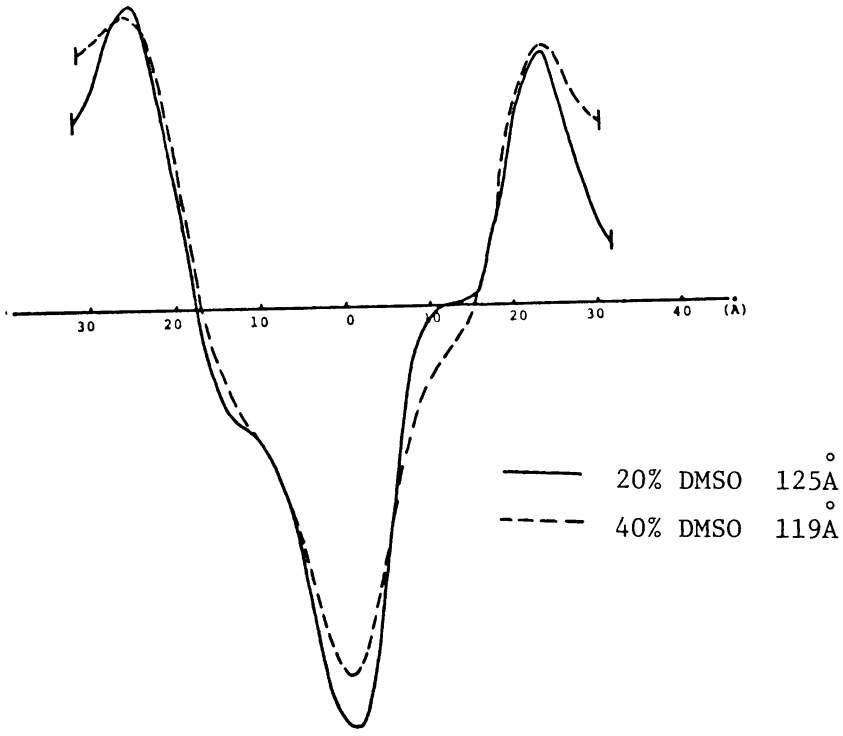

Fig. 3-14 Calculated electron density profiles of myelin membrane units for the collapsed phase from the 20% DMSO treated and 40% DMSO treated rabbit sciatic nerve myelin.

tions of sign relation in the case of the 20% DMSO treated nerve.

Fig. 3-14 shows the electron density profiles of the collapsed phases in 20% DMSO (125Å) and 40% DMSO (119Å) treated state, which are superposed with each other at the corresponding high density lipid polar group and the base lines. The separation between high density peaks is almost the same in both samples, as 47.5Å for 20% DMSO treated nerve and 47.6Å for 40% DMSO treated nerve. So the difference in periodicity (6Å) is due to the difference in the cytoplasmic and the external space. Of interest in the density profile is the remarkable bump at the central area of the lipid hydrocarbon chain which is located in the C phase from 20% DMSO treated nerve. Whereas there is no remarkable bump in the 40% DMSO treated nerve.

5) Summary of the experimental results

On the rabbit sciatic nerve immediately removed from the rabbit, DMSO effect was investigated taking account of the spontaneous denaturation. Using the nerve stored in Ringer's solution at 4°C overnight the response to the DMSO effect was quite different from that observed in freshly dissected nerve. So this experiment were made in two steps, the short exposure experiment using the same nerve to check the dependence of the reversible or irreversible modification on the DMSO concentration and the long exposure experiment to observe the higher order and weak

reflections. Through these experiments the effect of DMSO was given as below.

1. In the treatment with DMSO solution the collapsed phase is first observed at 10% DMSO concentration.

2. At the range frome 10% to 30% DMSO concentration, native-like phase (N phase) and the collapsed phase (C phase) coexist, the N phase is identical to the fresh nerve in periodicity, while the intensity distribution is different. The C phase shows approximately 120Å periodicity which gradually reduces with DMSO concentration. The 2nd order reflection is quite intense and the 3rd order is visible. On washing the treated nerve in normal Ringer's solution the fresh pattern is completely restored within this region.

3. Above the 40% DMSO treatment, the native-like phase is replaced by the expanded phase, whose periodicity is about 206Å and increases with DMSO concentration. Intensity distribution of this phase indicates the asymmetrical structure. On washing in Ringer's solution, the F' phase is obtained, which is a little expanded in periodicity than the fresh pattern, and with respect to the intensity distribution, odd order reflections are less intense than the fresh pattern. Half widths of the reflections from the F' phase show that it is more disordered than F phase.

4. In the treated state, at the critical concentration, the packing of the hydrocarbon chain is changed to a more ordered

state, which was demonstrated by the wide angle reflection at $4.6\mathring{A}$.

5. Schematically C and N phase in the treated state are replaced by C' and E phase at a certain concentration between 30% and 40% DMSO solution, at which on washing F phase turns to F' phase in the irreversible way.

reversible $F \rightleftharpoons N$, C

irreversible $F \longrightarrow E$, $C' \rightarrow F'$

3-3 Acetone effect on rabbit sciatic nerve

A. Experiment

Acetone effect is investigated in the same way as the DMSO experiment to compare the both effects.

B. Results

1) Short exposure experiment

Fig. 3-15 shows the densitometer traces of one series of 20 % acetone experiment on the same nerve, that is , fresh, treated and treated-and-washed state, whose diffraction pattern is recorded for one hour exposure. In short exposure experiment the reflections (2nd, 3rd, 4th and 5th order) were detected in fresh and treated-and-washed states, and the 2nd order reflection from the collapsed phase in the treated state. General view of the diffraction patterns in acetone treated or acetone treated-and-washed state corresponds well to that observed in the DMSO treatment experiment. In the same way as described in the case of DMSO treatment, periodicity, structure factor, diffracting power and half width were calculated from the densitometer traces.

Periodicity

In Fig. 3-16 and Table 3-4 are depicted the periodicities of the observable phases for one hour exposure in the treated (marked

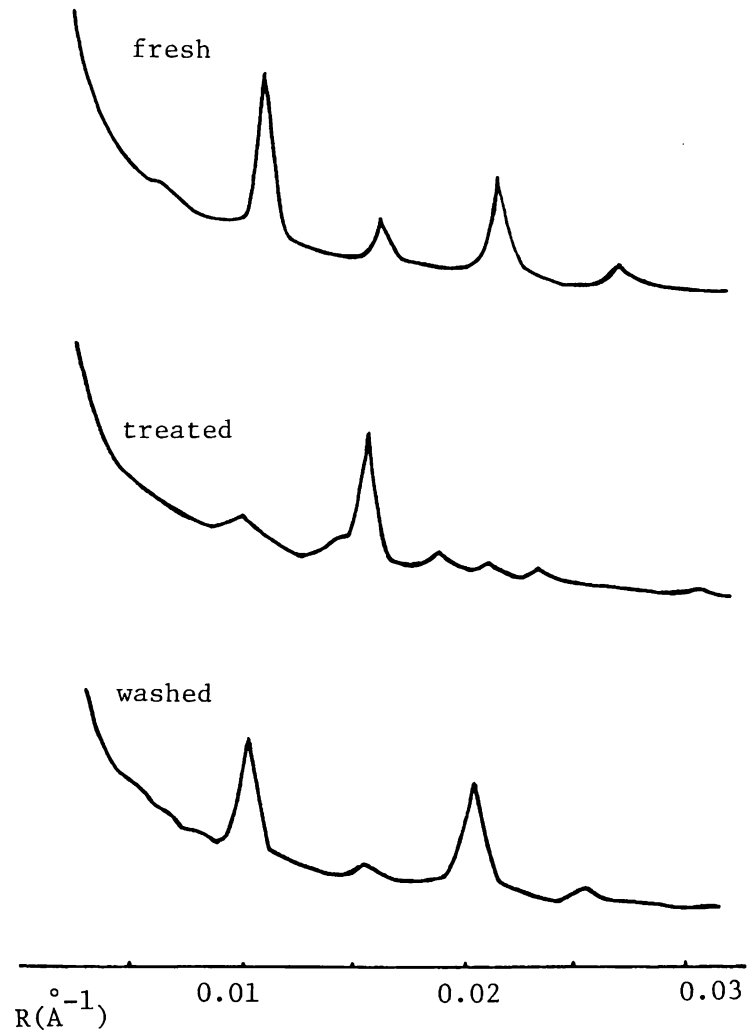

Fig. 3-15 Densitometer tracings vs. diffraction angle for the fresh, 20% acetone treated and 20% acetone treated-and-washed rabbit sciatic nerve myelin.

in circle) and the treated-and-washed state (marked in square).

In the treatment with acetone, at 10% acetone no modification can be observed in x-ray diffraction, whereas above 20% the collapsed and the expanded phase emerge and are detected. As acetone concentration increases, the periodicity of the collapsed phase decreases from 128Å at 20% acetone to 119Å at 50% acetone, while periodicity of the expanded phase increases from 212Å at 20% to 216Å at 30% acetone. At 20% acetone the 2nd reflection of the fresh like phase in period (189Å) can be seen in addition.

On washing the nerve for one hour after one hour exposure for recording the diffraction from fresh state, 2 hours treatment in acetone solution and one hour exposure for treated state, at 10% acetone the periodicity is recorded to be identical to the fresh state. Above 20% acetone the treated-and-washed state gives the reflections of the slightly expanded phase, of which periodicity increases with the concentration in such way that it varies from 192Å at 20% to 198Å at 50% acetone. So periodically, 20% acetone is the critical concentration at which reversible modification turns to irreversible modification in this short exposure experimental system.

Diffracting power of C phase in the treated state

Fig. 3-17 shows the dependence of the diffracting power of the collapsed phase in the treated state on the acetone concen-

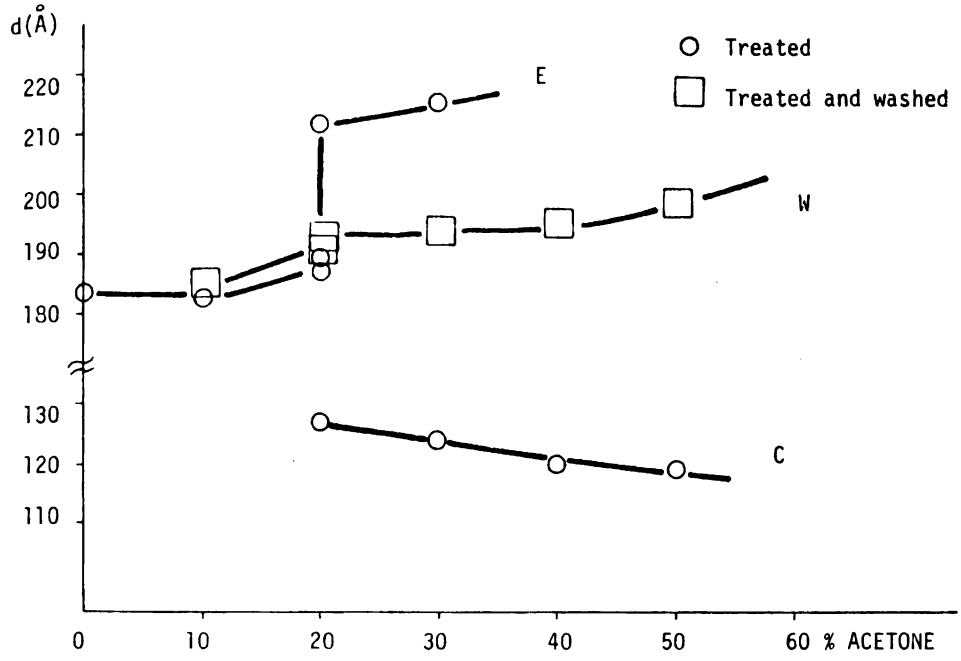

Fig. 3-16 Dependence on acetone concentration of the native-like phase, of the collapsed phase and of the expanded phase in the acetone treated state and of the washed phase in the acetone treated-and-washed state for rabbit sciatic nerve myelin.

Table 3-4 Periodicity of rabbit sciatic myelin membrane in fresh, acetone treated and acetone treated-and-washed state.

Acetone(%)	10	20	30	40	50
Fresh	184.0	184.0	184.0	184.0	184.0
Treated	182.5	188.7 212.0 127.5	215.8 124.2	- 119.5	- 119.1
Washed	185.2	192.1	193.7	195.0	197.9

tration, whose value is normalized so that the total diffracting power becomes 1.0 . At 20% acetone concentration the newly appeared collapsed phase attains 72% of the total diffracting power and above that concentration the collapsed phase gradually approaches to 100%. Practically at 40% acetone concentration it is quite difficult to measure the integrated intensity in the effective way.

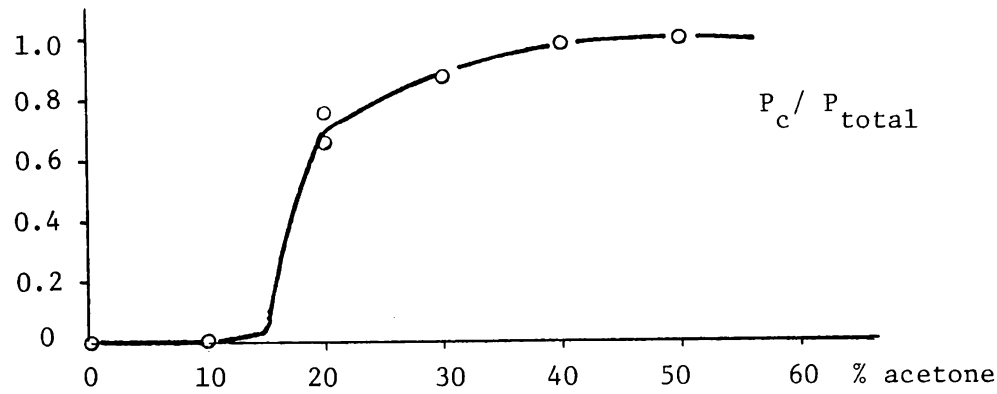

Fig. 3-17 Dependence of the diffracting power of the collapsed phase in the acetone treated state on acetone concentration for rabbit sciatic nerve myelin. Vertical axis shows the diffracting power ratio of the C phase to the total diffracting power.

Structure factors for acetone treated-and-washed rabbit sciatic nerve

In Fig. 3-18 and Table 3-5 are depicted the structure factors for the reflections in the washed state. Up to 10% concentration the structure factor is almost equal to that of the

fresh state. Above the critical 20% concentration the 3rd and the 5th order reflections decrease in intensity and in the concomitant way the 4th order reflection is relatively intensified.

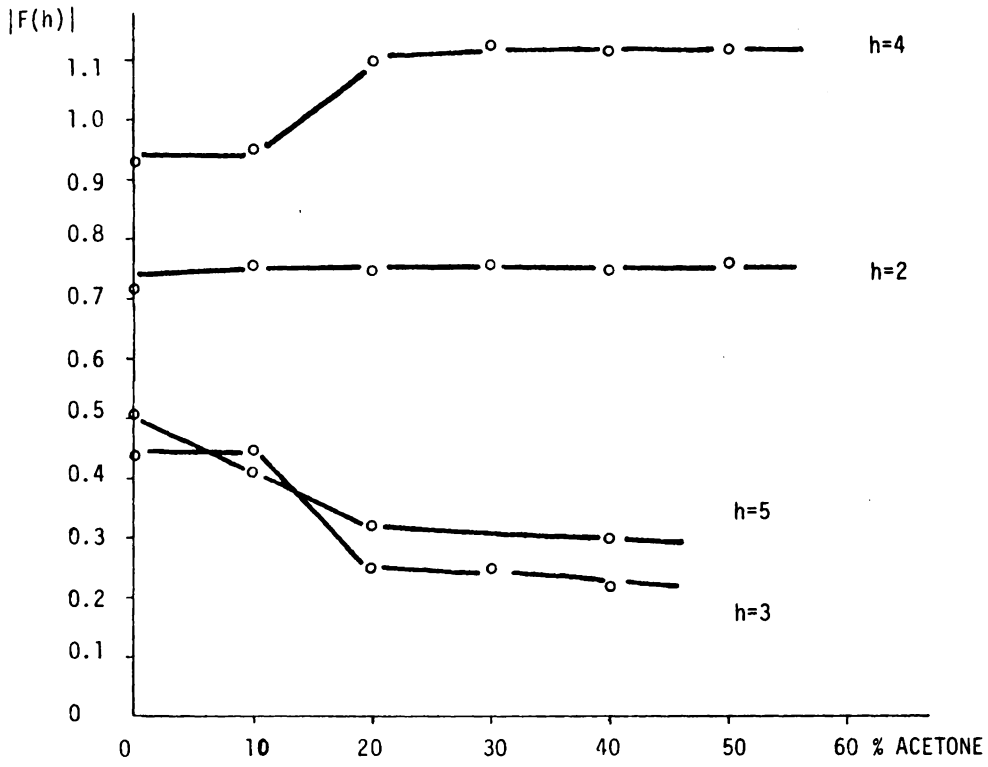

Fig. 3-18 Dependence of the structure factor in the acetone treated-and-washed state of rabbit sciatic nerve myelin on acetone concentration.

Table 3-5 Structure factor of rabbit sciatic myelin membrane in acetone treated-and-washed state at different acetone concentration.

% acetone	|F(2)|	|F(3)|	|F(4)|	|F(5)|
0	0.75	0.44	0.93	0.47
10	0.76	0.45	0.95	0.41
20	0.74	0.29	1.08	0.34
30	0.76	0.25	1.14	-
40	0.75	0.23	1.12	0.30
50	0.77	0.37	1.12	-

Half width broadening in the washed state of rabbit sciatic nerve

Fig. 3-19 shows the dependence of the half width of each reflection in the washed state on the acetone concentration. Half width of each reflection is given in the relative scale to that observed in the fresh state. Beyond the critical concentration at 20% acetone the half width of each reflection increases with the trend that the higher order reflection broadens more than the lower order reflection.

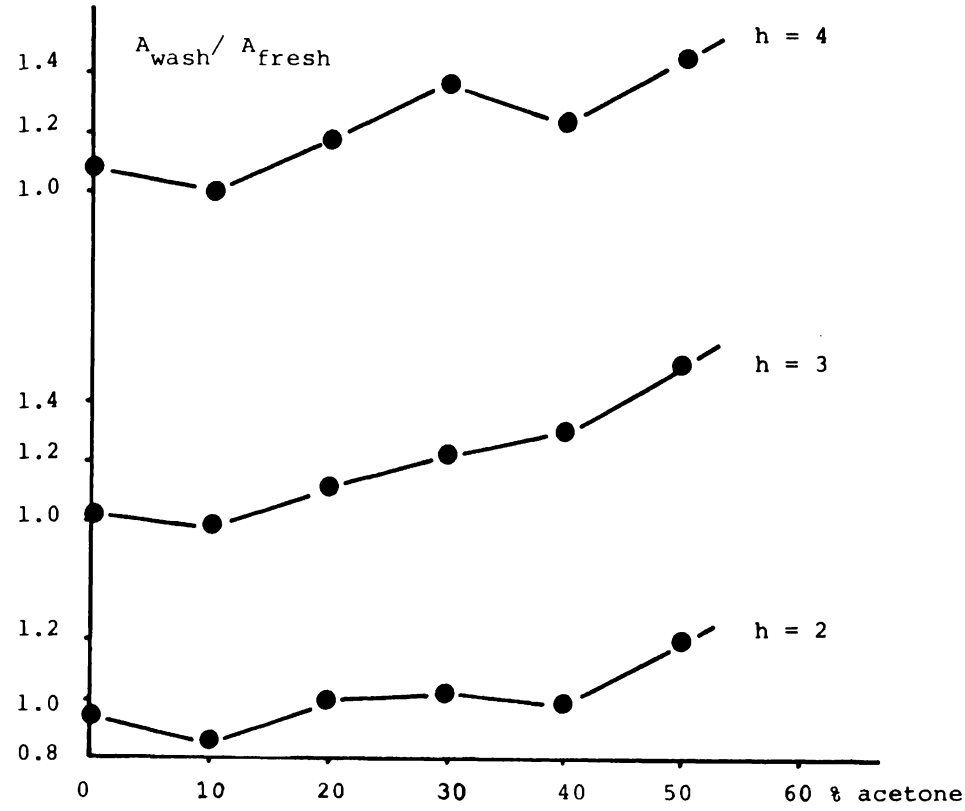

Fig. 3-19 Dependence of the half width of diffraction spectrum in the acetone treated-and-washed state on acetone concentration for rabbit sciatic nerve myelin.

In the short exposure experiment given above it is established that the acetone irreversibly modifies the nerve myelin above 20% acetone concentration. With attention to the structural relationship between fresh phase, expanded phase, collapsed phase and quasi fresh phase (in the washed state), a long exposure experiment was carried out.

2) Long exposure experiment

Fig. 3-20 shows the long exposure x-ray diffraction pattern from 20% acetone treated rabbit sciatic nerve, which was recorded for the nerve sealed in thin walled glass capillary tube with immersion medium after 2 hours' incubation in bulk acetone solution at room temperature. In this densitometer trace there appear three phases, the collapsed phase (128Å), the native-like phase (184Å) and the expanded phase (190Å), whose diffracting powers are 83%, 13% and 4%, respectively, of the total value. During the long exposure 20% acetone induces more collapsed phase than in the short exposure experiment.

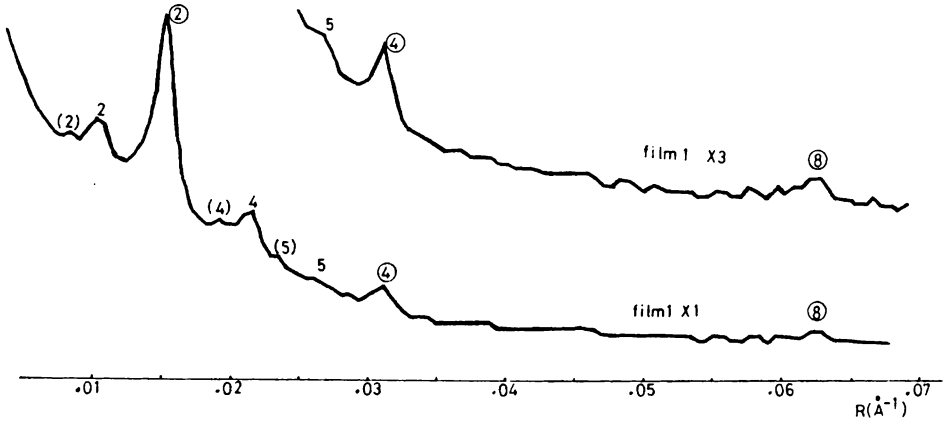

Fig. 3-20 Densitometer tracing vs. diffraction angle for 20% acetone treated rabbit sciatic nerve myelin.

In Fig. 3-21 (Table 3-6) is depicted the structure factor of the collapsed phase from the 20% acetone treated nerve myelin, which shows only measurable even order reflections, as $|F(2)| = 1.00$, $|F(4)| = 0.47$ and $|F(8)| = 0.29$. In 20% acetone treated nerve 190Å expanded phase shows the relatively equal intensity of each reflection. On increasing the acetone concentration or incubation time, the intensities of the 2nd and 4th order reflection decrease and reversely the 3rd and 5th order reflections intensify.

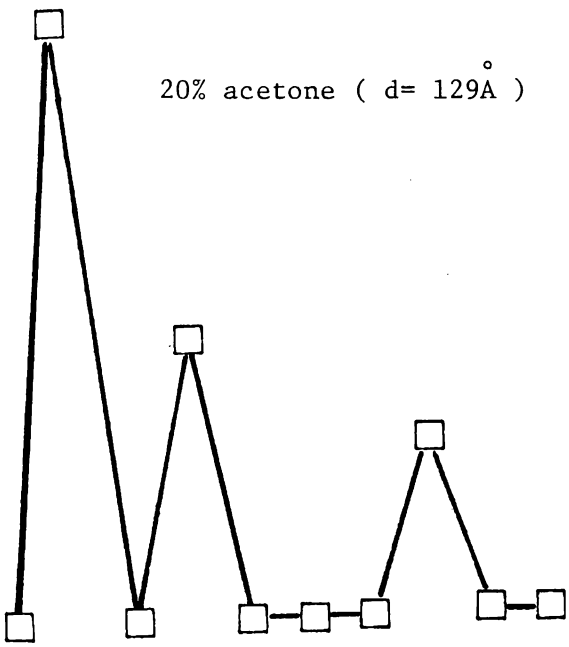

d	129Å
P_c	86%
F(h)	
1	-
2	1.00
3	-
4	0.47
5	-
6	-
7	-
8	0.29

Fig. 3-21 (Table 3-6) Structure factor of the collapsed phase vs. reciprocal coordinate for 20% acetone treated rabbit sciatic nerve myelin.

3) Electron density distribution

Acetone treated-and-washed nerve

Fig. 3-23 shows the electron density profiles for acetone treated-and-washed state which are calculated using up to 5th order reflections. On the same reason as in the case of DMSO treated-and-washed nerve the sign is assigned to as + + - - for the 2nd, 3rd, 4th and 5th order reflection, respectively. Density profiles calculated by all combinations of sign relation are shown in Fig. 3-22 for example in the case of 40% acetone treated-and-washed nerve.

On increasing the acetone concentration the periodicity of the washed phase gradually increases. From the low resolution electron density profile the separation between center to center high dense peaks and the separation at cytoplasmic boundary contribute to that periodical expansion. For example in the fresh state the cytoplasmic space is about 35Å width while in 40% acetone treated-and-washed sample 42Å can be calculated. Center separation expands from about 49Å at the fresh state to 53Å at the washed state. In both acetone treatments the separation of the external space gives almost an identical (48Å) to the separation observed in the fresh state (52Å).

Thus it is suggested that the myelin structure in the washed state is mainly modified at the cytoplasmic side.

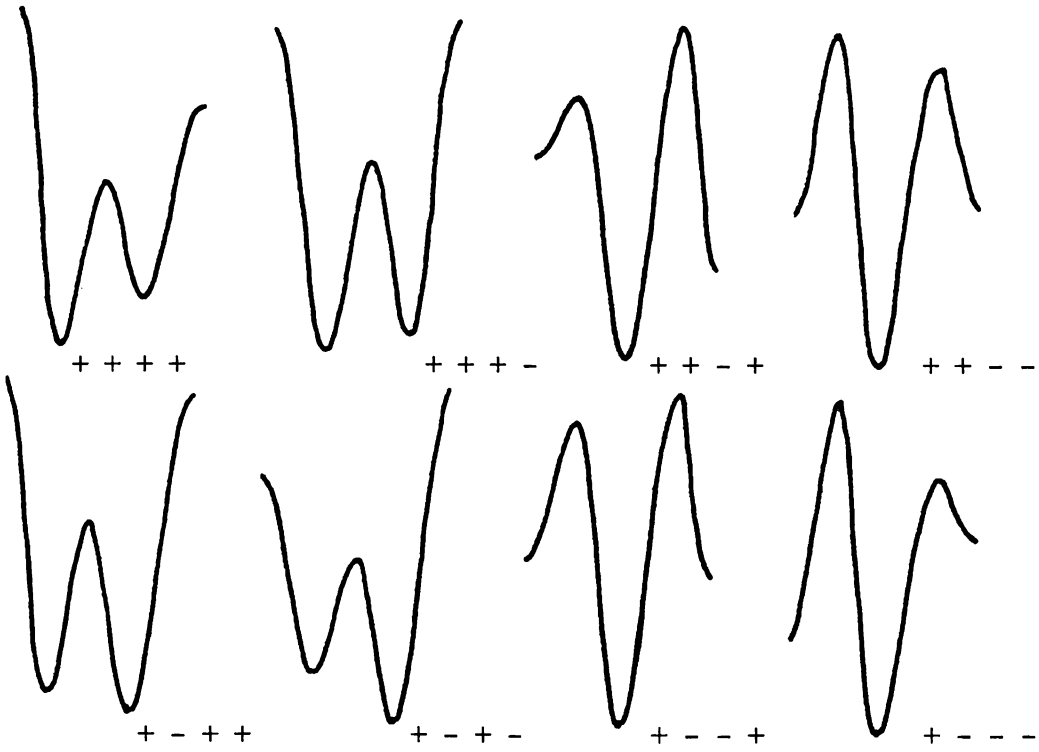

Fig. 3-22 Calculated electron density profiles with all sign relations of myelin membrane units for 40% acetone treated-and-washed rabbit sciatic nerve myelin.

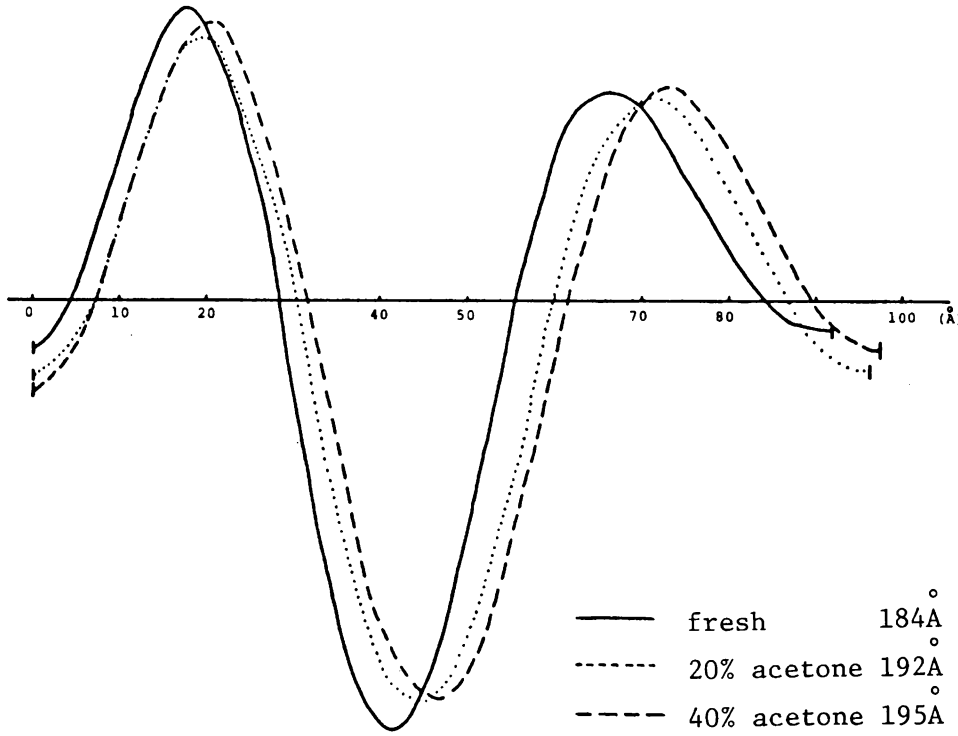

Fig. 3-23 Calculated electron density profiles of myelin membrane units for the fresh, 20% acetone treated-and-washed, and 40% acetone treated-and-washed rabbit sciatic nerve as a function of distance from the cytoplasmic boundary.

Collapsed phase

On the same reason as described in the former section the sign relations for the diffraction spectra were assigned as + - - for the 2nd, 4th and 8th order,respectively, which were observed in the collapsed phase (129Å) from the long exposure experiment. Fig. 3-24 shows the density profiles calculated by assigning all combinations of sign relation for 20% acetone treated state. Fig. 3-25 shows the density profile in arbitary unit. The separation between high dense peak to peak is 47.7Å long and the width of the extracellular or cytoplasmic space is 16.8Å long. Remarkable feature is that there is no bump at the center of the lipid bilayer, which was detected in that from 20% DMSO treated nerve.

4) Summary of the experimental results

To distinguish the acetone effect on the nerve myelin from the natural degeneration, the short exposure experiment in specimen chamber was carried out at first, then the long exposure experiment in capillary tube was performed to detect the higher order reflections for getting detailed structure. In the former experiment using the same nerve, periodicity, diffracting power , half width and structure factor were calculated and those parameters provided the framework of the acetone effect on nerve myelin. The long exposure experiment revealed the detailed structure of

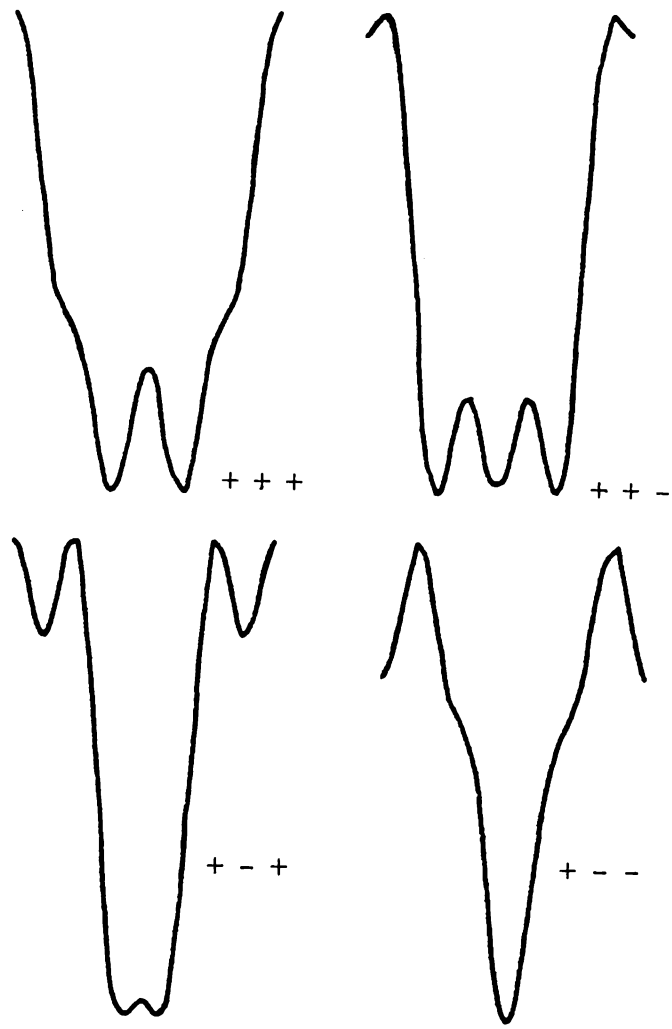

Fig. 3-24 Calculated electron density profiles with all sign relations of myelin membrane units for the collapsed phase from 20% acetone treated rabbit sciatic nerve myelin.

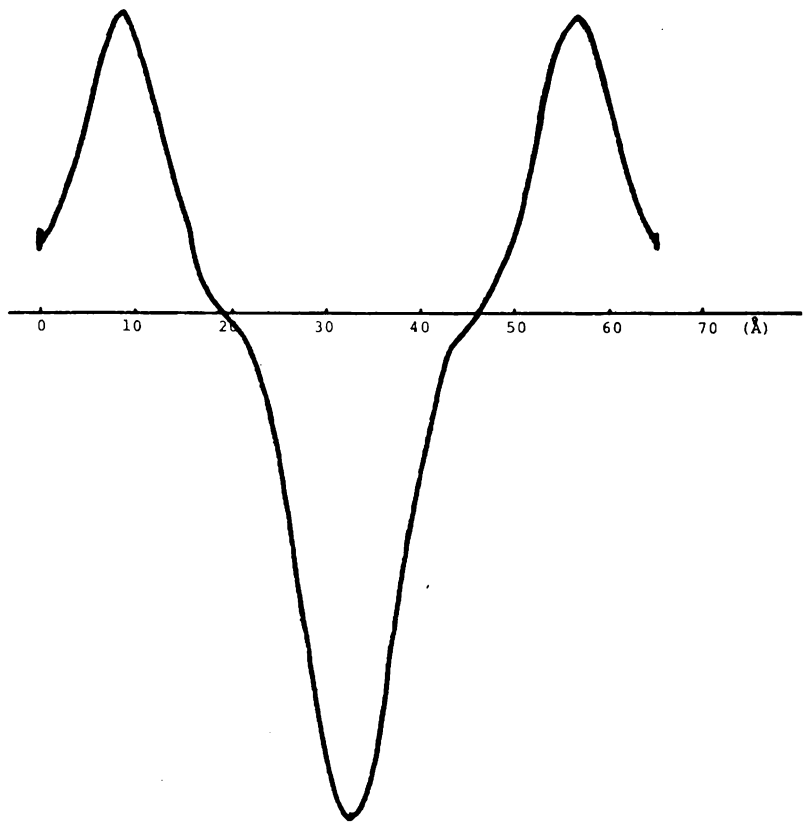

Fig. 3-25 Calculated electron density profile of myelin membrane unit for the collapsed phase from 20% acetone treated rabbit sciatic nerve myelin.

the detected phase.

1. In the treated state up to 10% acetone concentration, there appears no new phase to be detected, however beyond the critical point, 20% acetone, the collapsed phase and the expanded phase coexisting with native-like phase come to appear and as the acetone concentration increases, the expanded phase becomes more expanded in periodical distance, the collapsed phase shrinks in period and the native-like phase fades away. The collapsed phase was shown to have no odd orders and the expanded phase, gradually expanding, turned to be a more asymmetric structure.

2. On washing the treated nerve in Ringer's solution following the acetone treatment, up to 10% concentration fully restoration to normal fresh pattern was observed, whereas in the treatment with acetone above that concentration quasi fresh pattern was recorded, which wa expanded in periodicity and showed weak odd order reflections compared with those of fresh state. In addition, the washed phase structure is disordered.

3-4 Glutaraldehyde effect on rabbit sciatic nerve

A. Experiment

Sciatic nerves were removed from the freshly killed rabbit. Sections of the nerve were treated by immersion in bulk 0.025% glutaraldehyde (G.A.) in Ringer's solution at room temperature. After incubation for a predetermined time the nerve section was sealed into capillary tube and mounted on an x-ray camera with Franks type single mirror focussing. Exposures were routinely for 2 hours. All experimental procedures were carriedout at room temperature. Mammalian Ringer's solution is composed of NaCl 860mg, KCl 30mg, $CaCl_2 2H_2O$ 33mg in 100ml total volume. Glutaraldehyde solution was prepared just before use by dissolution of the 25% glutaraldehyde solution (Nakarai Chemicals, LTD., without further purification) in mammalian Ringer's solution. X-ray diffraction intensity and periodicity were measured using a Syntex AD-1 Autodensitometer.

B. Results

Fig. 3-26 shows the densitometer tracings of the diffraction patterns against the incubation time at room temperature in 0.025% glutaraldehyde solution. After 4 hours incubation a diffraction pattern different from the fresh pattern was obtained, which showed the existence of two phases, one of which is a fresh-like

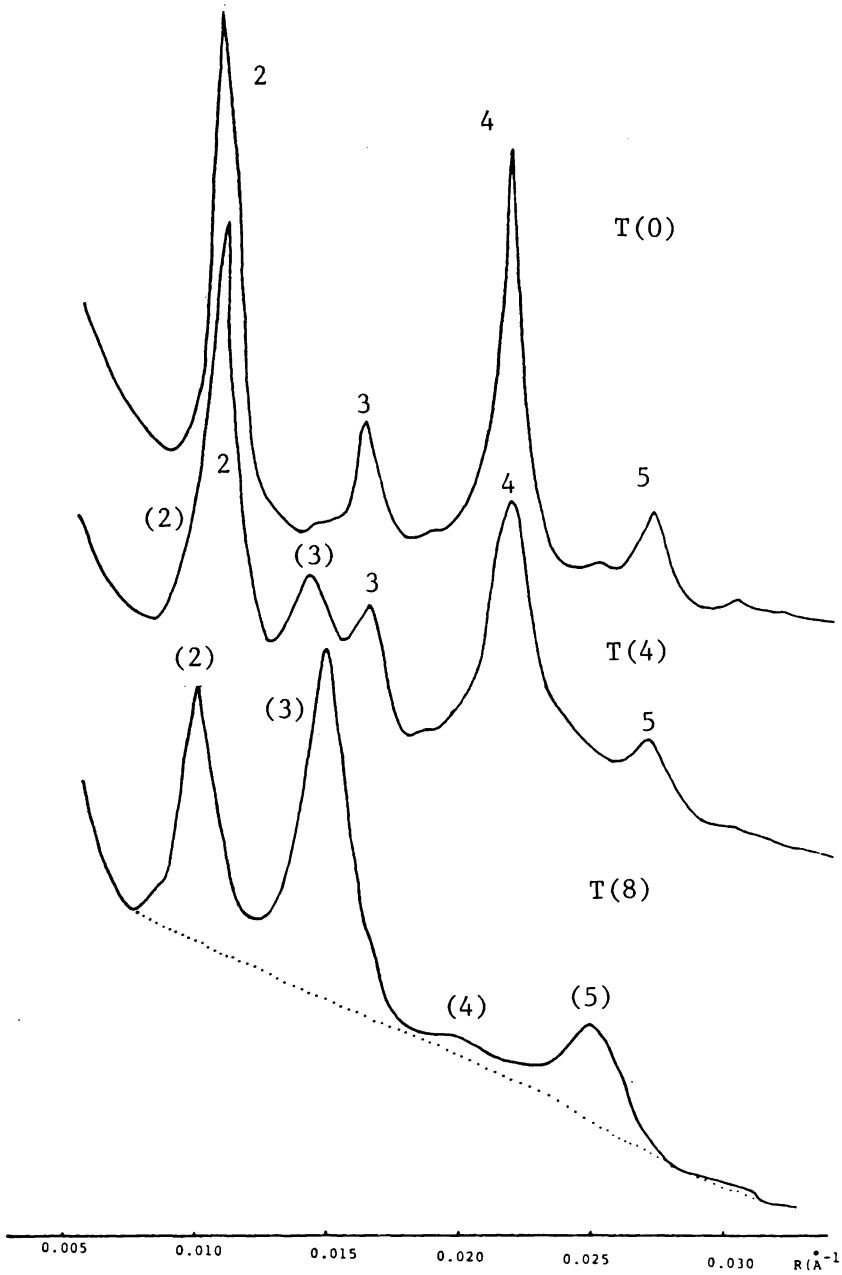

Fig. 3-26 Densitometer tracings vs. diffraction angle for 0.025% glutaraldehyde treated rabbit sciatic nerve myelin after different hours of incubation.

phase and the other a periodically expanded phase. On increasing the incubation time to 8 hours the new phase completely replaces the native phase and washing procedure into Ringer's solution gives no change on the newly appeared diffraction pattern.

In Fig. 3-27 is depicted the diffracting power ratio aginst the incubation time. After 4 hours, 16% of the total diffracting power is occupied by the expanded phase (G phase) whose periodicity is 207Å. On increasing the incubation time the G phase becomes dominant and a little shrinks to 197Å at 8 hours which keeps constant to 20 hours. The structure factor of the reflections from the G phase is given in Table 3-7, which suggests the intense odd order reflections. On the other hand the structure factor of native-like phase coexisting with the G phase at 4 hours also shows a structural modification induced by glutaraldehyde, even though it is identical to the fresh pattern in the periodicity.

The solution with higher concentration of glutaraldehyde modifies the structure of nerve myelin faster than that of lower concentration.

C. Electron dinsity distribution

Fig. 3-28 shows the electron density profiles from glutaraldehyde treated rabbit sciatic nerve. There is no unique information about the assignment of the sign to each reflection, so all combinations were calculated and appropriate profiles were

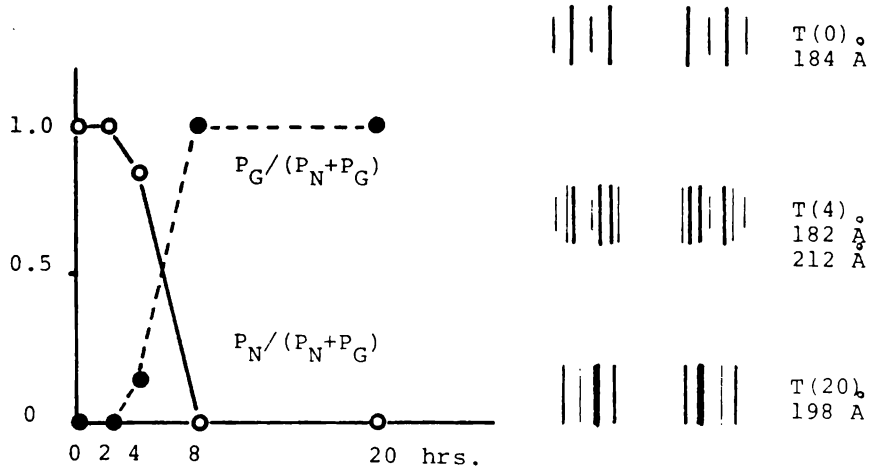

Fig. 3-27 Dependence of the diffracting power of the glutaraldehyde fixed phase on the incubation time. Schematic drawings of the diffraction pattern for glutaraldehyde treated rabbit sciatic nerve myelin after different hours of incubation.

Table 3-7 Periodicity and structure factor of the native phase and of the new phase for 0.025% glutaraldehyde treated rabbit sciatic nerve myelin after different hours of incubation.

incubation time (hrs.)	0	2	4		8	20
periodical distance (Å)	184	183	183	207	197	198
|F(h)|						
2	0.75	0.76	0.69	0.53	0.60	0.57
3	0.44	0.44	0.47	1.13	1.01	1.03
4	0.93	0.93	0.93	-	0.22	0.24
5	0.47	0.43	0.51	0.72	0.74	0.73

selected which clearly showed the existence of the lipid bilayer. In this way the phase of each reflection was determined as, + + - - , for the 2nd, 3rd, 4th and 5th order reflection, respectively.

Fig. 3-29 shows the density profiles of the glutaraldehyde treated and fresh nerve by superposing at the base line, whereby measuring the distance in the cytoplasmic, lipid bilayer and extracellular space. In comparison with the fresh profile, it is shown that the shrinkage in the cytoplasmic space by 7Å and the expansion in the extracellular space by 19Å. While the constant value in the lipid bilayer region can be detected.

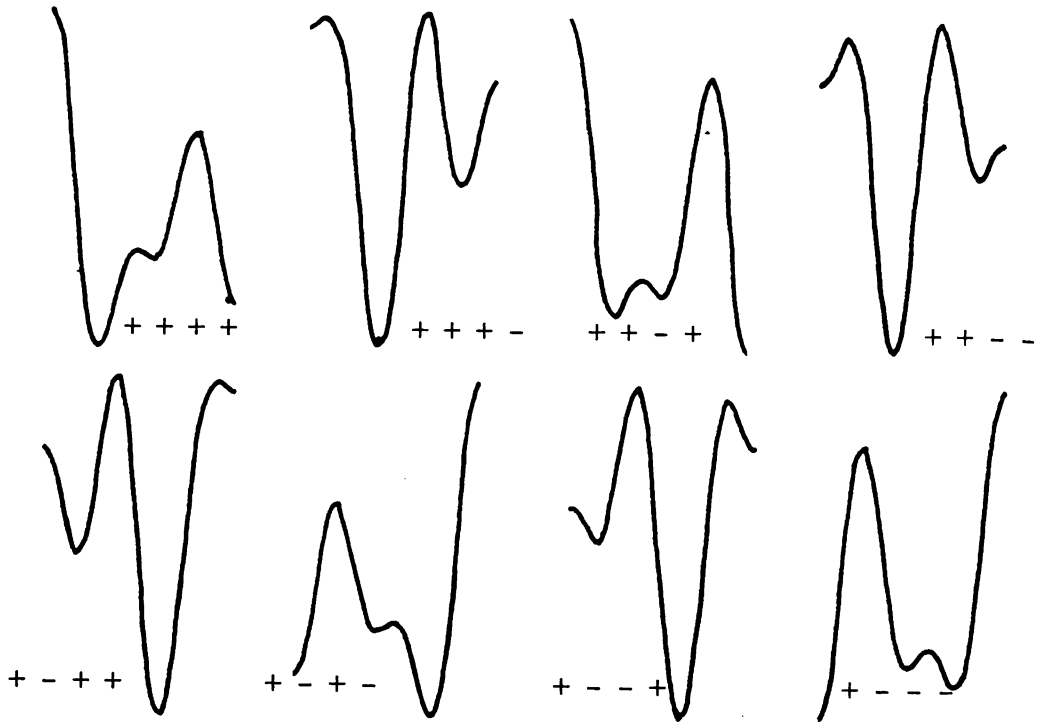

Fig. 3-28 Calculated electron density profiles with all sign relations of myelin membrane units for the glutaraldehyde fixed phase from 0.025% glutaraldehyde treated rabbit sciatic nerve myelin.

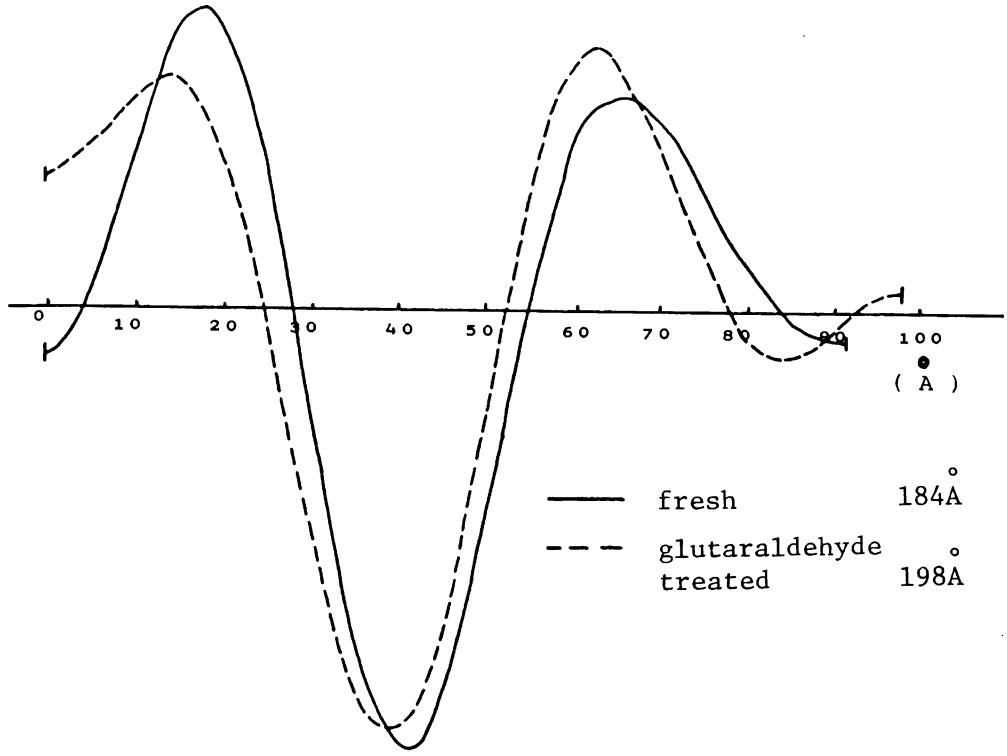

Fig. 3-29 Calculated electron density profiles of myelin membrane units for the fresh rabbit sciatic nerve myelin and 0.025% glutaraldehyde treated nerve myelin as a funtion of distance from the cytoplasmic boundary.

3-5 Cross experiments to rabbit sciatic nerve (DMSO and glutaraldehyde effect on the acetone treated-and-washed rabbit sciatic nerve)

In subsection 3-2, 3-3 and 3-4 there appeared quite similar structure phases. Therefore to establish the structural relationship between them the cross experiment is carried out. In this section 3-5, the modification of acetone treated-and-washed nerve is observed on application of DMSO or glutaraldehyde.

A. Experiment

Freshly dissected rabbit sciatic nerve was treated by immersion in 20% acetone in Ringer's solution for 3 hours, then replaced in Ringer's solution for 1 hour at room temperature. To this 20% acetone treated-and-washed nerve, DMSO was applied for 2 hours at various concentrations. All exposures were made for the specimen sealed in capillary tube with immersion medium. Exposures were routinely for 2 hours, with longer exposures of 15 hours to detect higher order diffraction.

For the comparison with DMSO effect on the fresh nerve myelin, the same experiments were carried out for the fresh nerve myelin in the same way as above. All the experimental procedures were performed at room temperature.

B. Relults

Figs. 3-30 and 3-31 show the dependence of the diffracting power ratio and periodicity on the DMSO concentration applying to the 20% acetone treated-and-washed nerve.

At zero % DMSO concentration (Ringer's solution), 20% acetone treated-and-washed nerve shows a 191Å periodicity and intensity distribution with less odd order reflections,which were described in former section. Applying the 10% DMSO, no collapsed phase is obtained, but a little shrunk native-like phase can be seen. On increasing the DMSO concentration the collapsed phase begins to emerge from the 20% DMSO concentration and gradually shrinks from 126Å at 20% to 112Å at 50% DMSO concentration. On the other hand the native-like phase at first shrinks then expands to 211Å in periodicity at 40% DMSO concentration. Diffracting power ratio of the collapsed phase which demonstrates the occupying ratio against the total diffracting region suggests 62% at the 20% DMSO where the collapsed phase is observed for the first time.

For the fresh nerve myelin, the segregation of the nerve myelin structure into the collapse phase and the native-like phase are observed at 10% DMSO concentration. On increasing the DMSO concentration the expanded phase is detected at a lower DMSO concentration, compared with the 20% acetone treated-and-washed nerve.

In addition the structure factors of the reflections of the

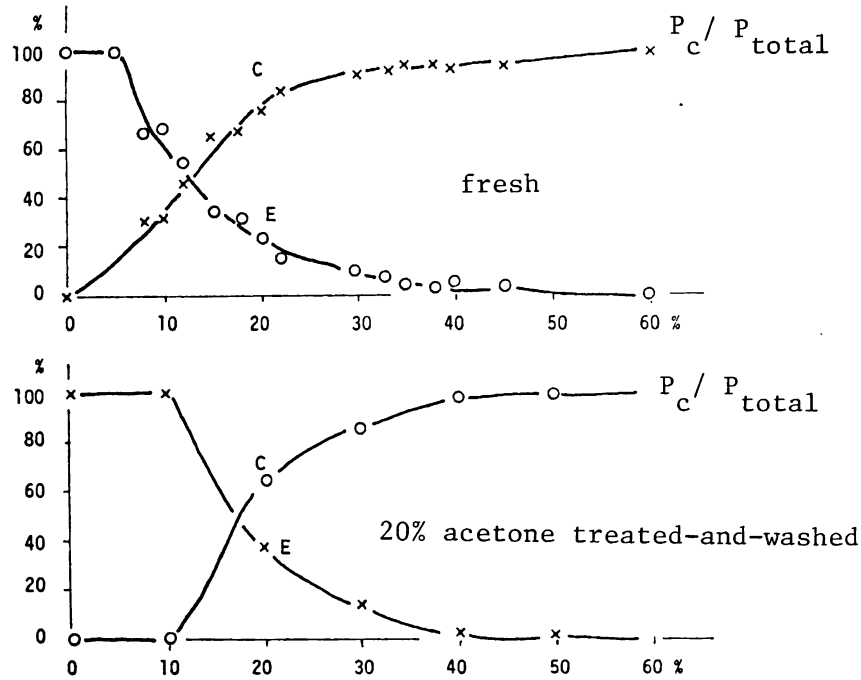

Fig. 3-30 Dependence on DMSO concentration of the diffracting power of the collapsed phase in the DMSO treated state for fresh rabbit sciatic nerve myelin and for 20% acetone treated-and-washed nerve myelin.

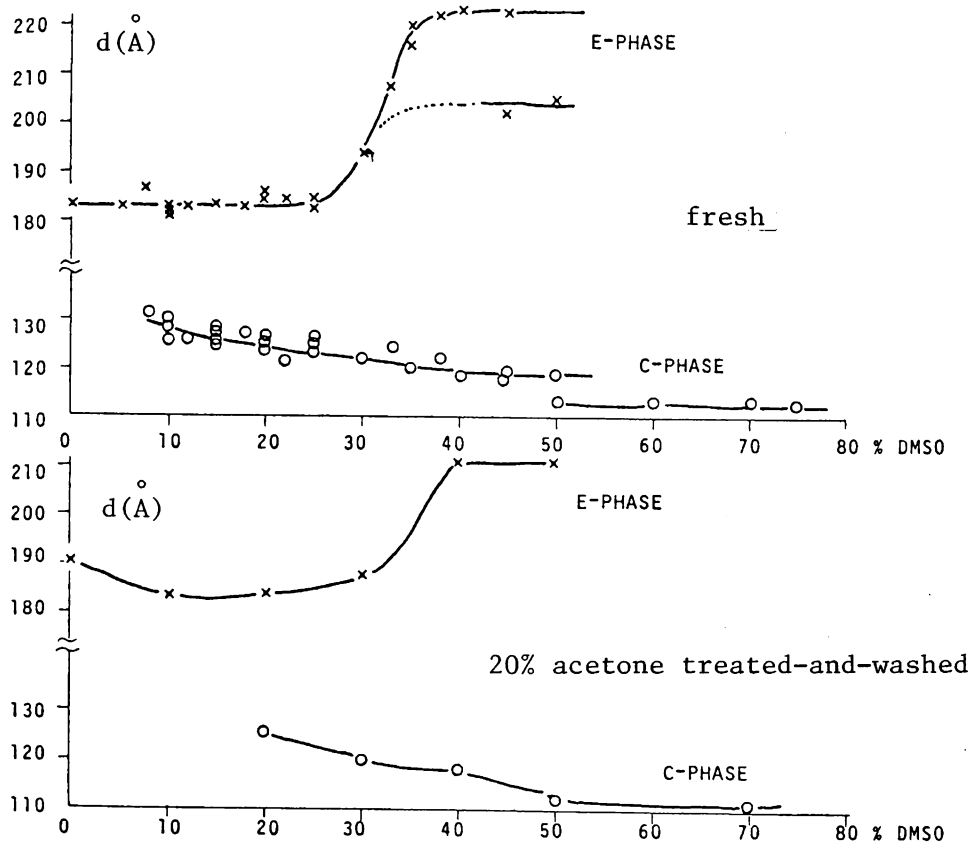

Fig. 3-31 Dependence on DMSO concentration of the periodicities of the different phases in the DMSO treated state for fresh rabbit sciatic nerve myelin and for 20% acetone treated-and-washed nerve myelin.

collapsed phase from acetone treated-and-washed nerve myelin are different from those for the fresh nerve myelin with respect to the intensity of the odd order reflections. 20% and 40% DMSO applying to the F' phase (see former section), the odd order intensity relatively reduces especially in the treatment of 40% DMSO, where no 3rd order reflection can be observed.

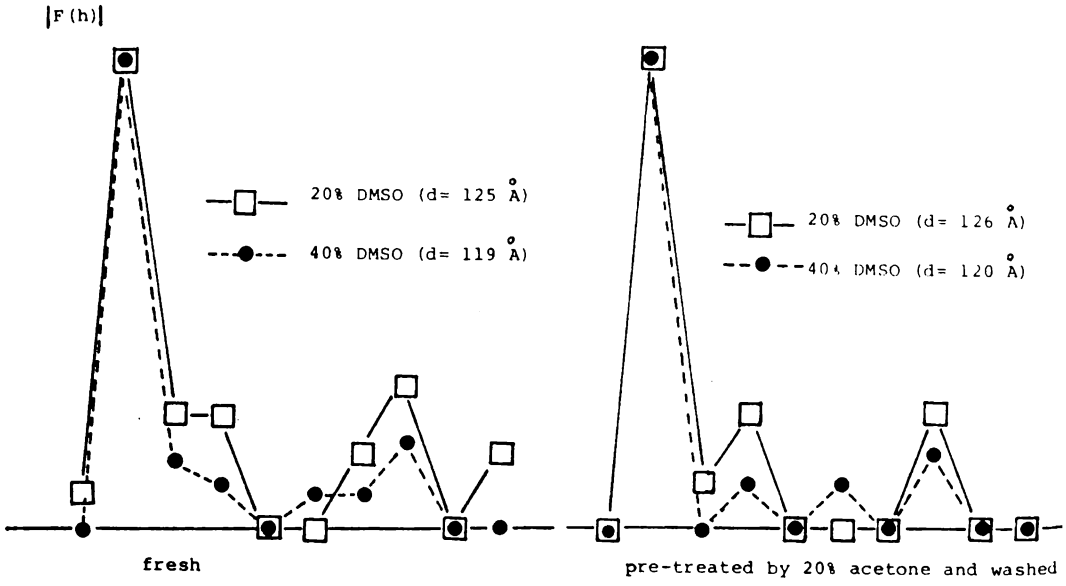

Fig. 3-32 Comparison of structure factors vs. reciprocal coordinatesof the collapsed phases in the DMSO treated state for fresh rabbit sciatic nerve myelin and for 20% acetone treated-and-washed nerve myelin.

Table 3-8 Periodicity, structure factor and P_c value of the collapsed phase in 20% and in 40% DMSO treated state for 20% acetone treated-and-washed rabbit sciatic nerve myelin. 20A.20D, 20% acetone treatment-and-washing and then 20% DMSO treatment. 20A.40D, 20% acetone treatment-and-washing and then 40% DMSO treatment.

	20A.20D	20A.40D
d	126Å	120Å
P_c	79%	86%
$\|F(h)\|$		
1	-	-
2	1.08	1.08
3	0.10	-
4	0.24	0.09
5	-	-
6	-	0.09
7	-	-
8	0.25	0.16

C. Electron density distribution

For the collapsed phase in the 20% and 40% DMSO treated nerve , the electron density profiles were derived using the 2nd, 3rd, 4th and 8th order reflections. On the same reason as described in the former section the sign relations were assigned as + + - - , for these reflections. Fig. 3-33 shows the electron density profiles with the scaling where there is superposition at the high electron density layers of the lipid bilayer and the base line. Both of them show the almost same separation in the lipid bilayer as 48.2Å for 20% DMSO and 48.4Å for 40% DMSO. Therefore the

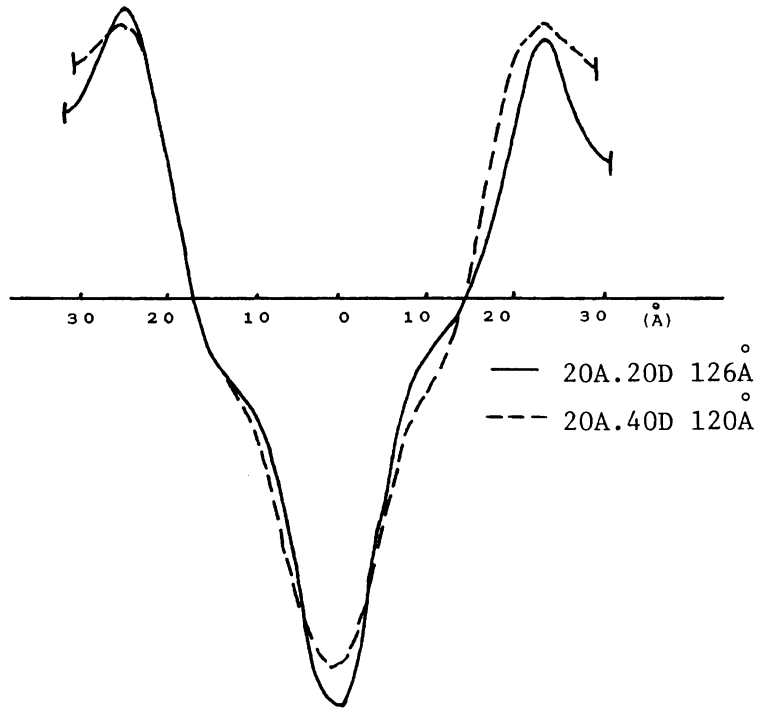

Fig. 3-33 Calculated elctron density profiles of myelin membrane units of the collapsed phases in 20% and 40% DMSO treated state for 20% acetone treated-and-washed rabbit sciatic nerve myelin.

difference in the periodicity, 6Å , is mainly due to the difference in the space separations of the cytoplasmic and the extracellular region. In addition it is confirmed that the more intense odd order reflection in the 20% DMSO treated nerve contributes to the asymmetrical density at the hydrocarbon chain region.

3-6 Cross effects of DMSO and glutaraldehyde on rabbit sciatic nerve

Glutaraldehyde which is known to crosslink the membranous components leads to the determination of a topology of the components in the membrane structure. In subsection 3-2 was shown that the reversible modification was induced by the DMSO below 30% concentration while above that point irreversible modification takes place. In subsection 3-4 was shown that glutaraldehyde fixes the modified structure, for on replacing the treated nerve into Ringer's solution no change could be detected. In this subsection DMSO effect was investigated on the glutaraldehyde treated

nerve and vice versa.

A. Experiment

Freshly dissected rabbit sciatic nerve was treated by immersion in 0.025% glutaraldehyde solution for 8 to 20 hours, in which sufficiently giving the only glutaraldehyde pattern shown in section 3-4. After washing out the glutaraldehyde, the nerve section was treated in the DMSO solution for 2 hours. Treated nerve sample was sealed in thin walled glass capillary tube with immersion medium. To detect the higher order reflection the longer exposure was made. All experiments were performed at room temperature.

B. Results

Applying the 20% and 40% DMSO in Ringer's solution to the glutaraldehyde treated nerve whose pattern was shown in the subsection 3-4, the collapsed phase and the other phase can be detected.

In the treatment with 20% DMSO solution the long exposure diffraction pattern shows the collapsed phase (124Å) with reflections up to the 8th order and the periodically fresh-like phase (183Å) with several reflections (2nd, 3rd, 4th and 5th order), where the collapsed phase occupies 75% of the total diffracting power. Increasing the DMSO concentration above the point at

which the irreversible modification can be induced, for example, 40% DMSO treatment gives 119Å collapsed phase (2nd, 3rd, 4th and 8th order) occupying 89% out of the total diffracting power and 184Å phase (1st, 2nd, 3rd, 4th and 5th order).

Detailed investigation of the structure factors of the collapsed phases from 20% and 40% treated nerves show relatively similar intensity distribution to that from the fresh nerve in the treatment with 20% DMSO solution, especially 40% DMSO treatment to the G phase (glutaraldehyde fixed pattern) gives rather intense 3rd order reflection compared with the native nerve. Fig. 3-34 and Table 3-9 show the structure factors of the reflections from the collapsed phase.

On the other hand native-like phase shows asymmetric structure in the 40% DMSO treatment.

On replacing the DMSO treated nerve into normal Ringer's solution, the glutaraldehyde pattern is almost restored, which is characterized by the approximate 205Å period and asymmetric intensity distribution.

C. Electron density distribution

By using the structure factors of the 2nd, 3rd, 4th and 8th order reflections of the collapsed phases in the 20% DMSO and 40% DMSO treated nerve, the electron density profiles were calculated. The sign relations were assigned as + + - - for each reflections,

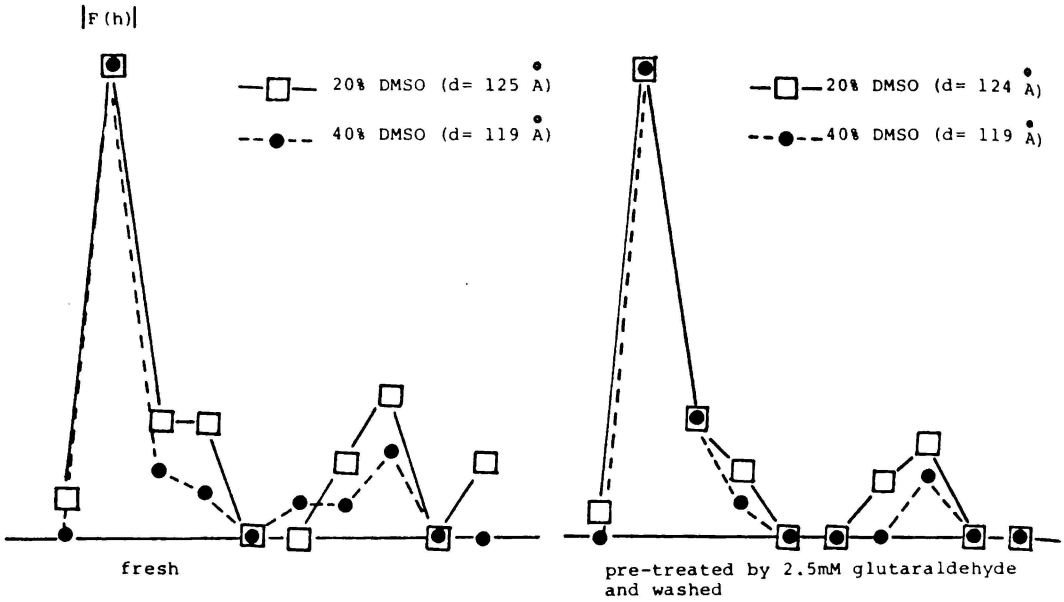

Fig. 3-34 Comparison of the structure factors vs. reciprocal coordinate of the collapsed phases in the DMSO treated state for fresh rabbit sciatic nerve myelin and for 0.025% glutaraldehyde treated-and-washed (fixed) nerve myelin.

	G.A.20D	G.A.40D
d	124Å	119Å
P_c	75%	89%
|F(h)|		
1	0.05	-
2	1.05	1.06
3	0.25	0.24
4	0.14	0.07
5	-	-
6	-	-
7	0.12	-
8	0.20	0.13

Table 3-9 Periodicity, structure factor and P_c value of the collapsed phase in 20% and in 40% DMSO treated state for 0.025% glutaraldehyde treated-and-washed rabbit sciatic nerve myelin. G.A.20D, 0.025% glutaraldehyde treatment-and-washing and then 20% DMSO treatment. G.A.40D, 0.025% glutaraldehyde treatment-and-washing and then 40% DMSO treatment.

respectively. Fig.3-35 shows the electron density profiles of the collapsed phase for 20% and 40% DMSO treated nerve myelin with the scaling where there is superposition at the base line. They are almost identical in the separation from the high dense peak to peak and in the similar shape in the lipid bilayer region. The 5Å shrinkage in the 40% DMSO treated nerve is due to the shorter widths in the cytoplasmic and the extracelluar space.

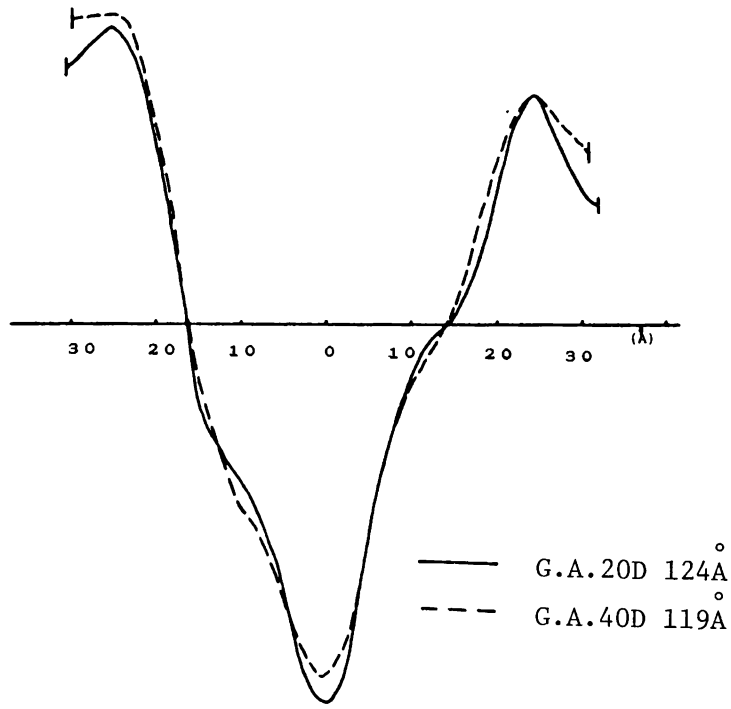

Fig. 3-35 Calculated electron density profiles of membrane units of the collapsed phases in 20% and 40% DMSO treated state for 0.025% glutaraldehyde treated-and-washed rabbit sciatic nerve myelin.

3-7 The behaviour of DMSO treated nerve during drying and subsequent heating and cooling

The behaviour of the treated nerve myelin in various organic solvents during drying has been extensively studied for the purpose of identifying the lipid phase or the lipo-protein phase when several phases were observed in the same x-ray diffraction pattern due to the physical or chemical perturbation. Comparative study of nerve myelin and of the extracted lipid provided the basis of identification of the reflection which originated from the lipid phase. In this subsection this technique was applied to the DMSO treated nerve.

A. Experiment

Freshly dissected rabbit sciatic nerve was treated by incubation in 35% DMSO solution in mammalian Ringer's solution for two hours at room temperature (23°C), and sealed in a thin walled glass capillary tube with DMSO solution. After the 35% DMSO treated pattern was recorded, the treated nerve was taken from the capillary and mounted on the camera under tension. The behaviour of DMSO treated nerve during drying was studied by recording the diffraction at intervals during the drying process. Heating experiments were performed using a frigister mounted sample holder with the temperature controlled to $\pm$ 1°C.

B. Results

In Fig. 3-36 is schematically depicted the diffraction pattern during drying for 35% DMSO treated nerve and Fig. 3-37 shows the periodicities as the function of time since when the nerve was exposed to air for drying.

Before drying DMSO treated nerve showed the 2nd order reflection of 120Å collapsed phase and the 2nd order reflection from 200Å expanded phase after a short exposure.

On drying, the periodicity of the expanded phase increased from 200Å to 230Å while that of the collapsed phase decreased from 60Å to 56Å. On heating to 50°C the expanded phase periodicity reduced to 200Å and the collapsed phase to 55Å. At this temperature there was a marked reduction in the intensity of the 55Å reflection and a new reflection appeared at 42Å. At higher temperatures the 55Å reflection intensity was further reduced and the 42Å reflection showed a corresponding increase. When the temperature was lowered to 23°C the 55Å reflection again became strong and the 42Å reflection much weaker. In the later stages of drying and during heating an additional reflection at about 61Å which could not be related to any of the other periodicities was also observed.

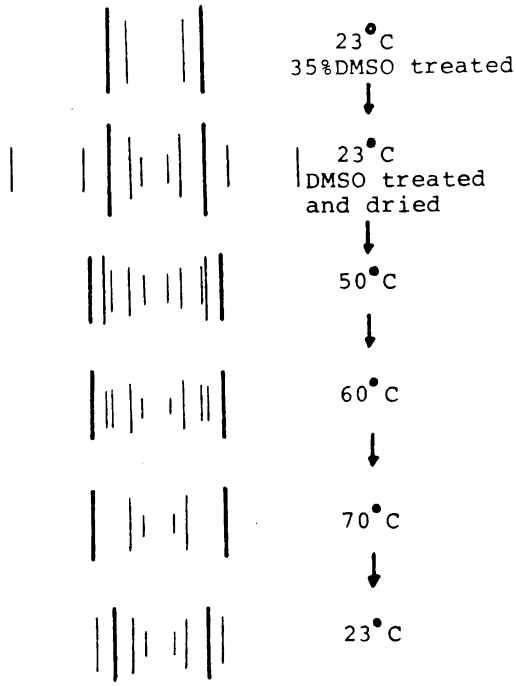

Fig. 3-36 Schematic drawings of the diffraction pattern for 35% DMSO treated rabbit sciatic nerve myelin during drying and subseqent heating and cooling.

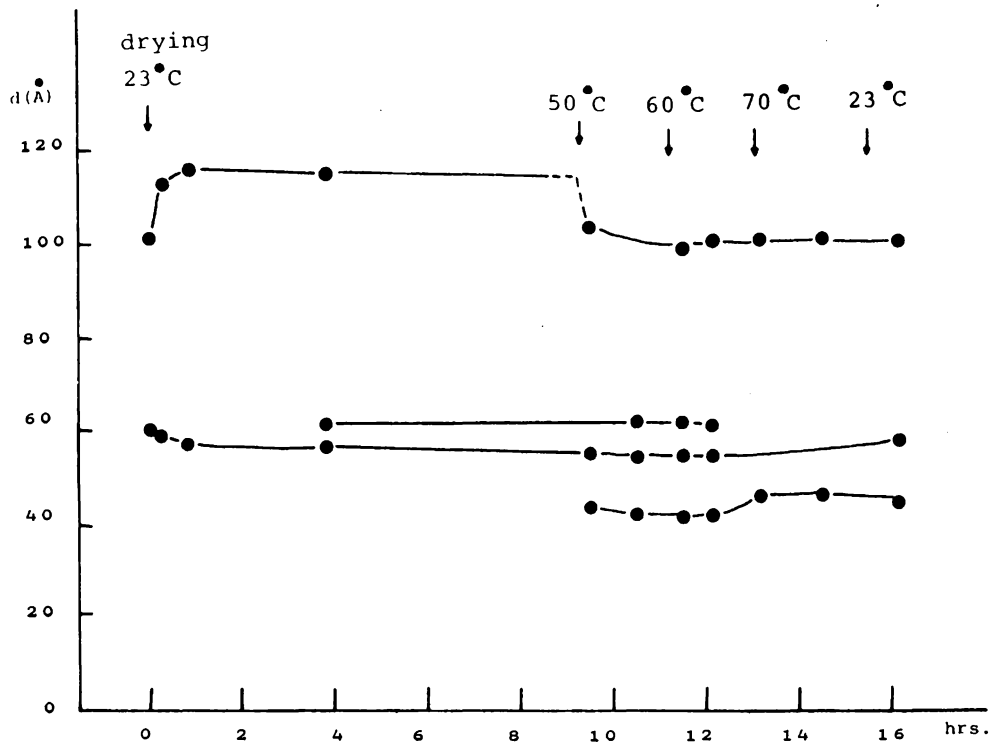

Fig. 3-37 Periodicity of the 35% DMSO treated rabbit sciatic nerve myelin during drying and subsequent heating and cooling.

C. Comparison between the drying studies on nerve myelin

Extensive studies on the modification of nerve myelin during drying and subsequent heating and cooling provide evidence that DMSO treated nerve has a similar structure to dried nerve. Elkes and Finean (1953b) found the changes in diffraction pattern with temperature of normal dried frog sciatic nerve and dry total lipid extracts, where at 20°C reflections of 43.0Å and 60.0Å were commonly observed in both, and above 60°C to 70°C, the 60Å band could not be seen. In dried nerve, in addition, longer periods of 74Å and 143Å observed, were shown to be relatively unaffected over the whole range of temperature from -20°C to 60°C, whereas in the extracted lipid no long period bands could be seen. In the present specimen, DMSO treated and then dried rabbit sciatic nerve, showed similar features, at 23°C 110Å reflection and 60Å reflection. On increasing the temperature the 110Å remained relatively unchanged, and the lower periodicity, from 50°C to 70°C was replaced by 55Å and 42Å reflection and above 70°C only 46Å reflection. Thus it is suggested that the expanded phase is a lipo-protein structure and the collapsed phase is a structure mainly composed of lipids. However, slight differences were also observed between dried nerve and DMSO treated and dried nerve, 1) during drying the periodic distance of the expanded phase increases from 100Å to 115Å at 23°C, while above 50°C

decreases to 100Å, 2) above 50°C for the first time 42Å reflection begins to emerge, 3) throughout the drying process 34.5Å reflection indicating free cholesterol cannot be observed. These differences suggest the dried nerve does not completely represent the DMSO treated and dried nerve, especially in the DMSO treatment the distribution of the cholesterol could be significantly modified.

Thus it is speculated in the gross sense DMSO treatment induces the segregation into the lipo-protein structure and lipid structure.

3-8 DMSO, acetone and glutaraldehyde effects on rabbit optic nerve

In an attempt to compare the structural difference between PNS (peripheral nervous system) and CNS(central nervous system), freshly dissected optic nerve of rabbit was treated by immersion in DMSO, acetone and glutaraldehyde. The effects of these chemicals on the optic nerve are described.

A. DMSO and acetone effect

Fig. 3-38 shows the dependence of the periodicity on the DMSO

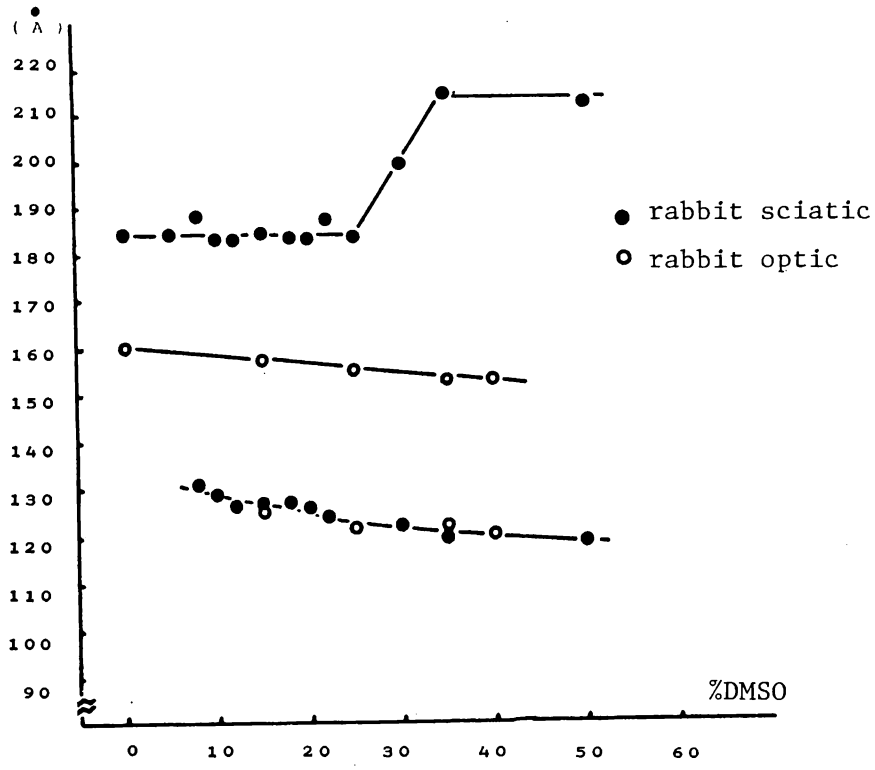

Fig. 3-38 Dependence on DMSO concentration of the periodicity in the DMSO treated state for rabbit sciatic nerve myelin and for rabbit optic nerve myelin.

concentration for rabbit optic and sciatic nerve which were treated by immersion in DMSO or acetone for 2 hours, sealed in thin walled glass capillary tube and mounted on the x-ray camera. All experimental procedures were carried out at room temperature. Under such experimental conditions, PNS and CNS show similar behaviour in the periodicity of the collapsed phase, which

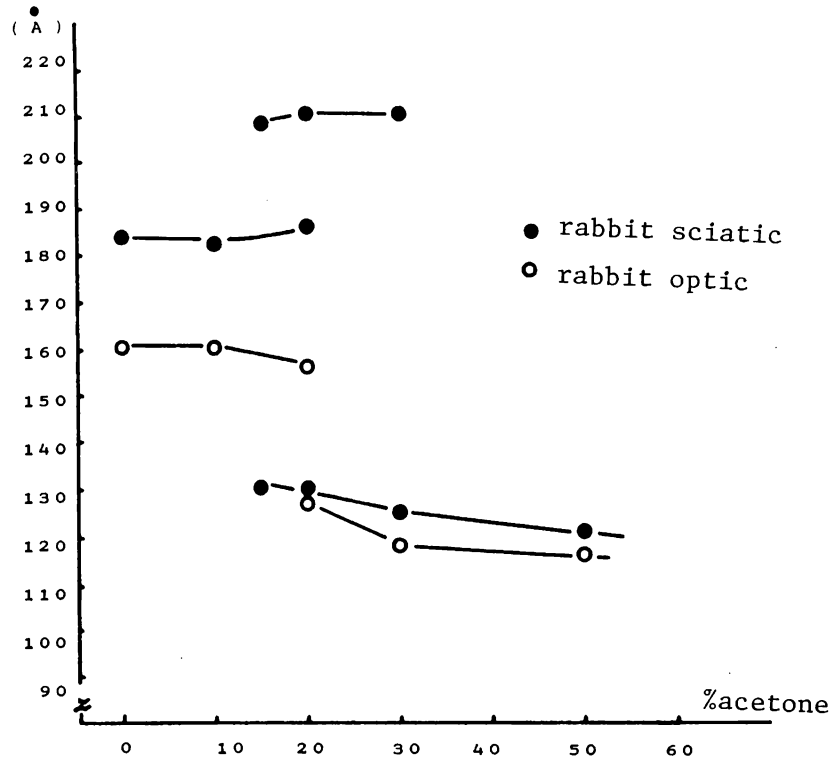

Fig. 3-39 Dependence on acetone concentration of the periodicity in the acetone treated state for rabbit sciatic nerve myelin and for rabbit optic nerve myelin.

gradually reduces with increased DMSO or acetone concentration. However the second phase in rabbit optic nerve shows a decrease in periodicity, while rabbit sciatic nerve gives expanded above 40% concentration for DMSO treatment and 15% for acetone. Fig. 3-39 shows periodicities observed in the acetone treated optic nerve as the function of the acetone concentration.

B. Glutaraldehyde effect

Freshly removed rabbit optic nerve showed the 2nd and 4th order reflections of 160Å phase after a short exposure (Fig.3-40). When applying 0.025% glutaraldehyde solution in mammalian Ringer's solution, after 5 hours, a weak 3rd order reflection of a 160Å phase emerges. On increasing the incubation time, the 3rd order reflection becomes stronger and after 21 hours the periodicity reached 152Å and remained constant after 25 hours. On replacing in normal Ringer's solution no change in the diffraction pattern could be observed. In the longer exposure the 1st, 2nd, 3rd, 4th, 6th and 10th order reflections were observed. Fig.3-41 shows the densitometer tracing for glutaraldehyde treated rabbit optic nerve myelin and the structure factors of the reflections from this G phase are given in Table 3-10.

35% DMSO treatment of the glutaraldehyde treated optic nerve gave the 60Å reflection and the 2nd and 4th order reflections of 146Å phase, on washing the DMSO treated nerve with normal Ringer' solution the typical glutaraldehyde fixed pattern was restored. This collapsed phase was not so dominant as that given from fresh optic nerve. Following treatment by 0.025% glutaraldehyde solution, 35% DMSO treated nerve gave an intense 58Å reflection and the 2nd order reflection of 151Å phase and on replacing into normal Ringer's solution, 159Å original fixed phase was restored.

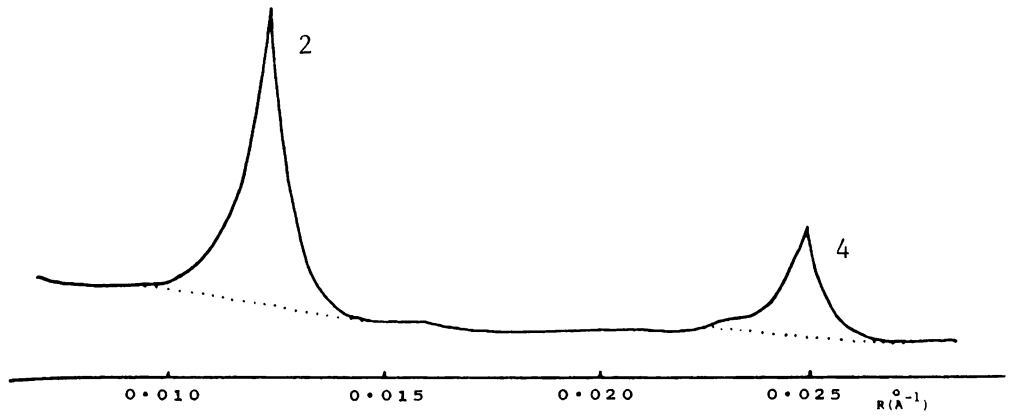

Fig. 3-40 Densitometer tracing vs. diffraction angle for fresh rabbit optic nerve myelin.

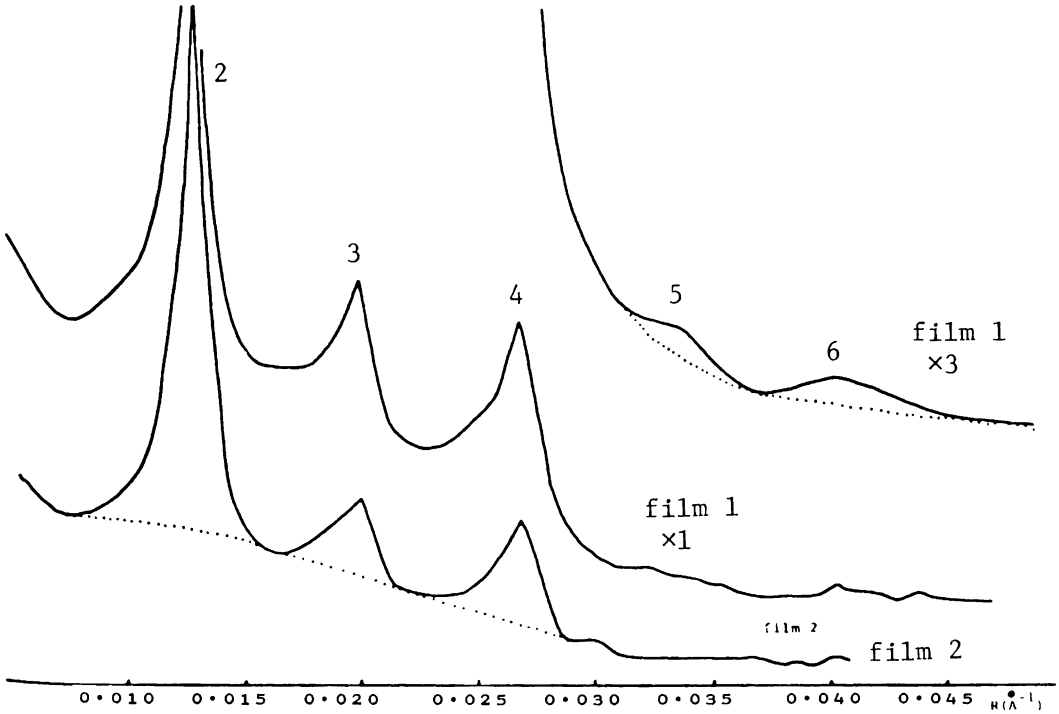

Fig. 3-41 Densitometer tracing vs. diffraction angle for 0.025% glutaraldehyde treated rabbit optic nerve myelin.

Table 3-10 Periodicity and structure factor for fresh and for 0.025% glutaraldehyde treated rabbit optic nerve myelin.

	fresh	G.A. treated
d	160Å	152Å
|F(h)|		
2	1.02	0.96
3	-	0.50
4	0.75	0.60
5	-	-

C. Electron density distribution profile for the glutaraldehyde treated rabbit optic nerve myelin

Fig. 3-42 shows the electron density profiles of the glutaraldehyde treated and fresh optic nerve, which are drawn with the superposition at the base line by using the 2nd, 3rd, 4th and 5th order reflections of 152Å glutaraldehyde treated phase and 160Å fresh phase, respectively. The phase problem is solved by calculation of electron density profiles with all combinations of sign relation (Fig. 3-43) and + + - - is chosen as appropriate to give the apparent lipid bilayer corresponding with the other nerve myelins so far reported. From this figure it is determined that the cytoplasmic lipid bilayer and the extracellular space

are 20Å, 48Å and 36Å, respectively. Hence it is shown that the difference in periodicity (8Å) from fresh nerve is due to the shrinkage in the cytoplasmic (10Å) and the lipid bilayer space (2Å) and the expansion in the extracellular space (5Å).

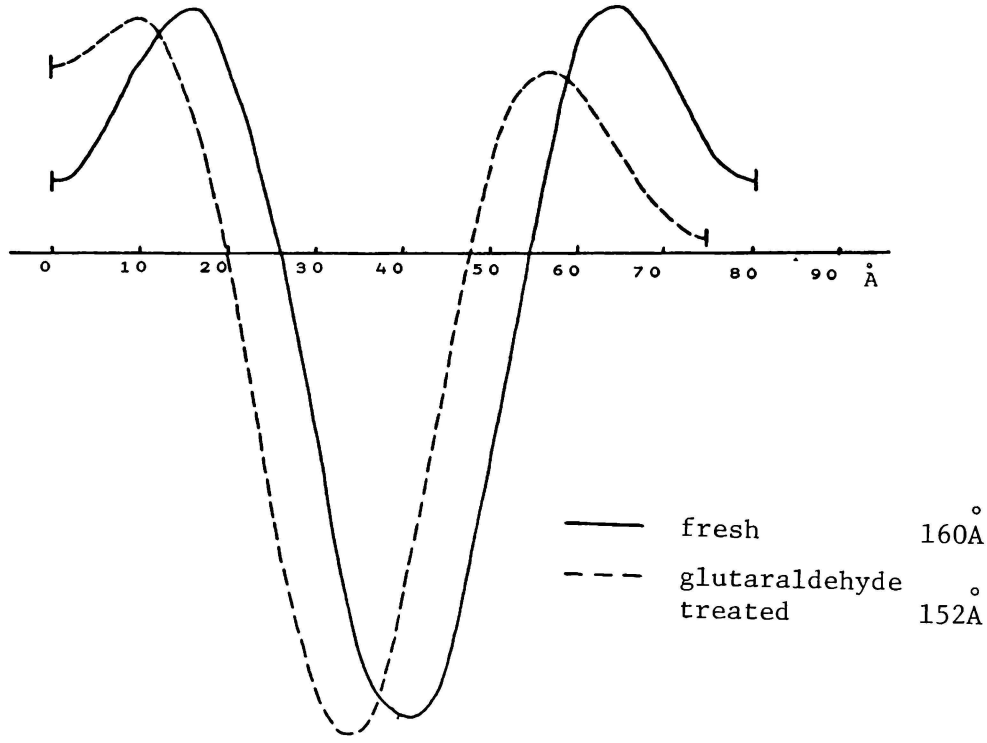

Fig. 3-42 Calculated electron density profiles of myelin membrane units for rabbit optic nerve myelin and for 0.025% glutaraldehyde treated rabbit optic nerve myelin as a function of distance from the cytoplasmic boundary.

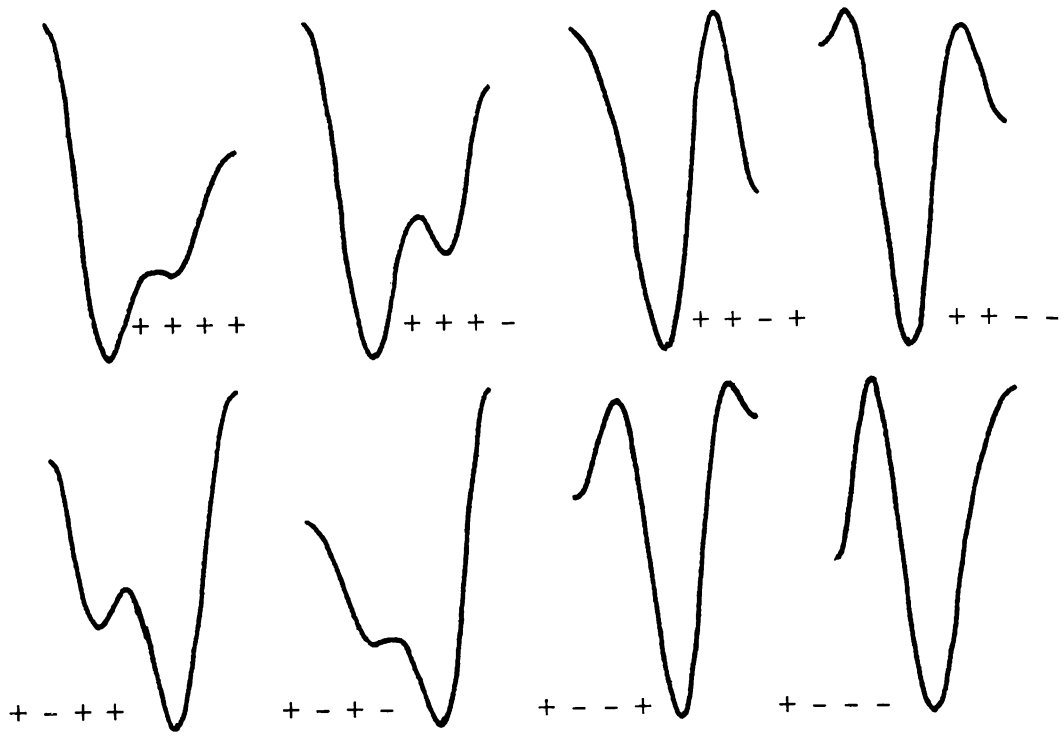

Fig. 3-43 Calculated electron density profiles with all sign relations of myelin membrane units for 0.025% glutaraldehyde treated rabbit optic nerve myelin.

D. Comparison between rabbit sciatic and optic nerve with the effects of DMSO, acetone and glutaraldehyde

Comparing the DMSO effects on the rabbit sciatic nerve with those on the rabbit optic nerve, the behaviour of the collapsed phase with the change in DMSO or acetone concentration is quite similar in such a way that it gradually shrinks on inreasing the concentration. This suggests that the segregated collapsed phase is similar in structure. Finean et al. (1968) has already demonstrated that various isolated dried membranes show a similar diffraction pattern, which is characterized by a sharp reflection at 60Å which on subsequent heating and cooling behaves as extracted lipid, with a longer periodicity much more stable during temperature variation. In this regard the labile lipid exists in common in the sciatic and optic nerve myelin. While the other phases, which are considered to be lipo-protein complexes, expand for sciatic nerve and shrink for optic nerve. Corresponding behaviour in periodicity was observed in the glutaraldehyde treated nerve. Glutaraldehyde fixed pattern showed asymmetric structure in both nervous systems, while the reflections from fixed optic nerve give sharp spectra and can be detected up to 10th order reflection, but in fixed sciatic nerve myelin only 4 reflections were apparent and these were quite broad.

Applying DMSO solution to the fixed optic nerve, intensity of 60Å reflection is not so marked. While applying DMSO to the

fresh state or applying glutaraldehyde to DMSO treated state the 60Å reflection appears quite intense. On washing the fixed nerve no change in diffraction pattern can be detected. These observations suggest glutaraldehyde crosslinks the lipid and protein, so there remain less labile lipids to segregate from lipid-protein complex to form a collapsed phase.

Following Finean's generalization (Finean et al.,1968) that " membranes are fundamentally similar in structure for the same behaviour exhibited in the drying process in every isolated membrane ", glutaraldehyde may attack the lipid and protein complexes and crosslink them. So such an assembly of lipo-protein complex may provide the difference between optic and sciatic nerve myelin.

3-9 Discussion

In this subsection the following aspects are discussed on the basis of the experimental results obtained in the former sections, such as 1) the framework of the reversible to irreversible transformation which is given as the correlation

between the external perturbation and the induced x-ray diffraction pattern in result, 2) the interpretation on the modification of the myelin structure in terms of the chemical components, 3) the comparison between the DMSO, acetone and glutaraldehyde effects and other external perturbation, which will lead to the clarification of the stabilizing factor of the structure of nerve myelin, 4) the comparison between PNS and CNS nerve myelin with respect to the response to the external perturbation, 5) correlation between the natural degradation, demyelinating deseases and the present documented modifications, 6) concluding remarks on the structure stability of nerve myelin sheath.

Framework of the reversible to irreversible transformation

On close comparison between DMSO and acetone effects, similar points can be detected in respect of the periodicity, diffracting power, half width of x-ray reflection and the structure factor.

From the experimental results on the periodicity for DMSO or acetone treated state and for treated-and-washed state, 10% DMSO segregates the fresh phase (184Å) into the collapsed phase (129Å) and the native-like phase (184Å), while acetone does not produce two phases separation until 20% concentration. Therefore in the competence for the phase segregation in the membrane structure DMSO is more effective than acetone. However, in the power of modifying the myelin structure irreversibly acetone is stronger

than DMSO. There is no concentration range observed where acetone exerts reversible modification as DMSO does. In the range from 10% to 30% DMSO the reversible modification can be detected. Hence in the acetone treatment, once the segregation is incurred the washing procedure does not restore the original fresh phase. Above the critical concentration of the reversible to irreversible transformation the periodicity of the expanded phase (212Å at 20%) observed in the acetone treatment is 10Å longer than that in 40% DMSO treatment. And in accord, the acetone treated-and-washed phase (192Å at 20%) shows more expanded periodicity than that of DMSO (187Å at 40%). As to the collapsed phase, however, an almost identical behaviour with respect to concentration can be observed in both cases. Thus the lower critical concentration which shows the effectiveness of the irreversible modification, can be well correlated with the longer periodicity in the expanded and the quasi fresh phases.

At the critical concentration, 40% for DMSO and 20% for acetone treatment, the induced collapsed phase occupies 80% of the total diffracting power which is common in both treatments.

For the structure factor and the electron density distribution 20% acetone does not give the odd order reflection and as already shown 40% DMSO also gives weaker odd order reflection than 20% DMSO does. Low resolution electron density profiles show that the distances of the polar to polar head group in lipid

bilayer region are almost identical as 47.6Å, 47.9Å and 47.7Å for 20% DMSO, 40% DMSO and 20% acetone respectively, while the cytoplasmic and the external space is equal in each case. Thus the difference in the 3rd order reflection intensity can be ascribed to the asymmetric profile in the lipid bilayer part. Even though the periodicity of the collapsed phase in 40% DMSO treatment is shorter than that in 20% acetone treatment by 10Å, the density profile of the lipid bilayer part is quite similar. In this regard, above the critical concentration the gross structure of the collapsed phase is commonly characterized by the weak 3rd order reflection. So because of the close similarities in the case of the acetone treatment the collapsed phase is to be called as C' phase against C phase by the treatment of low DMSO concentration. The weaker odd order reflection correlates with the lower critical concentration in acetone treatment than DMSO.

Concerning the treated-and-washed state, in the range of the irreversible modification the common features are detected as, 1) the relative intensity of the 3rd and 5th order reflection become weaker than that in the fresh state, 2) the half width of the Bragg reflections increases with the concentration, and 3) the periodicity increases with the concentration. Fig. 3-44 shows the structure factors against the reciprocal space for the washed state after the various treatments. All of them fit the Fourier transform obtained by Caspar and Kirshner (1971) for rabbit sciatic

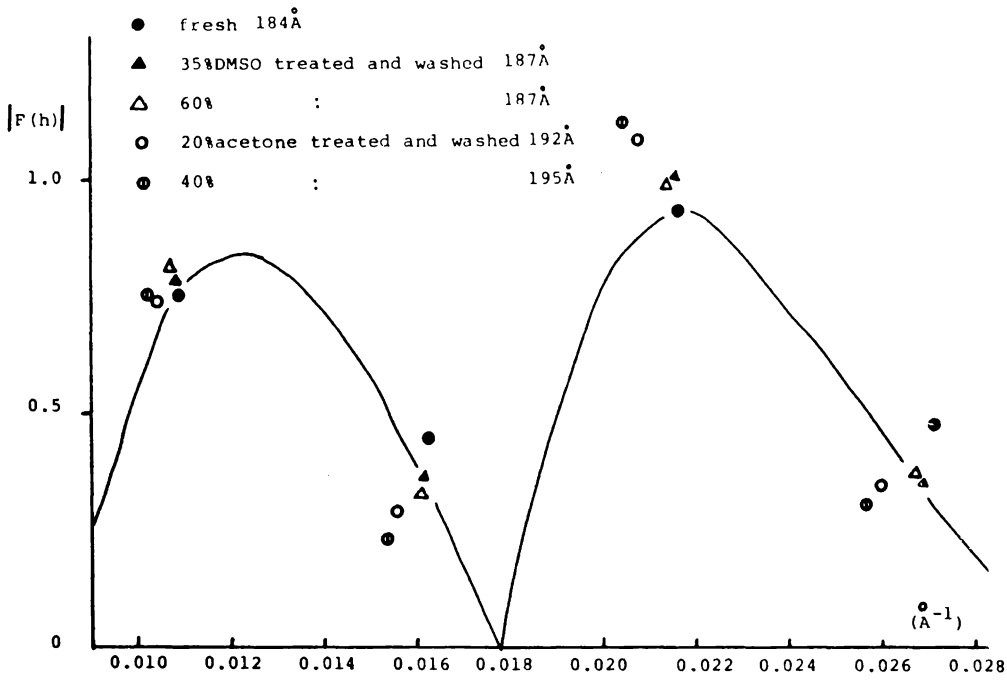

Fig. 3-44 Structure factors vs. reciprocal coordinate in fresh, DMSO treated-and-washed and acetone treated-and-washed state for rabbit sciatic nerve myelin.

nerve myelin, but deviate gradually to the lower coordinates with increasing the periodicity. This is interpreted by the cytoplasmic expansion mainly induced on the transformation from the fresh phase to the quasi fresh phase. In fact the electron density profiles give the evidence that the weak odd order reflections mainly contribute to the cytoplasmic expansion and the increase of the distance of polar to polar head group in the lipid bilayer region, with almost preserving the external space.

Applying the DMSO on the washed state (quasi fresh, F' phase) the collapsed phase with weak odd order could be obtained, thus the F' phase reversibly transforms to C' phase.

In this way may be extracted the common features of the relationship between DMSO and acetone effect on the nerve myelin sheath. Namely, with regard to the framework of the reversible to irreversible transformation the following schematic figure can be established.

$$F \rightleftharpoons C \quad , \quad N$$

$$F \longrightarrow C' \quad , \quad E \longrightarrow F' \rightleftharpoons C'$$

However acetone is more effective than DMSO to induce the irreversible modification, while DMSO is stronger in the segregation of the myelin structure into two distinct phases.

Why such a fomulation could be established must be clarified through the combination of the interpretation of the electron density profiles in terms of the chemical composition and the physico-chemical property of the DMSO and acetone.

Comparison between F phase and F' phase

The comparison between F phase and F' phase is studied for the better understanding about what F' phase is.

Low resolution electron density profiles of the F' phase

(40% DMSO treated-and-washed, 70% DMSO treated-and-washed, 20% acetone treated-and-washed, 40% acetone treated-and-washed) show the cytoplasmic expansion and the separation between the peaks in the lipid bilayer region. Associating with them the half width shows the increase of the disorderness in the stacking of myelin layers. According to the Hoseman's definition (1962) the distortions of the second kind could be induced in the irreversible modification, for the higher order reflection becomes broader than the lower. Hyble (1977) reported the fresh myelin holds the same property. The distortions in the fresh state is also exhibited in the present data that even in the fresh phase half width of the higher order reflection is larger than that of the lower order reflection.

What is the collapsed phase

Table 3-11 shows the structure factors of the collapsed phases detected in the various experiments. Of the periodicity, 20D (20% DMSO treatment to fresh nerve), 20A.20D (20% DMSO treatment to 20% acetone treated-and-washed nerve), G.A•20D (20% DMSO treatment to 0.025% glutaraldehyde treated-and-washed nerve) show the almost identical values as 125Å, 126Å and 124Å, respectively. For 40% DMSO treatment to the various pre-treated nerves, the almost identical periodicity was observed.

Electron density profiles are, in the gross sence, quite

Table 3-11 Periodicities, structure factors and P_c values of the different collapsed phases for rabbit sciatic nerve.

treat-ment	20D	20A.20D	G.A.20D	40D	20A.40D	G.A.40D	20A
d(Å)	125	126	124	119	120	119	129
P_c(%)	76	79	75	93	86	89	86
|F(h)|							
1	0.08	-	0.05	-	-	-	-
2	1.00	1.08	1.05	1.06	1.08	1.06	1.00
3	0.24	0.10	0.25	0.14	-	0.24	-
4	0.24	0.24	0.14	0.09	0.09	0.07	0.47
5	-	-	-	-	-	-	-
6	-	-	-	0.07	0.09	-	-
7	0.16	-	0.12	0.07	-	-	-
8	0.30	0.25	0.20	0.18	0.16	0.13	0.29
9	-	-	-	-	-	-	-
10	0.16	-	-	-	-	-	-

similar each other and these resemble the multi-lamellared lipid artificial membrane (Franks,1976) in the point of the periodicity and the equality in distance between the cytoplasmic and extracellular space. The experiment of drying, subsequently heating and cooling, gives the evidence that the collapsed phase behaves like an extracted lipids , which is fully

described in former section. In addition no experimental results so far have appeared to support that fully dried nerve shows the 120Å lipo-protein complex. Schmitt et al. (1941) reported 144Å for amphibian and 158Å for mammalian nerve myelin in the drying experiment.

However there are marked differences in the region of lipid bilayer between C phase and C' phase, the former of which was derived from 20D, G.A.20D and G.A.40D nerves and the latter was from 40D, 20A.20D, 20A.40D and 20A nerves. C phase has the bump at the external side of the lipid bilayer, while C' phase shows a symmetric feature in this part, which is obvious in the 20A. The superposition of the electron density profiles of the 20D and of the fresh nerve clearly shows that this bump is the same as the peak appeared in Caspar and Kirshner's density profile (Fig. 3-45).

On this asymmetically located bump, according to Caspar and Kirshner (1971), it was assumed to be the asymmetric location of the cholesterol. Recently, however, Nelander and Blaurock (1978) interpreted this bump as the protein inserted into the half of the bilayer. In fact Pinto da Silva and Miller (1975) detected such protein inserted in the membrane bilayer by the freeze fracture electron microscopy. Further the biochemical studies also suggested the existence of such integral protein (Boggs and Moscarello,1978). In addition Wood (1973) reported

that glutaraldehyde fixes the protein and some lipids except cholesterol. In our result is shown that the glutaraldehyde preserves the asymmetrical bump against the DMSO effect to induce the phase segregation. In this connection membranous proteins might mainly contribute to this peak halfway at the half of the lipid bilayer. It is well known that there are two major proteins in myelin, basic protein (A_1 protein for CNS and P_1, P_2 proteins for PNS) and hydrophobic protein (P_0 protein for PNS and proteo-lipid protein for CNS). So there remains unclarified which protein resides in this part, but it is reasonable to assume the hydrophobic protein on physico-chemical reasons, for basic protein is a peripheral protein to interact ionically with the acidic lipid (London and Vossenberg,1973) and is reported to be in the cytoplasmic space (Carnegie and Dunkley,1975). The artificial membrane composed of the purified hydrophobic protein from human brain myelin and of dipalmitoyl lecithin (DPL) or of dimyristyl lecithin (DML) showed the very similar lamellae thickness as exhibited by the pure lipid alone and that the hydrophobic protein is mainly embedded within the lecithin bilayer (Rand et al.,1976). Furthermore Mateu et al. (1973) showed that the model membrane composed of basic protein of nerve myelin and lipid gives equivalent periodicity as the fresh nerve myelin. As the present results show that C phase having the bump gives very similar spacing of lipid alone, hydrophobic protein might be crucial to contribute to

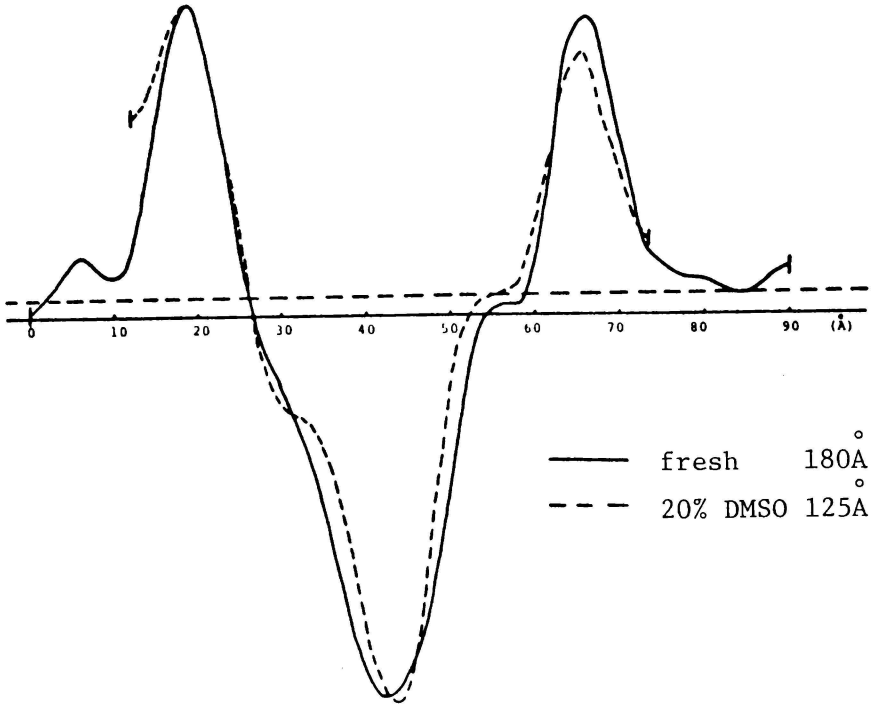

Fig. 3-45 Comparison of electron density profiles for fresh rabbit sciatic nerve myelin (Caspar et al.,1971) and the collapsed phase of 20% DMSO treated rabbit sciatic nerve myelin.

this area.

Wide angle reflection clearly shows the molecular rearrangement at the critical concentration where reversible to irreversible modification can be detected. Wide angle reflection is known to give the packing of the hydrocarbon chain of the lipids and broad ring reflects the fluidized structure in the hydro-

carbon chain (Engelman,1970). Since in the treated state the collapsed phase occupies most part of the total diffracting region, it is reasonable to speculate that the wide angle reflection reflects the molecular rearrangement in the collapsed phase. At 20% DMSO concentration the C phase shows normal broad 4.6Å reflection, whereas at 40% DMSO the C' phase gives the sharp 4.6Å reflection at room temperature (20°C), which is associated with the appearance of the E phase. According to Freeman et al. (1975), at 35% DMSO there also appears the sharp ring and at 50°C it becomes broad. Therefore the bump above mentioned might contribute to the packing of the hydrocarbon chain. Ladbrook et al. (1968) reported the endothermic transition at 35°C and 49°C, then they interpreted it due to the cholesterol and phospholipid precipitation.

Taking consideration of the fluidizing effect of cholesterol (reviewed by Demal,1976) on nerve myelin, in addition, the phase transition described above is closely involved in the rearrangement of the cholesterol. In addition, hydrophobic protein also fluidizes the hydrocarbon chain packing in the similar way as cholesterol (Papahadjopoulos et al.,1975). In these regards, at present it is appropriately stated that the cholesterol and hydrophobic protein are at least needed to integrate the structure of the rabbit sciatic nerve myelin. Thus the collapsed phase is not only the lipo-protein phase with preserving the lipid bilayer region

as in the native nerve myelin.

Conclusively, paying attention to the reversible to irreversible modification, the fresh phase changes to the quasi fresh phase when some asymmetrically located substances are modified by DMSO or acetone. Above constituents are fixed by glutaraldehyde and are effective to make the myelin to be compact.

CHAPTER 4

STRUCTURE STUDY OF CARP NERVE MYELIN

4-1 Introduction

With the exception of fish nerve myelin the x-ray diffraction pattern of vertebrate nerve myelin is known to vary with species and types of the nervous system, in such a way that the higher taxonomic groups have myelin with longer periodicity than that of lower taxonomic groups and that myelin in peripheral nervous system has 170Å to 180Å periodicity, while that in central nervous system has 150Å to 160Å. As to the intensity distribution, the odd order reflection of the PNS type myelin is more intense than that of CNS type myelin. It means PNS myelin membrane is packed more asymmetric relative to the cytoplasmic surface and the external surface.

Fish nerve myelin, however, was reported to show the presence of two phases in the native state by the x-ray diffraction method, one of which corresponds to PNS type and the other to CNS type in regard to the periodicity. However, with respect to the intensity distribution, CNS type phase in fish myelin is more asymmetric than the PNS type phase (Blaurock and Worthington,1969).

On the comparison between PNS and CNS nerve myelin, numerous studies so far appeared and clarified in part the difference and similarity between them in respect of morphology, chemical com-

position and the response to the perturbation. Nonethless no explanation has yet been given as to the difference between them at a molecular level.

In this chapter, therefore, the structural difference between PNS and CNS type myelin is used as a basis for the examination of the two phases in fish nerve myelin.

As it has not yet been established to what extent the in situ experiment correctly represents the structure in vivo condition, so the correlation between the in vivo system and in situ experimental system the author selected is considered.

This subsection lays the basis of the following experiments. Afterwards is discussed the external perturbation on the fish nerve myelin, namely effects of mammalian Ringer's solution, pH, glutaraldehyde and calcium.

4-2 Experiment

A. Correlation between in vivo and in situ experimental condition

Previously reported x-ray diffraction studies on fish nerve myelin (Blaurock and Worthington,1969) (Hoglund and Ringertz,1961) (Finean,1960) have provided no detailed description of the experimental conditions in particular of animal (species, weight, acclimatization condition), preparation of the specimen, the composition of the immersing solution and temperature at which exposure is carried out.

Animal

Previously it has been shown (Cossins,1977) (Miller et al., 1976) that the fatty acid composition of goldfish intestinal phospholipids can be modified by a change in environmental temperature. It is assumed that the increase in membrane fluidity of cold acclimatized goldfish is correlated with a decrease in the proportion of saturated fatty acids of the major phospholipids and with increased unsaturation index in choline phosphoglycerides and that this is essential to maintain the normal cellular function at a lower environmental temperature.

In this dissertation, consequently, 2 years old carp are used for experiment which are 10 to 15cm in length, approximately 20g weight, perchased from aqua-pet-shop and kept in aerated water at 20°C - 29°C at least one week before use.

Fish saline

Walf and Quimky (1969) described that mammalian type solutions are entirely satisfactory for many fresh water teleosts and the pH of the medium necessary for good growth of fish cells does not appear to be particularly critical and most cells seem to fare well in the range of pH 7.2 - 7.8. Similar physiological fish saline was proposed by Yamamoto (1949) as, NaCl 0.75%, KCl 0.02%, $CaCl_2$ 0.02% and $NaHCO_3$ 0.002%. In a preliminary experiment, on measuring at room temperature the osmolarity of fish blood by using vapor

pressure osmometer (Mechrolab. Vapor pressure osmometer Model 301A)calibrated by KCl at various concentration, within an accuracy of 2.3%, the blood osmolarity showed the value from 260 mOsM. to 300mOsM., which decreased during the process of coagulation. Kato (1942) also measured the concentration of the body fluid as 0.11M - 0.16M in teleosts by means of freezing point depression.

Hereby the author determined that a suitable fish physiological saline as NaCl 860mg, KCl 30mg, $CaCl_2 2H_2O$ 33mg in 100ml, the pH adjusted with either $NaHCO_3$ or Tris (5mM).

Postmortem deterioration

When the animal is killed, natural denaturation proceeds in unknown way. Intracellular proteases have been implicated in the degeneration through the secondary demyelination of Wallerian degeneration (Gabrieleson,1975). It is impossible to avoid this factor when studying the nerve myelin in situ, even though presently there exists no way to effectively remove this problem. So in this study, carp spinal cord is freshly dissected out and x-ray diffraction pattern is recorded as a function of time after execution.

B. Modification of carp spinal cord by the external perturbation

2-years old carp measuring 10 - 15cm long, purchased from

an aqua-pet-shop were kept in aerated water at 20°C - 29°C for at 1east one weak before use.

Carp spinal cord was dissected out and chopped sections (about 3mm long), stored in mammalian Ringer's solution at 4°C immediately after decapitation. Sectioned nerve was sealed into glass capillary tube (0.7mm in diameter) with immersing medium and mounted on the x-ray camera with the water circulating system to control the temperature ($\pm$ 1°C). X-ray diffraction patterns were obtained at various time of intervals from the specimens at particular temperature on a Franks camera using singe mirror focused Ni filtered, Cu Kα radiation from a Toshiba sealed-off x-ray tube operated at 40KV, 18mA.

Glutaraldehyde effect was studied on the specimen soaked in glutaraldehyde solution for 1 hour followed by washing in normal Ringer's solution for 1 hour at 4°C in the same way as for the non-treated nerve. Exposure time routinely was 2 or 4 hours. Glutaraldehyde solution (0.25% or 3%) was prepared by dissolving glutaraldehyde solution (25% solution, Nakarai Chemicals LTD., without further purification) in mammalian Ringer's solution. The effect of glutaraldehyde in monomeric form (0.25% in mammalian Ringer's solution) on carp spinal cord was studied preliminarily , where the concentration of glutaraldehyde was determined chemically (Frigerio and Shaw,1969) and optically (Gillett and Gull,1972) (Rasmussen and Albrechtsen,1974).

Mammalian Ringer's solution for carp nerve myelin experiment was composed of NaCl(860mg), KCl(30mg), $CaCl_2 2H_2O$(33mg) in 100ml total volume adjusted to pH 7.3 by $NaHCO_3$ or by Tris (5mM).

For the comparison between the in vivo and in situ experimental systems and to establish the effects of natural degradation, x-ray diffraction patterns from freshly dissected carp spinal cord sealed in capillary tube without Ringer's solution were recorded at various intervals after the animal was killed.

The pH effects were studied on carp spinal cord myelin (3mm long and 0.7mm in diameter) immersed in incubation medium (100ml) at 23°C for 16 hours after execution. Incubated nerve section was sealed in the thin walled glass capillary tube with immersion medium and mounted on the x-ray camera. Exposure was carried out for 2 hours at 23°C. Incubation medium in 100ml total volume was prepared by dissolving NaCl(860mg), KCl(30mg), $CaCl_2 2H_2O$(33mg) and reagent(5mM) to adjust pH to the desired value, Glycine for pH 3.1, Potassium Biphthalate for pH 4.0 and pH 5.3, Histidine Monohydrochroride Monohydrate for pH 6.2, Tris for pH 7.3 and Glycylglycine for pH 9.1.

In addition the effect of calcium ions was studied for carp spinal cord by detecting the x-ray diffraction patterns from carp spinal cords incubated at various intervals in Ringer's solution without calcium which was composed of NaCl(880mg), KCl(30mg) and Tris(60.6mg=5mM) in 100ml to be osmometrically identical to normal

Ringer's solution (pH 7.3). Experimental procedures (incubation of carp spinal cord and x-ray exposure) were carried out at 23°C ±1°C. As a control carp spinal cord incubated in Tris buffered Ringer's solution containing calucium ions was in parallel exposed to x-rays. Exposure time was 2 or 4 hours long.

4-3 Results

A. Time dependence of x-ray diffraction pattern from carp spinal cord

Fig. 4-1 shows the x-ray diffraction patterns from the same carp spinal cord preincubated in Ringer's solution at 4°C for 2 hours at various periods after execution. All figures are depicted on the same scale by microdensitometer tracings. At 3 hours after execution two phases can be recognized, one of which shows 2nd, 3rd, 4th and 5th order reflections of 155Å phase (I-phase) and the other shows 2nd, 3rd and 4th order reflections of 183Å phase (II-phase). The former is more dominant than the latter at first. As time goes on reflections of the I-phase gradually decrease in intensity, while the II-phase reflections become dominant. At 23 hours after execution almost only the II-phase reflections can be detected. From this densitometer tracings, respective parameters as periodicity, diffracting power, structure factor and half width

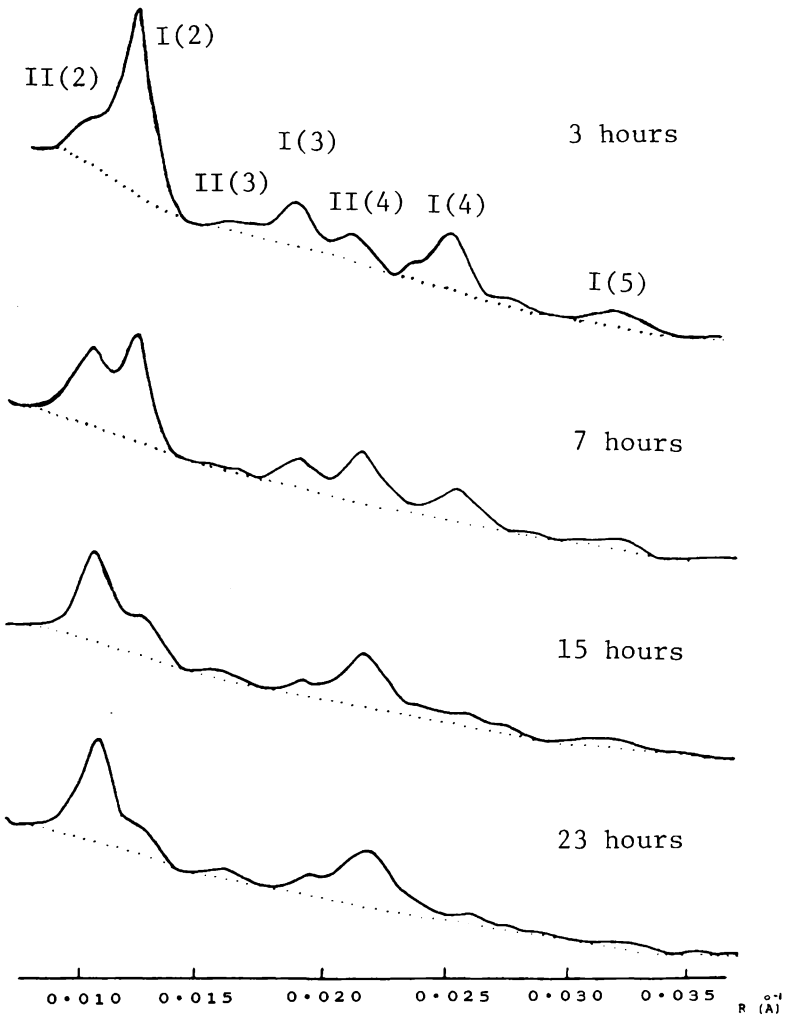

Fig. 4-1 Densitometer tracings vs. diffraction angle for carp spinal cord myelin with time after execution.

of each reflection were calculated to make this structural change more clearly understood.

Periodicity

As rigorously discussed in chapter 2, throughout the experiment up to 40 hours after execution the periodicities of both phases keep constant within the accuracy (1.2%), and are 155Å and 183Å, respectively. No other reflections can be seen which can be ascribed to other phases.

Diffracting power

In Fig. 4-2 are shown the diffracting power of the I-phase (P_I) marked in black circle and the diffracting power of the II-phase (P_{II}) marked in white circle, which are normalized to $P_I(3) + P_{II}(3) = 1.0$, where $P_I(3)$ means the diffracting power of the I-phase at 3 hours after execution. As time passes, the total diffracting power (dotted line) substantially decreases in the similar way as that of the I-phase, while the II-phase at the initial stage increases and reaches a plateau at 9 hours, then keeps constant for up to 40 hours. The decrease is not due to the x-ray damage which was checked and compenstated by the variation of the recording time.

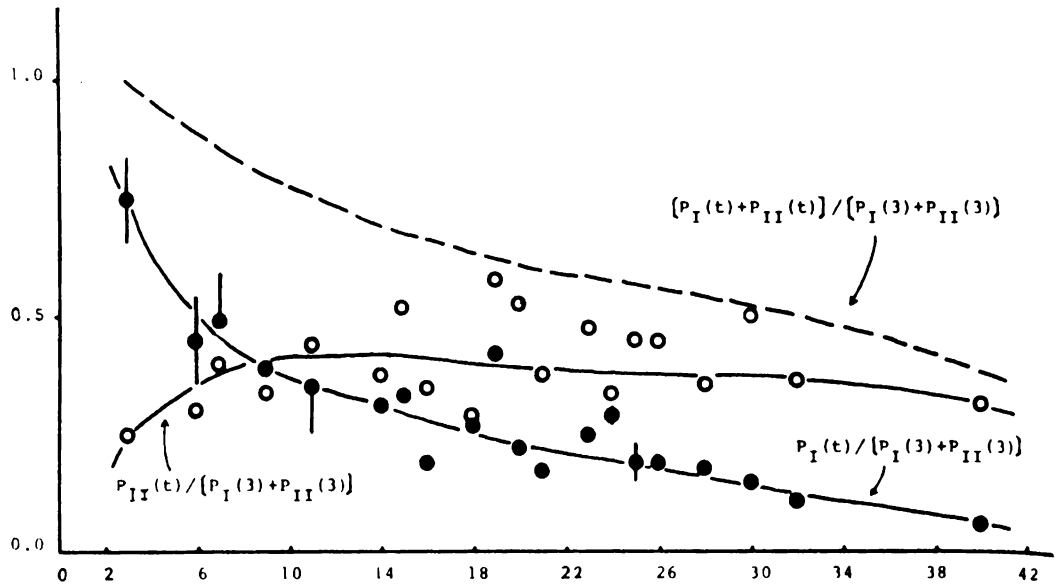

Fig. 4-2 Dependence of the diffracting power on time after execution for the I-phase and the II-phase of carp spinal cord myelin.

Structure factor

In Fig. 4-3 and Fig. 4-4 are shown the structure factors of the I-phase and the II-phase as a function of time after execution. No change can be observed with time in either phase within the limit of detection, thus during the degeneration of nerve myelin the structure of each phase remains unchanged. Therefore it confirms that the asymmetric I-phase structure discretely turns into an symmetric II-phase structure, with a change in periodicity from 155Å to 183Å.

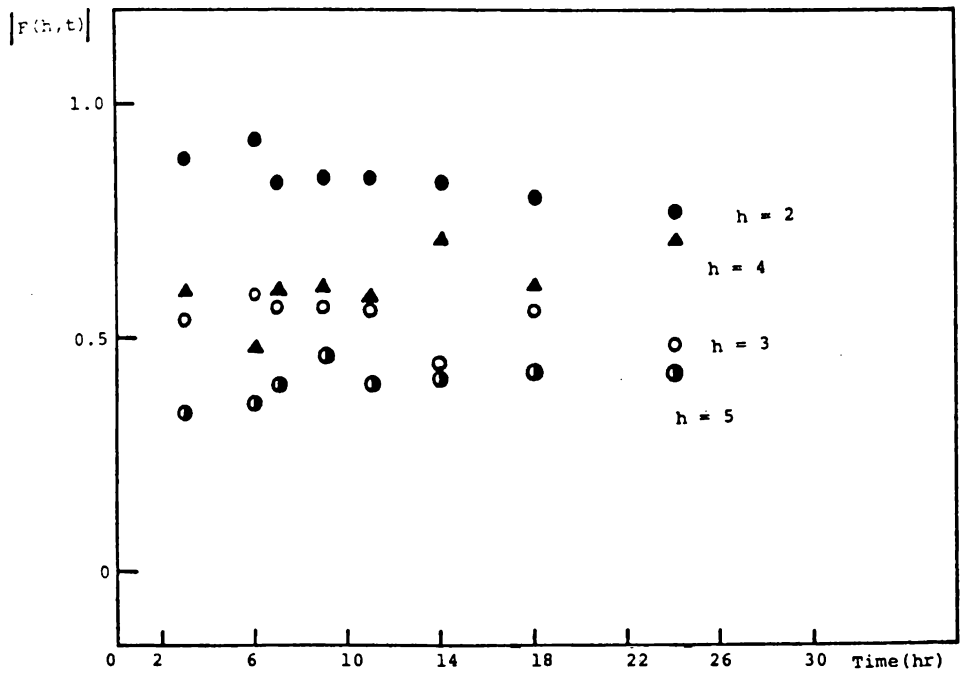

Fig. 4-3 Dependence of the structure factor on time after execution for the I-phase of carp spinal cord myelin.

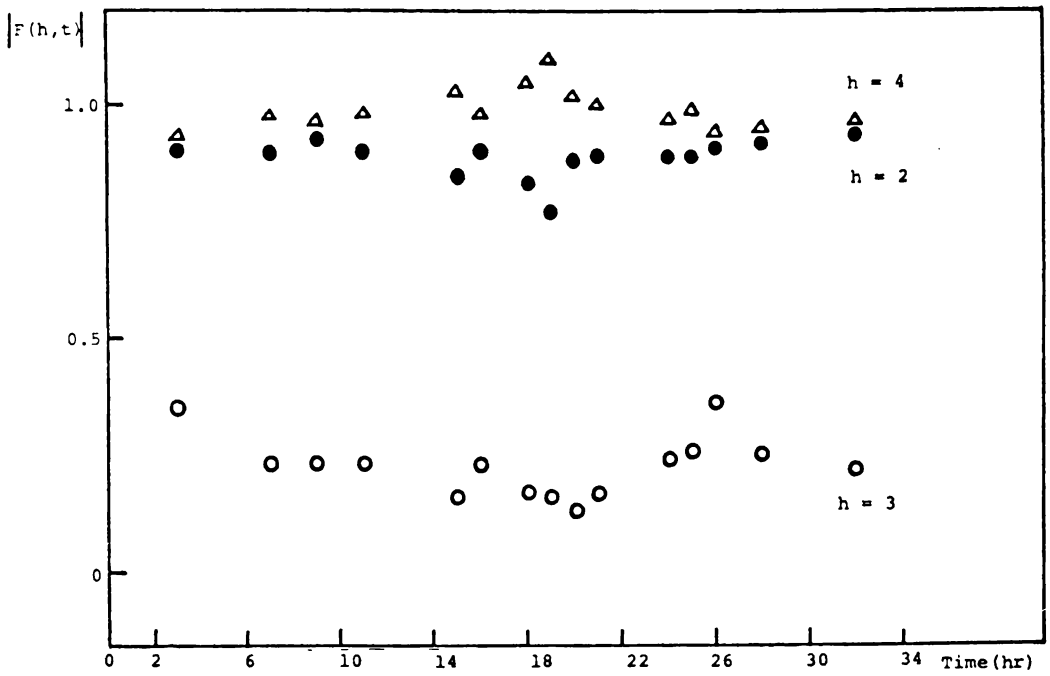

Fig. 4-4 Dependence of the structure factor on time after execution for the II-phase of carp spinal cord myelin.

Half width

Fig. 4-5 and 4-6 show the half widths of the reflections from each phase at various times after execution. As difficulty is encountered in the absolute estimation of the half width, each plot is a value relative to the 2nd order reflection of the I-phase observed at 3 hours. In both phases a common feature is observed, that is the marked broadening with time of the higher order reflections. The slope of the curve in the 4th order reflection from the I-phase is more acute than that from the II-phase, which corresponds, more or less, the increase in the diffracting power of the II-phase. Thus the I-phase is assumed to be a live structure, which after execution decreases in intensity and transforms to the II-phase concomitant with the increase of amorphous region.

B. Temperature effect

In Fig. 4-7 is depicted the I-phase diffracting power ratio, $P_I/(P_I+P_{II})$, as a function of time after execution at 15°C, 23°C and 33°C. Temperature effect was investigated for the sectioned nerve preincubated in mammalian Ringer's solution at 4°C for 2 hours. Fig. 4-7 apparently shows that lower temperature restrains the transformation from the I-phase to the II-phase, while a higher temperature facilitates such a trend. In the range of the temperature from 15°C to 33°C, no change in intensity distribution

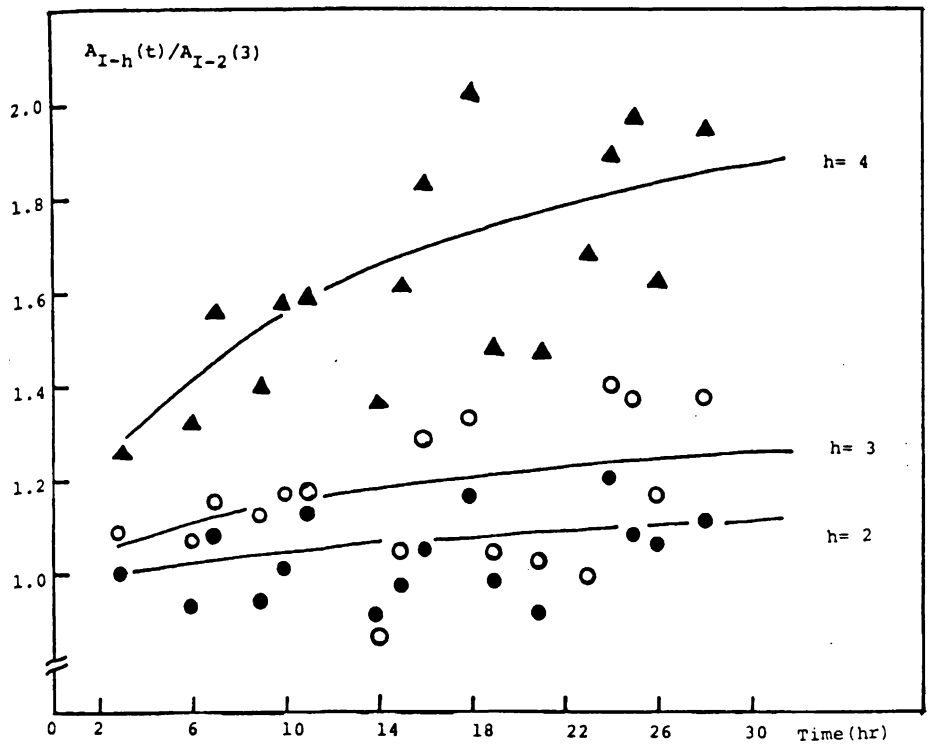

Fig.4-5 Dependence of the half width of reflection on time after execution for the I-phase of carp spinal cord myelin.

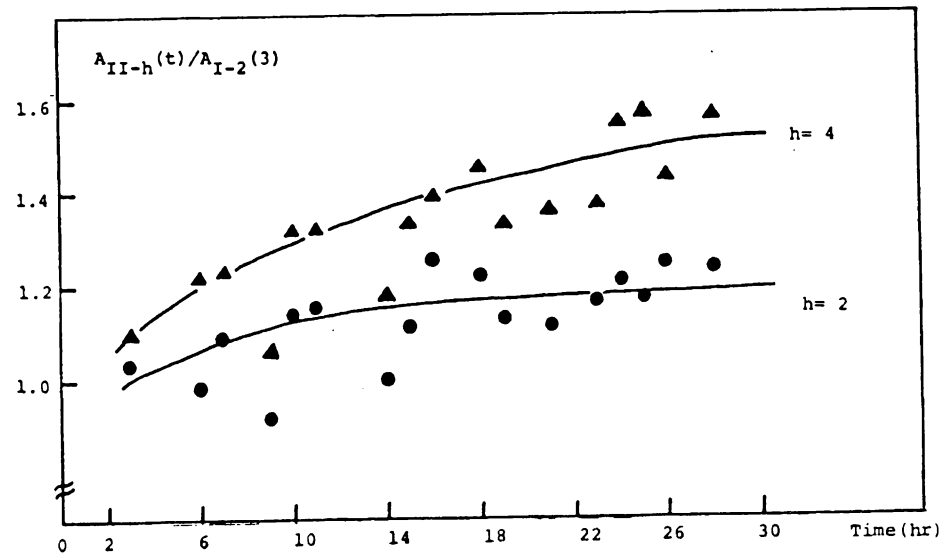

Fig. 4-6 Dependence of the half width of reflection on time after execution for the II-phase of carp spinal cord myelin.

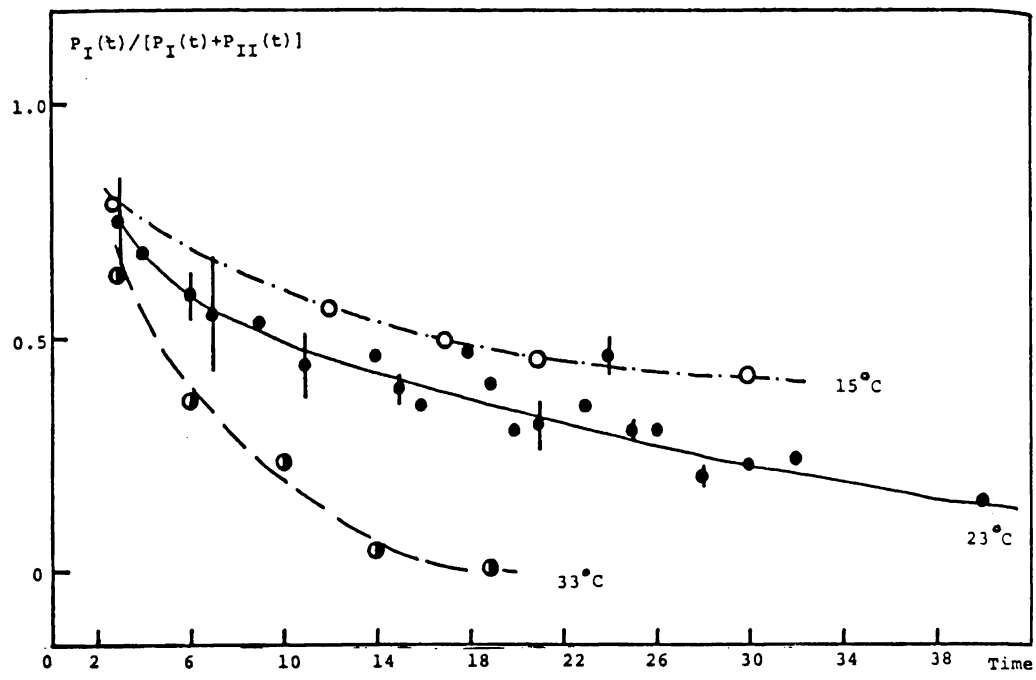

Fig. 4-7 Diffracting power of the I-phase of carp spinal cord myelin with time after execution at 15°C, 23°C and 33°C.

Table 4-1 Periodicity and structure factor of the I-phase and of the II-phase for carp spinal cord myelin at 15°C, 23°C and 33°C.

	15°C		23°C		33°C
$\|F(h)\|$	$d_{I\ 155(1)}$	$d_{II183(1)}$	$d_{I155(1)}$	$d_{II\ 183(1)}$	$d_{II\ 183}$
2	0.81(0.02)	0.84(0.02)	0.84(0.03)	o.89(0.03)	0.89(0.07)
3	0.53(0.02)	0.28(0.04)	0.54(0.04)	0.23(0.05)	0.20(0.03)
4	0.68(0.01)	1.03(0.02)	0.61(0.05)	0.99(0.03)	1.00(0.06)
5	0.40(0.04)		0.41(0.03)		

and in periodicity are observed within limits of detection, which are shown in Table 4-1.

In Fig. 4-8 is depicted the total diffracting power, $P_I(t)+P_{II}(t)$, as a function of time after execution, which is shown as a relative value to the total diffracting power observed at 3 hours after execution. On time passing the total diffracting power gradually decreases, but there is no recognizable dependency on the temperature.

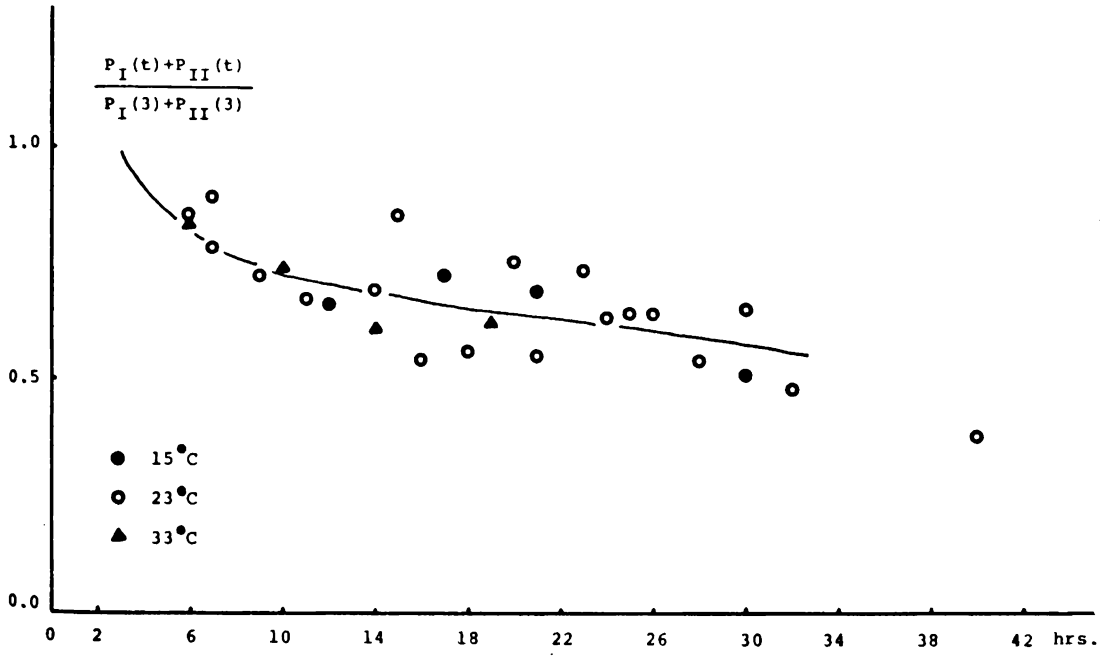

Fig. 4-8 Total diffracting power vs. time after execution for carp spinal cord myelin at 15°C, 23°C and 33°C.

C. Glutaraldehyde effect

Glutaraldehyde effect was examined by recording the diffraction pattern from 0.25% and from 3% glutaraldehyde treated-(for one hour)-and-washed (for one hour) freshly dissected carp spinal cord at various intervals from the time when carp was killed. Glutaraldehyde treatment was carried out at 4°C and the diffraction pattern was recorded at 23°C.

Fig. 4-9 shows the diffraction patterns of the 0.25% and 3% glutaraldehyde treated-and-washed carp spinal cord nerves at 3 hours after execution. In 0.25% treated nerve, the 2nd, 3rd, 4th and 5th order reflections of the I-phase and 2nd and 4th order reflections of the II-phase are visibly identified. The periodicities in both of them, shrink a little to 154Å and 181Å. It is of interest that 3% glutaraldehyde treated-and-washed nerve only gives the broader reflection of the I-phase.

Fig. 4-10 shows the ratio of the diffracting power of the I-phase to the total diffracting power as a function of time after execution for the specimen incubated in glutaraldehyde solution followed by washing the excess glutaraldehyde in mammalian Ringer's solution. Apparent restraining effect of the glutaraldehyde to the transformation from the I-phase to the II-phase is shown. Especially in the 3% glutaraldehyde treatment there is observed no reflections of the II-phase throughout the experiment.

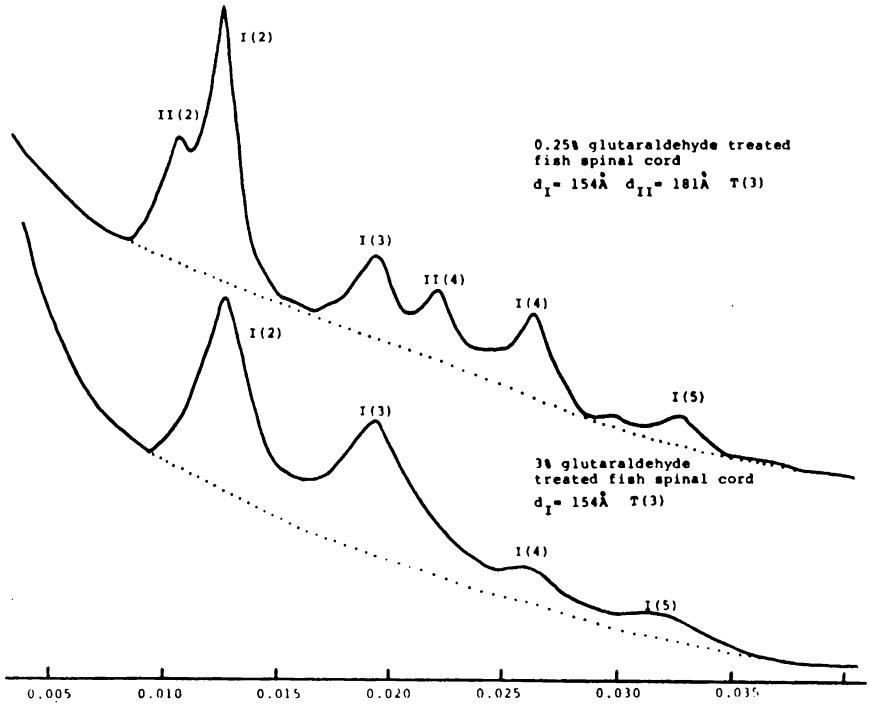

Fig. 4-9 Densitometer tracings vs. diffraction angle ($R=2\sin\theta/\lambda$) for 0.25% and 3% glutaraldehyde treated carp spinal cord myelin.

In Fig. 4-11 is depicted the total diffracting power, $P_I(t)+P_{II}(t)$, as a function of time, which is shown in ratio to the total diffracting power at 3 hours. On time passing no remarkable decrease in intensity was observed for the 3% glutaraldehyde treated nerve, while the total diffracting power of the 0.25% glutaraldehyde treated nerve shows an almost equal decrease as that of the specimen in normal Ringer's solution.

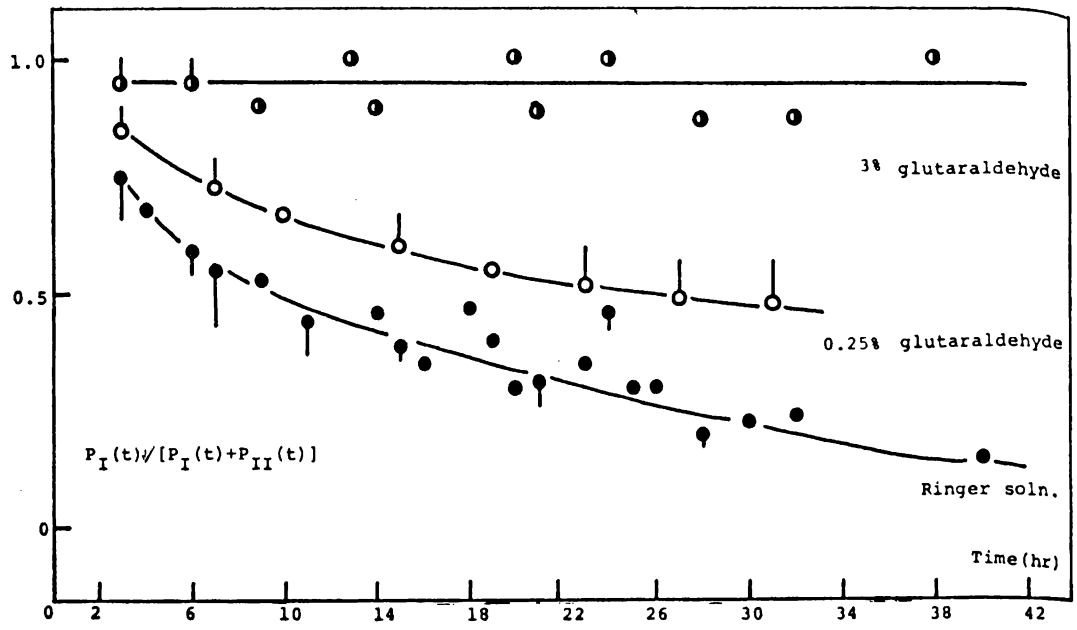

Fig. 4-10 Diffracting power of the I-phase vs. time after execution for glutaraldehyde treated carp spinal cord myelin.

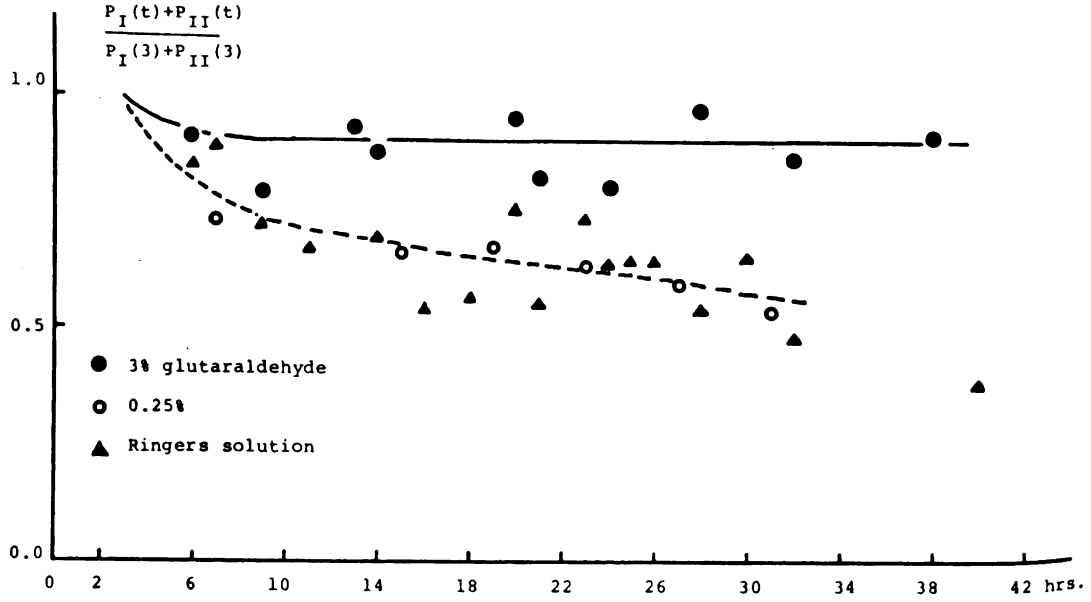

Fig. 4-11 Total diffracting power vs. time after execution for glutaraldehyde treated carp spinal cord myelin.

Throughout the experiment up to 28 hours after execution, the constant values are almost maintained, in periodicity and the intensity distribution. In Fig. 4-12 and 4-13 are shown the structure factors of the 2nd, 3rd, 4th and 5th order reflections in the I-phase from 3% and 0.25% glutaraldehyde preincubated-and-washed carp spinal cord. In the treatment of the glutaraldehyde solution the I-phase and the II-phase shrink slightly and the intensities of the 2nd and 3rd order reflections relatively increase. Those are given in Table 4-2.

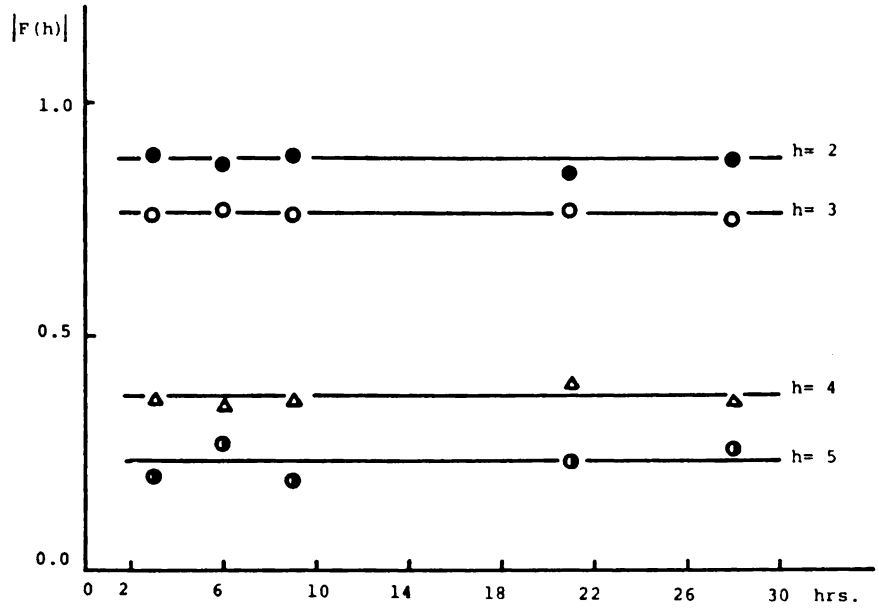

Fig. 4-12 Structure factor of the I-phase vs. time after execution for 3.0% glutaraldehyde treated carp spinal cord myelin.

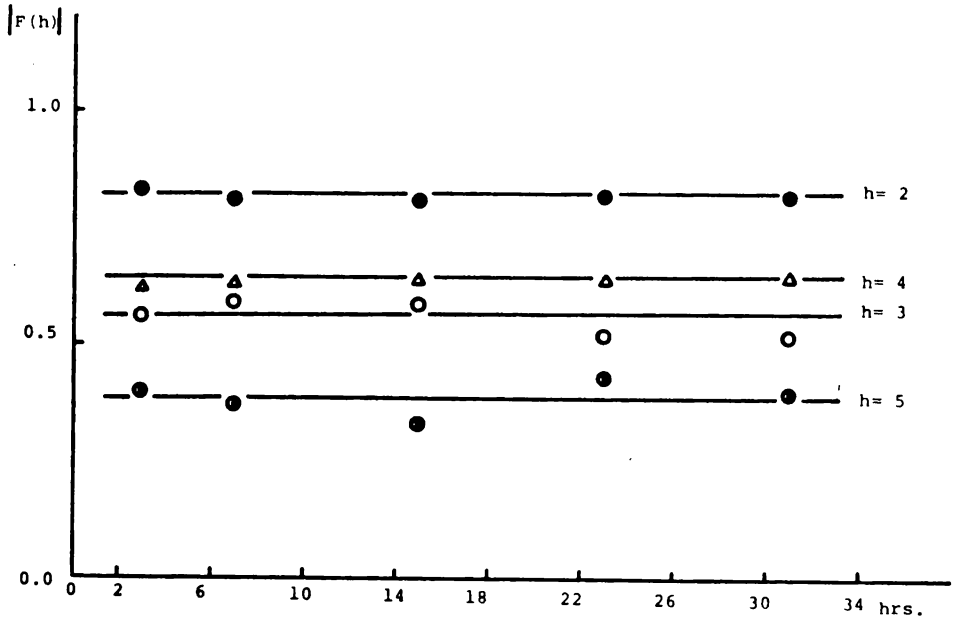

Fig. 4-13 Structure factor of the I-phase vs. time after execution for 0.25% glutaraldehyde treated carp spinal cord myelin.

Table 4-2 Periodicities and structure factors of the I-phase and of the II-phase for 0.25% and 3% glutaraldehyde treated carp spinal cord myelin.

	0.25% G.A.		3% G.A.
	d_I 154 (0.4) Å	d_{II} 181 Å	d_I 154 (1.1) Å
|F(h)|			
2	0.82 (0.01)	0.89	0.88 (0.01)
3	0.56 (0.03)	-	0.76 (0.01)
4	0.64 (0.01)	1.01	0.37 (0.01)
5	0.38 (0.03)	-	0.23 (0.03)

D. The pH effect

X-ray diffraction patterns were observed for carp spinal cord incubated in the various pH buffered bulk Ringer's solutions in the pH range from 3.1 to 9.1 at 23°C. Fig. 4-14 shows the diffracting power ratio of the short period phase to the total diffracting power, $P_I/(P_I+P_{II})$, and the schematic diffraction patterns as a function of pH value. Each point is calculated from the diffraction pattern from carp spinal cord treated for 16 hours at pH buffered bulk Ringer's solution, which has the identical osmometric pressure to the normal Ringer's solution.

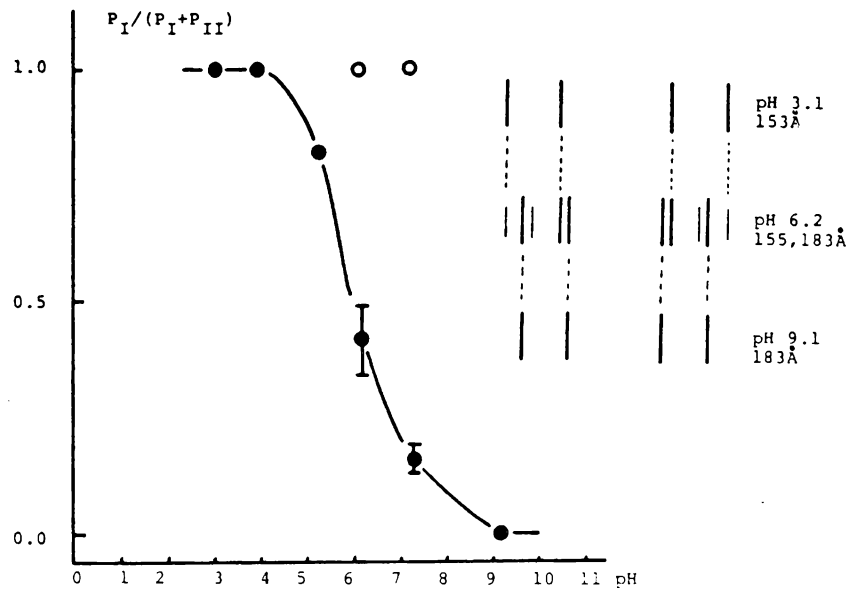

Fig. 4-14 Dependence of the diffracting power of the I-phase on the pH value for carp spinal cord myelin. Glycine for pH3.1, Potassium Biphthalate for pH4.0 and 5.3, Histidine Monohydrochroride Monohydrate for pH6.2, Tris for pH7.3, Glycylglycine for pH9.1, each in marked in (•), Phosphate fuffered solution for pH6.2 and 7.3,(o)

On increasing the incubation time, at pH from 5.3 to 9.1, the sharp increase of the long period phase (II-phase) and the decrease of the short period phase (I-phase) in intensity were observed, although the periodicities and the intensity distributions of the two phases (155Å and 183Å) were preserved. As the pH increases the transformation from the I-phase to the II-phase was accerlerated. Below the pH value 4.0, however, the intensity of the odd order reflection of the I-phase (155Å) gradually decreases, concomitantly the periodicity also decreases. For example Fig. 4-15 shows the dependence on the incubation time of the diffraction pattern from the nerve treated by the buffered solution at pH 3.1. After the nerve is incubated for 2 hours at 23°C then sealed in the thin walled glass capillary tube with treatment solution, 2 hours long exposure gives the 155Å and 183Å phase, whose intensity distribution each is equal to the observed value at pH 7.3. After 3 hours long incubation the 2nd, 3rd, 4th and 5th order reflections of 152Å phase are observed and the intensity distribution is changed in such a way that the 3rd and 5th order reflection decrease in intensity. On further treatment for example after 16 hours, there is no odd order reflection. In Table 4-3 are shown the structure factor and the periodicity of the I-phase observed at pH 3.1.

When Tris buffered Ringer's solution without calcium ions is applied to freshly dissected carp spinal cord for up to 28 hours

at 23°C the long period phase cannot be detected from any nerves. But the 2nd, 3rd, 4th and 5th order reflections of the 155Å phase can be observed. The intensity distribution is identical to that from carp spinal cord incubated in Tris buffered Ringer's solution containing calcium ions.

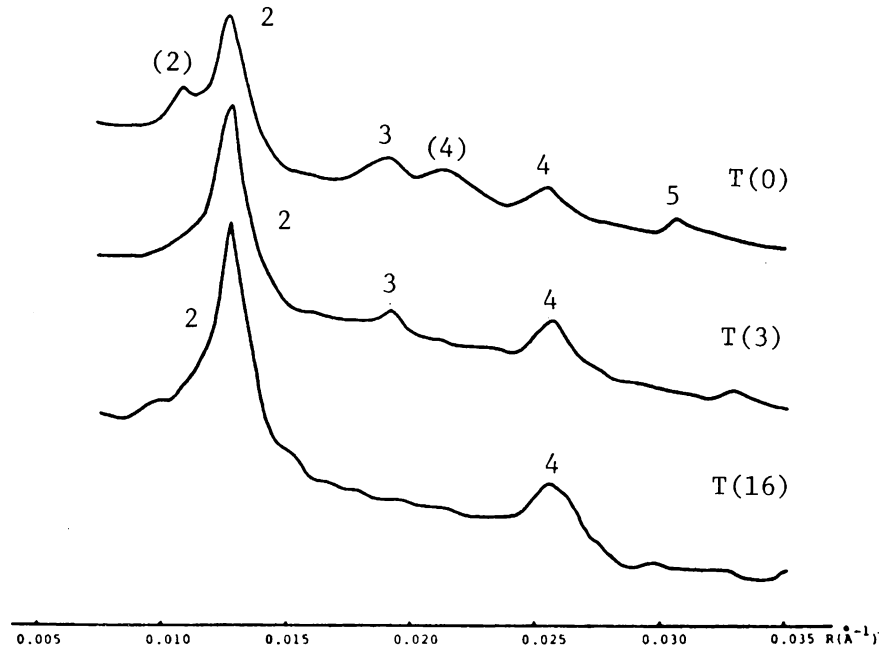

Fig. 4-15 Densitometer tracings vs. diffraction angle for carp spinal cord myelin in pH 3.1 Ringer's solution after different hours of incubation.

Table 4-3 Periodicity and structure factor of a short period phase for carp spinal cord incubated for different time in pH 3.1 bulk Ringer's solution.

Incubation time (hrs.)	0	3	16
periodical distance	155 Å	152 Å	152 Å
|F(h)|			
2	0.88	0.94	1.00
3	0.52	0.37	-
4	0.61	0.68	0.72
5	0.36	0.18	-

E. Behaviour of x-ray diffraction pattern for carp spinal cord without Ringer's solution and deterioration in the carcass

In an attempt to study the natural denaturation of the carp nerve myelin the x-ray diffraction pattern was observed for the freshly dissected nerve and for the nerve kept in the carcass. The former nerve was sealed in the capillary tube without Ringer's solution and the latter was dissected out from the animal which was killed 26 hours before, then sealed in capillary tube with no solution. In both of them the diffraction pattern was taken at various intervals after the head was cut off. For comparison x-ray diffraction pattern was also observed from the nerve sealed with Tris buffered Ringer's solution. All the experimental pro-

cedures were carried out at 23°C.

On time passing the reflections from the short period 155Å phase (I-phase) weaken and those from the long period 183Å phase (II-phase) are intensified. For both phases no significant changes in intensity distribution and the periodicity were observed.

Fig. 4-16 shows the behaviour of the diffracting power ratio for the I-phase as a function of time after execution. For both cases, freshly dissected and kept in carcuss, the transformation of the I-phase to the II-phase occurred with almost the same velocity. However, the diffracting power ratio for the I-phase of the nerve kept in carcass throughout the experiment is smaller than that forthe freshly dissected nerve. Of interest is the fact that the nerve soaked with no solution gives appreciably high value of the diffracting power ratio for the I-phase in comparison with that for the nerve soaked in pH 7.3 buffered Ringer's solution. This transformation is not due to the dehydration, because when nerve was sealed in capillary tube with distilled water just to maintain the humidity, the same transformation was also detected.

F. Comparison of the x-ray diffraction patterns from carp spinal cord (CNS), optic nerve (CNS) and lateral line (PNS)

X-ray diffraction patterns from carp optic nerve and lateral line were observed. Freshly dissected lateral line and optic nerve were sealed into thin walled glass capillary tube with mammalian

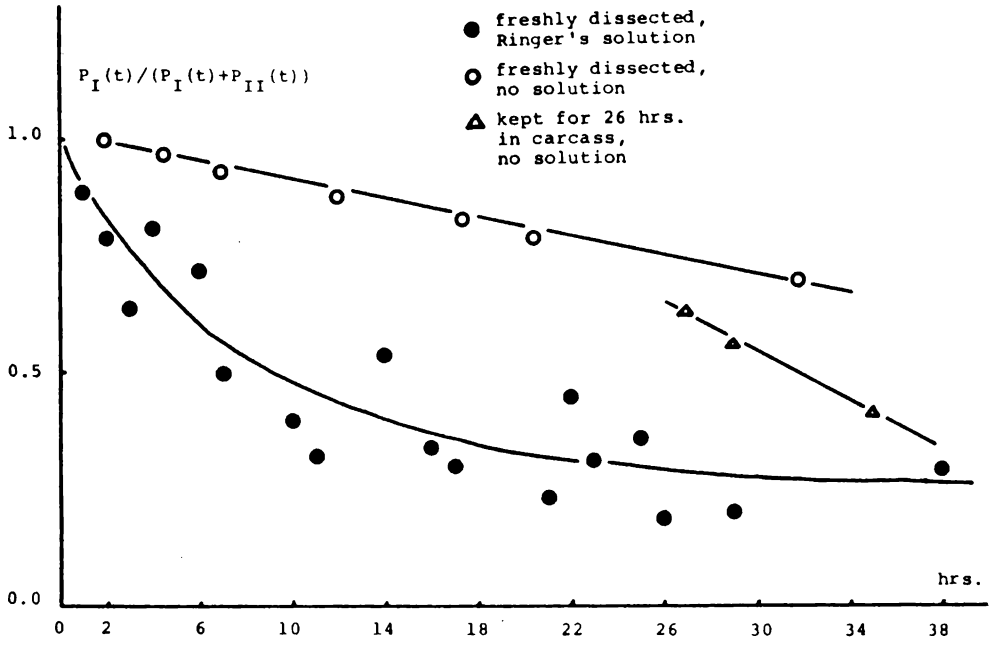

Fig. 4-16 Diffracting power of the I-phase vs. time after execution for freshly dissected carp spinal cord in Ringer's solution, freshly dissected carp spinal cord without solution and carp spinal cord kept in carcass.

Ringer's solution. X-ray diffraction patterns were observed from them at various intervals. Temperature of the specimen was maintained at 23°C $\pm$ 1°C, which was controlled by the constant temperature water circulating system. Exposure was routinely two or four hours long.

In Fig. 4-17 and 4-18 the diffraction patterns for lateral line and optic nerve are shown by their densitometer traces. At one hour after execution the lateral line shows the 1st, 2nd, 3rd

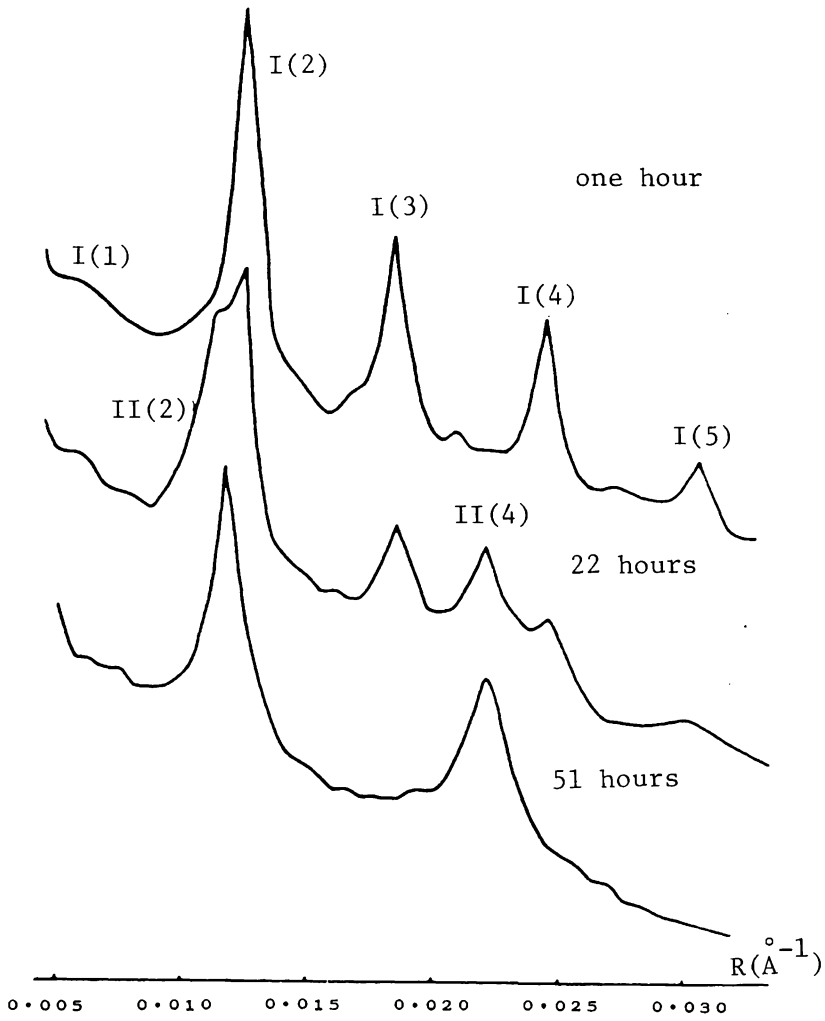

Fig. 4-17 Densitometer tracings vs. diffraction angle for carp lateral line with time after execution.

, 4th and 5th order reflections of 154Å phase. On time passing there come to appear the new phases, which have 179Å and 182Å periodicity for lateral line and optic nerve, respectively. In the

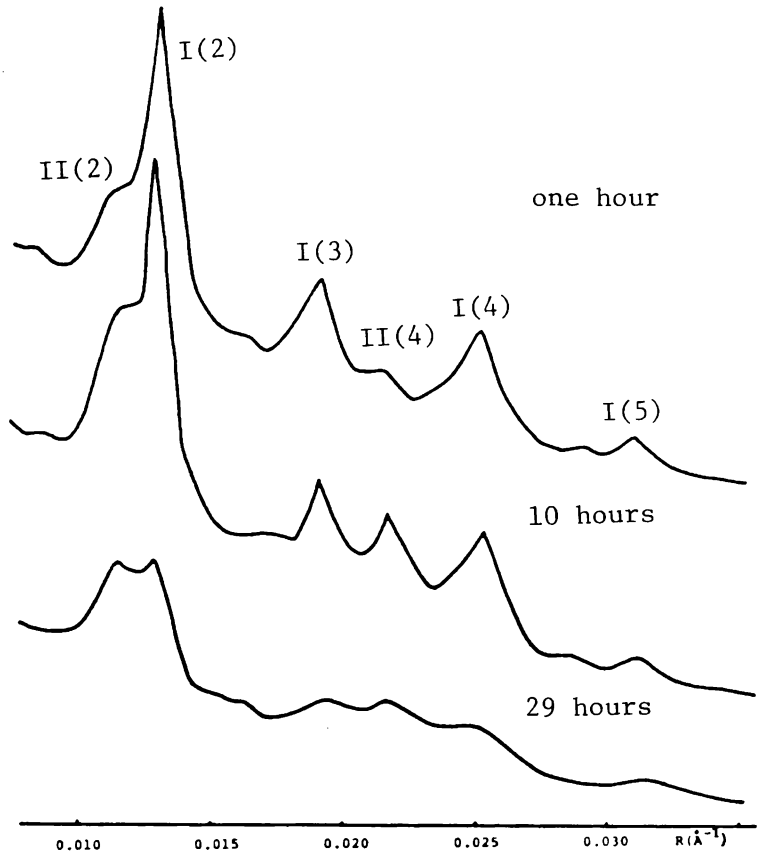

Fig. 4-18 Densitometer tracings vs. diffraction angle for carp optic nerve with time after execution.

end the short period phase cannot be detected. Throughout the experiment no reflections ascribed to other phases were observed. Fig. 4-19 shows the diffracting power ratio of short period phase (I-phase) to the total diffracting power. As time passes the occupancy of the I-phase decreases in all nerves, spinal cord, optic nerve and lateral line. However, as to the velocity of the

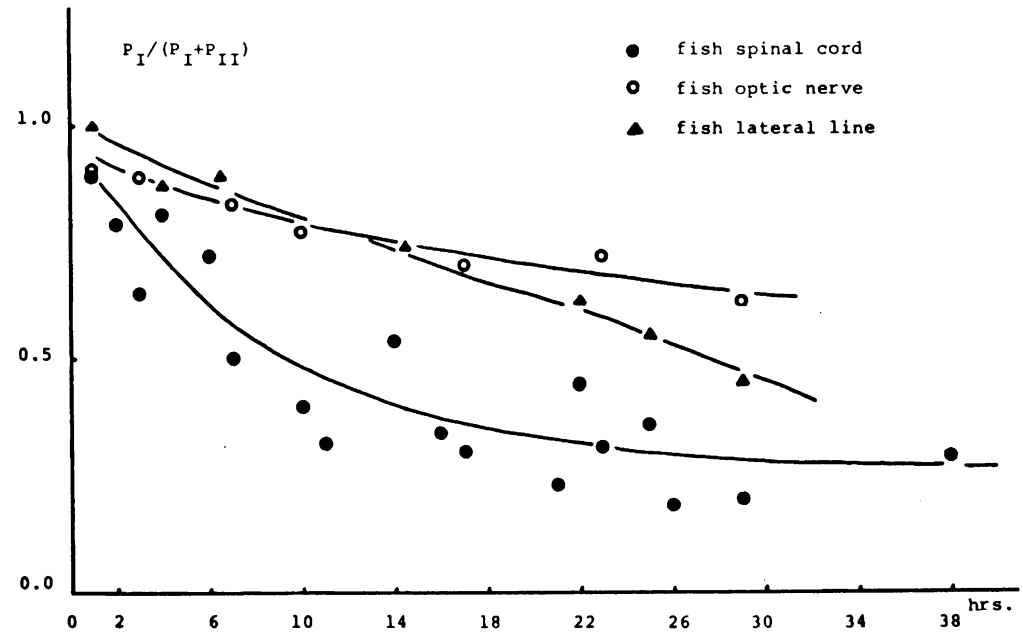

Fig. 4-19 Diffracting power of the I-phase vs. time after execution for carp spinal cord, carp optic nerve and carp lateral line.

transformation, the lateral line and the optic nerve do not show the marked reduction as the spinal cord does.

During the course of the transformation there are no significant changes in the periodicity and the intensity distribution for the short and the long period phase, which are shown in the Fig. 4-20, Fig. 4-21 and Table 4-4. At any time the optic nerve gives almost an identical structure after execution as that of the spinal cord, while the I-phase of the lateral line gives a little longer period and rather intense 3rd order reflection. No remarkable

change was detected for the II-phase.

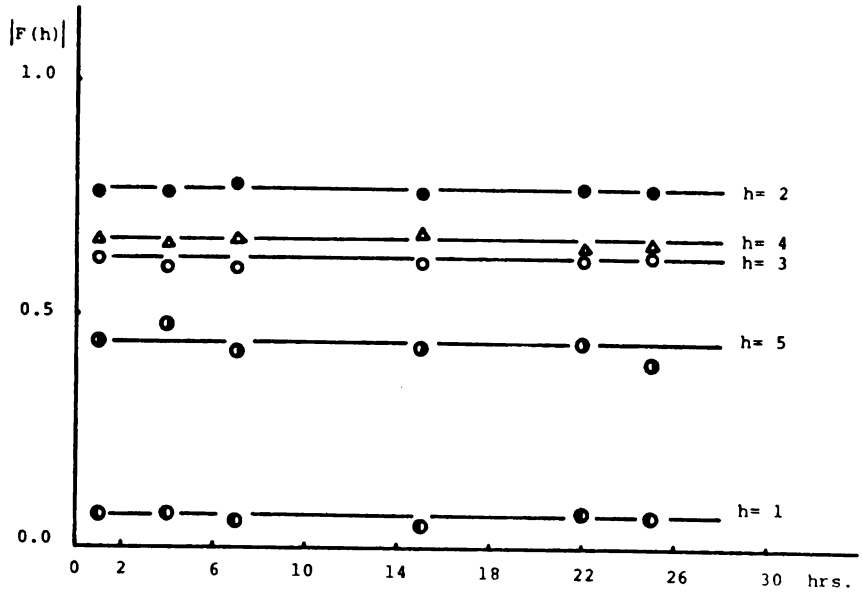

Fig. 4-20 Structure factor of the I-phase vs. time after execution for carp lateral line.

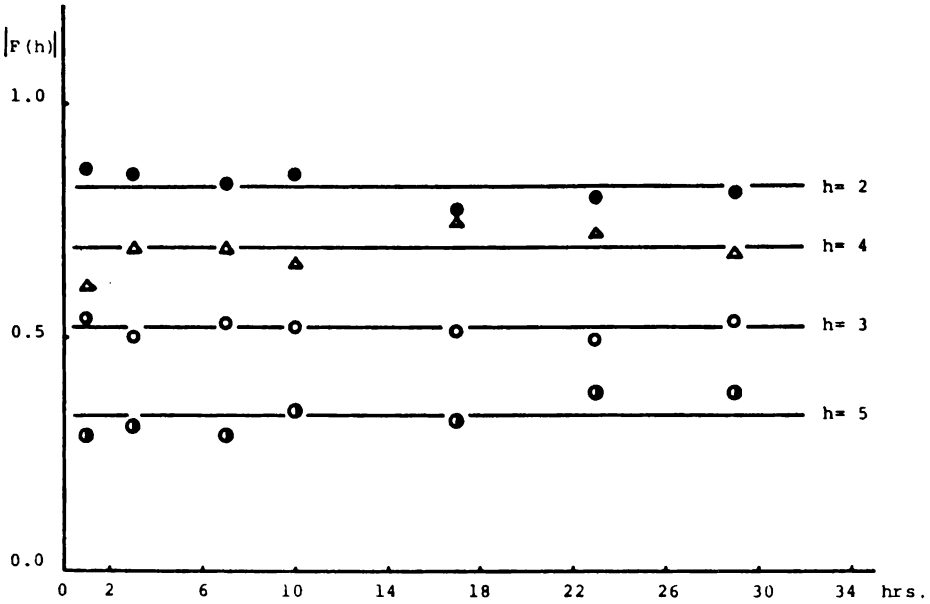

Fig. 4-21 Structure factor of the I-phase vs. time after execution for carp optic nerve.

Table 4-4 Periodicity and structure factor of the I-phase and of the II-phase for carp lateral line (F.L.) and for carp optic nerve (F.OP.).

	F.L.		F.OP.	
	d_I	d_{II}	d_I	d_{II}
$\|F(h)\|$	160(1)	179(2)	154(1)	182(1)
1	0.07(0.01)	-	-	-
2	0.77(0.01)	0.94(0.04)	0.82(0.03)	0.93(0.05)
3	0.62(0.01)	-	0.52(0.01)	-
4	0.66(0.01)	0.95(0.04)	0.69(0.02)	0.97(0.05)
5	0.44(0.02)	-	0.33(0.03)	-

G. Electron density profiles for the I-phase and the II-phase

Fig. 4-22 and 4-23 show the electron density distribution profiles for the I-phase (155Å) and the II-phase (183Å) from carp spinal cord and the I-phase (160Å) from carp lateral line. These profiles were calculated using diffraction data to 31Å (2, 3, 4 and 5 order) for the 155Å, up to 46Å (2, 3 and 4 order) for the 183Å phase and to 32Å (1, 2, 3, 4 and 5 order) for the I-phase (160Å) from carp lateral line. Sign relations for the diffraction spectra were assigned so that the density profiles correspond with the established membrane bilayer profiles of peripheral and central nerve myelin, thus + + - - for the I-phase of the carp spinal cord, + + - for the II-phase of the carp spinal cord and

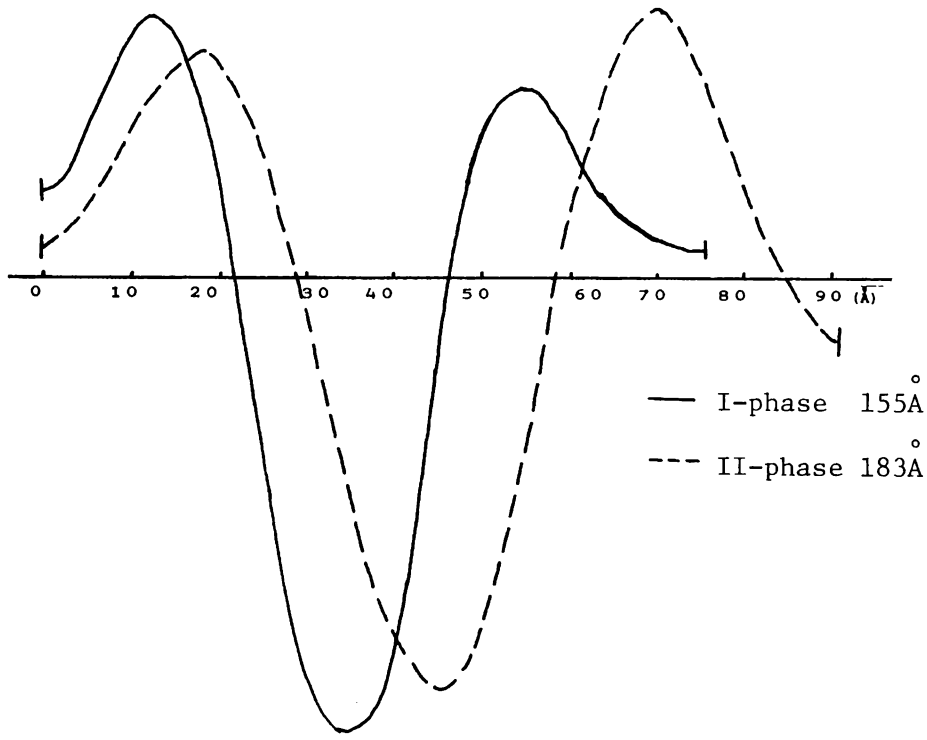

Fig. 4-22 Calculated electron density profiles of myelin membrane units for the I-phase and the II-phase of carp spinal cord myelin as a function of distance from the cytoplasmic boundary.

- + + - - for the I-phase from carp lateral line, respectively, were assigned. Fig. 4-24 and 4-25 show the electron density profiles calculated by assigning all sign relations.

From those profiles from carp spinal cord the distances from peak to peak at the cytoplasmic interface and at the extracellular interface and the width of the lipid bilayer are calcu-

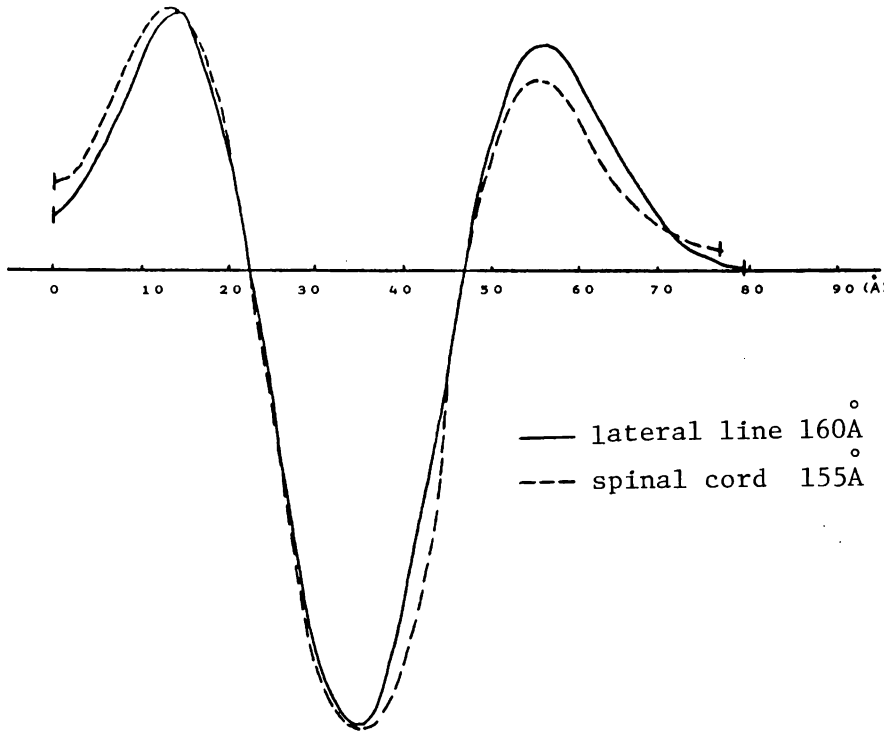

Fig. 4-23 Calculated electron density profiles of myelin membrane units for the I-phase of lateral line myelin and the I-phase of spinal cord myelin as a function of distance from the cytoplasmic boundary.

lated as 26Å, 44Å and 42Å for the I-phase and 37Å, 52Å and 45Å for the II-phase. As to the half of the lipid bilayer at the external side the I-phase and the II-phase are similar in peak to peak distance and in the shape of the peak. The II-phase shows marked expansion of the lipid bilayer and of the cytoplasmic space. In addition the electron density of the II-phase at the cyto-

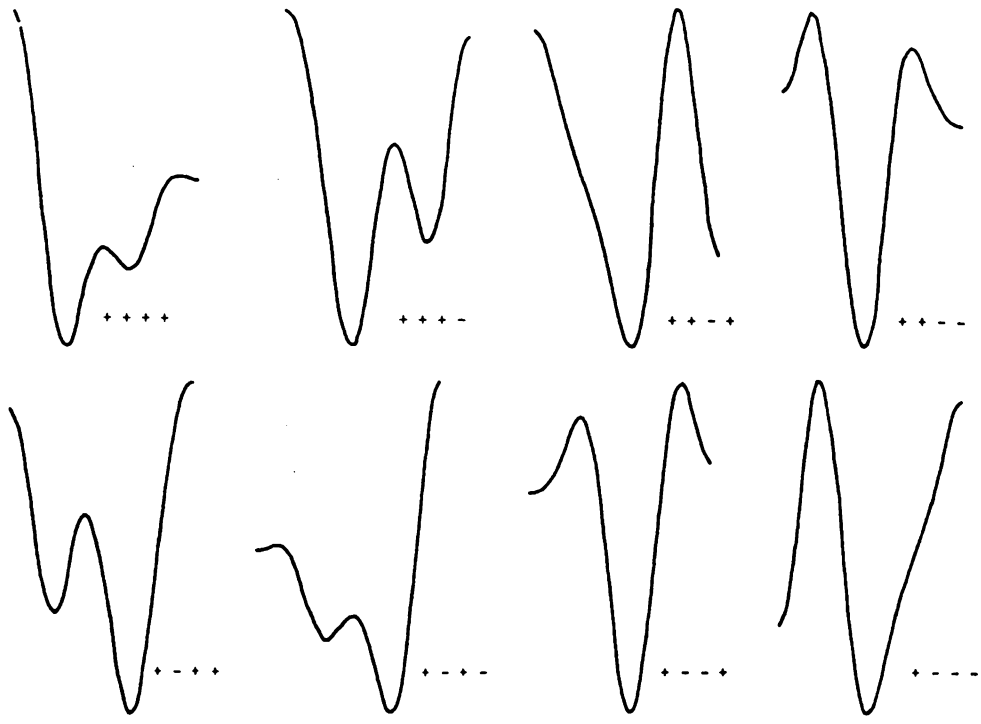

Fig. 4-24 Calculated electron density profiles with all sign relations of myelin membrane units for the I-phase of carp spinal cord myelin.

plasmic peak is lower than that of the I-phase. In both phases, however, a symmetric shape of the lipid bilayer portion is commonly observed.

Hence it is shown that the components in the cytoplasmic layer are most seriously affected in accord with the transformation from 155Å (I-phase) phase to 183Å (II-phase) phase, and

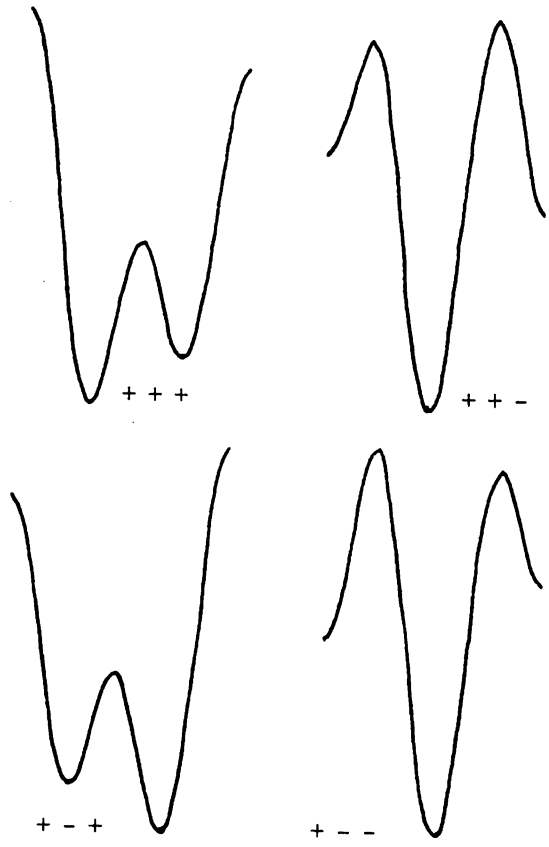

Fig. 4-25 Calculated electron density profiles with all sign relations of myelin membrane units for the II-phase of carp spinal cord myelin.

the changes of these components in distribution or in conformation might effect the packing of the lipid bilayer.

Comparison between the profiles of carp spinal cord (FSP) and carp lateral line (FL) shows that the difference in the periodicity by 5Å is mainly due to the separation at the external space. For the overall shape of the density profile they share the same

features in several points such as the electron density at the high dense peak on the cytoplasmic side is higher than that at the external side and that the electron density of the lowest trough is identical in both nerves. Thus the main structural difference between them lies in the external space.

Carp lateral line (FL) also shows the irreversible transformation from the I-phase (160Å) to the II-phase (179Å) which has the same structure as observed in spinal cord (FSP) or optic nerve (FOP).

Therefore it is suggested that the cytoplasmic side is closely correlated with the abnormal structural fragility of the fish nerve myelin. Furthermore it may be associated with the structural difference between fish nerve myelin and other vertebrate's nerve myelin.

4-4 Discussion

The significance of the in situ experimental system

Up to now there has been no explanation given as to the reason of the coexistence of the two structure phases in fish spinal cord, which are defined as the longer period phase (II-phase) and the shorter period phase (I-phase). In this x-ray diffraction study the following points are especially taken into

consideration to get reliable data, that is 1) adaptation condition, 2) immersion medium, 3) the effect of postmortem deterioration.

The effect of temperature acclimation on fish has been reported to induce a change in the chemical composition of fish membrane such that the structure is maintained in a fluid state. For example Miller et al. (1976) showed an increase in the proportion of unsaturated fatty acid chains as the environmental temperature falls in microsomal fractions of goldfish intestine. Similar adaptive changes have been mainly observed in microorganisms. One reason for such changes in lipid composition is the need to keep the viscosity of membrane lipids at a constant level , a process for which Sinensky (1974) has coined the term " *homeoviscous adaptation* ". For this reason fish were maintained at 20°C - 29°C for at least one week before use in this study.

As immersion medium, mammalian Ringer's solution (5mM Tris buffer, pH 7.3) was used, the osmolarity of fish blood having been found to be almost identical to that of mammalian blood.

In this study to estimate the postmortem deterioration the exact times at which fish are killed, dissected and when x-ray diffraction pattern is recorded are carefully noted. As shown in the section of experimental results x-ray diffraction patterns for sectioned carp spinal cord with mammalian Ringer's solution (pH 7.3) observed at intervals from execution show a certain system

atic modification of carp spinal cord myelin in such way that the shorter period phase is replaced by the longer period phase. Up to 40 hours after execution reflections ascribed to other phases have not been detected and the structures of the two original phases do not change in either periodicity or structure factor. Even though the total diffracting power reduces with time, a substantial increase in the contribution of the II-phase (183Å) to the diffracting power was observed.

Thus it is concluded that in situ the shorter period phase discretely transforms to the longer period phase.

From this experimental result it is presumed that in the physiological live state carp spinal cord nerve myelin exists in the short period phase structure. In fact the carp spinal cord dissected out from the animal which was killed one or two days previously showed a marked reduction of 155Å phase and increase of 183Å phase. In addition, as shown in Fig. 4-16 sectioned nerve sealed in a capillary tube without solution also gives a reduction of the I-phase with time. However such a reduction is not so marked as for the nerve perfused in mammalian Ringer's solution. In the former sample the shorter period phase has approximately 80% of the total diffracting power at 24 hours after execution, whereas in the latter case it has only 30%.

On the other hand from the experiments in situ, the close correlation between two phases was demonstrated, so the trans-

formation from the I-phase to the II-phase must be induced on the membrane just like a phase segregation.

Thus there are two interest problems in this in situ system, one of which is the mechanism of nerve degeneration and the other is the structureal relationship hetween PNS and CNS nerve myelin. Using this system it might give useful information on how nerve myelin degenerates and on what is the structural difference between peripheral and central nerve myelin.

Structural difference between two phases

On the treatment by glutaraldehyde solution in mammalian Ringer's solution carp spinal cord does not give a significant reduction of the I-phase and increase of the II-phase. Particularly in the case of 3% glutaraldehyde solution, no expanded long period phase can be seen. This shows that glutaraldehyde restricts the transformation from the I-phase to the II-phase. As glutaraldehyde is extensively used as a crosslinking or fixing reagent in the electron microscopy or biochemical studies (Sabatini et al., 1963) (Steck,1972), it appears that crosslinking of some components in nerve myelin may restrain this modification. Wood (1973) reported glutaraldehyde crosslinks basic protein, proteolipid protein and higher molecular weight components, which indicates that membranous proteins are at least responsible for the gross structural transformation. Other external perturbations, high

pH and calcium ion exert facilitating effect on the transformation from the I-phase to the II-phase. These factors are involved in the ionic interactions, so it is possible to deduce the intimate relationship between the basic protein and the structural modification, for basic protein is easily extracted by acid solution and salt solution.

It is well known that in demyelinating disease such as multiple sclerosis the basic protein selectively disappears with an increase of the acid proteinase (Einstein et al.,1972) and in vitro system it was also shown that the basic protein is readily hydrolyzed by acid proteinase (Einstein,1972) (Marks and Lajtha,1971) (Sammeck et al.,1972). These observations also suggests the intimate involvement of basic protein in structural modification. The electron density distribution profiles suggest the marked alteration during the process of the natural degradation. Recent biochemical research agrees in that the basic protein resides in the cytoplasmic side (Carnegie and Dunkley,1975). Hence, distribution or conformation of the basic protein is primarily affected and the protein to protein interaction may be altered. Then in result the above transformation can be induced.

Such natural degradation cannot be clearly observed in other animals, so the question remains as to why fish spinal cord especially shows this curious behaviour. Some reason may be ascribed to the protein composition, for Mehl and Halaris (1970)

reported that when cerebral myelin samples are subjected to gel electrophoresis in phenol solvent, fish nerve myelin gives two protein zones (Mc 0.71 and Mc 1.00) as the basic protein which gives a single band (Mc 0.82) from other vertebrates. As to the lipid composition in fish there is no marked difference from that in other vertebrates (Cuzner, Davison and Gregson,1965).

Two phases present in fish spinal cord are quite similar in period to mammalian PNS and CNS nerve myelin. Mateu et al. (1973) demonstrated that a model membrane composed of PNS or CNS basic protein and acidic lipids shows an almost identical periodicity to that of intact membrane, while the complex of proteolipid and lipid was reported to give lipid-like diffraction pattern (Rand et al.,1976).

Therefore it is speculated that the distribution of the basic protein might be involved in the structural difference between the 155Å phase and 183Å phase.

CHAPTER 5

CORRELATION OF X-RAY DIFFRACTION PATTERNS OF CENTRAL AND PERIPHERAL NERVE MYELIN

5-1 Introduction

There are two types of nervous systems, peripheral (PNS) and central (CNS) nervous systems, in the former of which the myelin sheath is derived from infolded plasma membrane of Schwann cell and in the latter from that of the oligodendroglia cell. Morphologically and chemically the differences in these two types bave been extensively studied by many workers, of which some characteristics are summalized in the appendix. As to the periodicity of vertebrate nerve myelin in the fresh state x-ray diffraction method showed 170Å - 185Å for PNS and 154Å - 160Å for CNS except for the fish nerve myelin (see appendix Table A-1). Except for fish , in addition, it was clarified that PNS type pattern is quite different from CNS type pattern in the intensity distribution. PNS nerve myelin gives rather intense odd order reflections than CNS nerve myelin. (Fig. 5-1) The external perturbation techniques also elucidated the difference in the structural organization which is integrated by the short and long distance interactions among membranous constituents.

Laying the similar way in this dissertation, information obtained on the correlation of x-ray diffraction patterns for

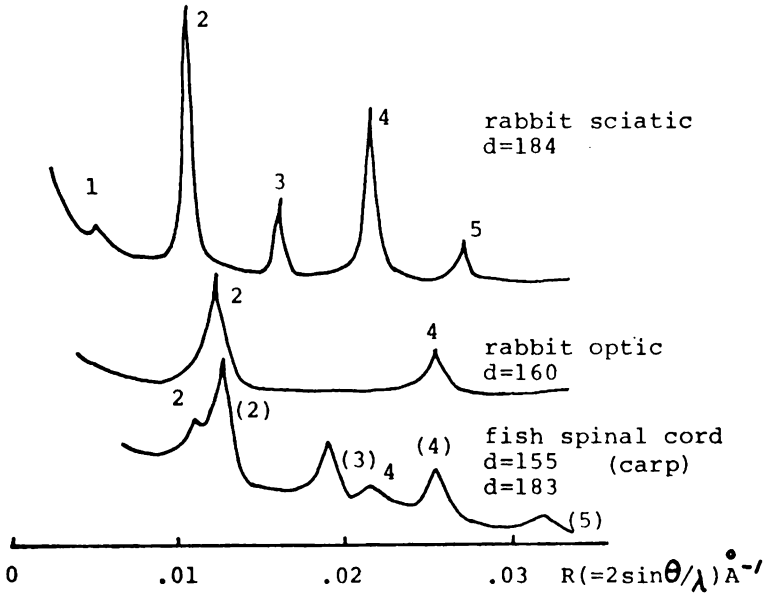

Fig. 5-1 Densitometer tracings vs. diffraction angle for rabbit sciatic nerve myelin, rabbit optic nerve myelin and carp spinal cord myelin.

central and peripheral nerves has been given in former chapters. Hence in this chapter the author aims to extract the differences in the way of integrating membranous components between PNS and CNS nerve myelin for the vertebrates of various origin.

In this regard, the comparison among the x-ray diffraction patterns from various nerve myelins are studied with respects to the periodicity, structure factor and electron density profiles. In the same way comparative studies of the x-ray diffraction

patterns from PNS and CNS nerve myelins were made for each vertebrate. These subjects are depicted in the subsection 5-2.

In the subsection 5-3 are shown the external perturbation experiments on the various nerve myelins.

Concludingly, in subsection 5-4 are described the structural differences in the PNS and CNS.

5-2 The x-ray diffraction patterns for the nerve myelins for various vertebrates

Fig. 5-2 shows the structure factors up to 5th order reflections plotted in the reciprocal space for frog sciatic (Fg.S,171Å), frog optic (Fg.O,155Å), chicken sciatic (Ch.S,182Å), chicken optic (Ch.O,155Å), rat sciatic (Rt.S,176Å), rat optic (Rt.O,159Å), rabbit sciatic (Rb.S,184Å), rabbit optic (Rb.O,160Å), carp spinal cord I-phase (FSP-I,155Å), carp spinal cord II-phase (FSP-II,183Å) and carp lateral line (FL,160Å). Except for rabbit nerve myelin and carp nerve myelin they are reported structure factors from Blaurock and Worthington (1969). Those values of rabbit and carp nerve myelin are presented in this dissertation. As shown in former chapters the higher taxonomic groups show longer periodicity than the lower taxonomic groups. It is also described before that PNS type nerve myelin has a longer period than CNS type nerve myelin. All the samples except the carp nerve myelin follow the Fourier

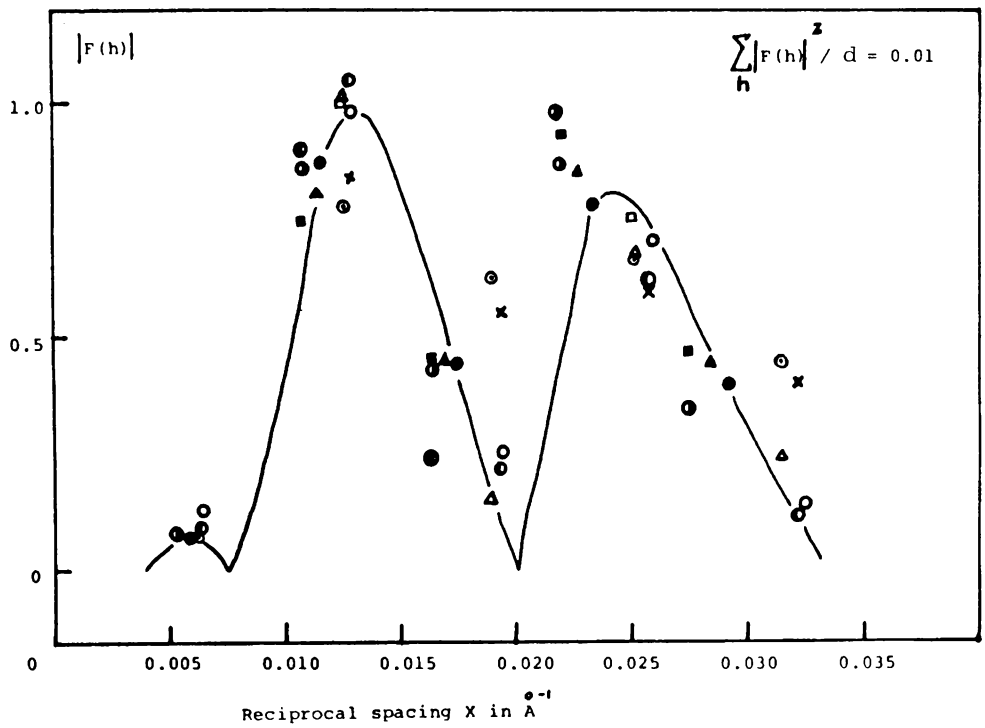

rabbit sciatic(■)184Å, rabbit optic(□)160Å, frog sciatic(●)171Å, frog optic(○)154Å, chicken sciatic(◑)182Å, chicken optic(◐)155Å, rat sciatic(▲)176Å, rat optic(△)159Å, carp spinal cord(×) 155Å, carp spinal cord(⊗)183Å, carp lateral line(⊙)160Å.

Fig. 5-2 Structure factors vs. reciprocal coordinate for different vertebrate nerve myelins.

transform of the frog sciatic nerve calculated by McIntosh and Worthington (1974) in low resolution. Hereby it is concluded that the gross structures of the nerve myelins, irrespective of PNS or CNS, are similar to each other and the relative signs of the reflections are identical in all specimens, namely - + + - - , which is determined by several workers independently by using different methords. In the carp case, as described in chapter 4, the author derived the same sign relations, - + + - - , to account for the best matching of the typical lipid bilayer profile by appling all combination of phases. Thus the electron density profiles can be calculated by using the above phases for respective reflections, whereby more substantial comparison between PNS and CNS can be made.

Table 5-1 shows the values of the half distance of the peak to peak separation in the cytoplasmic space (d_c), in the lipid bilayer region (d_l), and in the external space (d_e), which are measured from electron density profiles. The ratio of each space against the periodicity is indicated as $2d_c/d$, $2d_l/d$ and $2d_e/d$, respectively. Assuming the uncertainty involved in the periodicity to be 1%, as described in chapter 2, there are no significant changes in periodicity among rabbit (Rb.), rat (Rt.) and chicken (Ch.) for PNS and CNS. However the 13Å shorter period of frog sciatic (Fg.S) from rabbit sciatic (Rb.S) is significant and this difference is mainly due to the shrinkage by 2Å in cytoplasmic

Table 5-1 Distances across cytoplasmic space, lipid bilayer space and extracellular space for different vertebrate nerve myelins.

	(Å) d	(Å) d_c	(%) $2d_c/d$	(Å) d_l	(%) $2d_l/d$	(Å) d_e	(%) $2d_e/d$
Rb.S	184	17.5	(19)	48.8	(53)	25.8	(28)
Rt.S	176	16.7	(19)	46.6	(53)	24.7	(28)
Ch.S	182	17.1	(19)	50.0	(55)	23.8	(26)
Fg.S	171	15.3	(18)	47.3	(55)	22.9	(27)
F.L	160	13.6	(17)	42.7	(53)	23.7	(30)
Rb.O	160	15.2	(19)	49.6	(62)	15.2	(19)
Rt.O	159	15.3	(19)	48.5	(61)	15.7	(20)
Ch.O	155	13.2	(17)	48.8	(63)	15.5	(20)
Fg.O	154	13.5	(18)	47.4	(62)	16.0	(21)
FSP(I)	155	13.4	(17)	43.3	(56)	20.8	(27)

space, 2Å in lipid bilayer region and 3Å in external space. Comparison between rabbit sciatic (Rb.S) and carp lateral line (F.L) gives the 24Å difference in the periodicity which is due to the shrinkage (6Å) in the lipid bilayer region, 4Å in cytoplasmic space and 2Å in external space. Fig. 5-3 shows the electron density profiles for rabbit sciatic (Rb.S), frog sciatic (Fg.S) and carp lateral line (F.L) in an arbitary unit, which are superposed each other at the center trough of the lipid bilayer region.

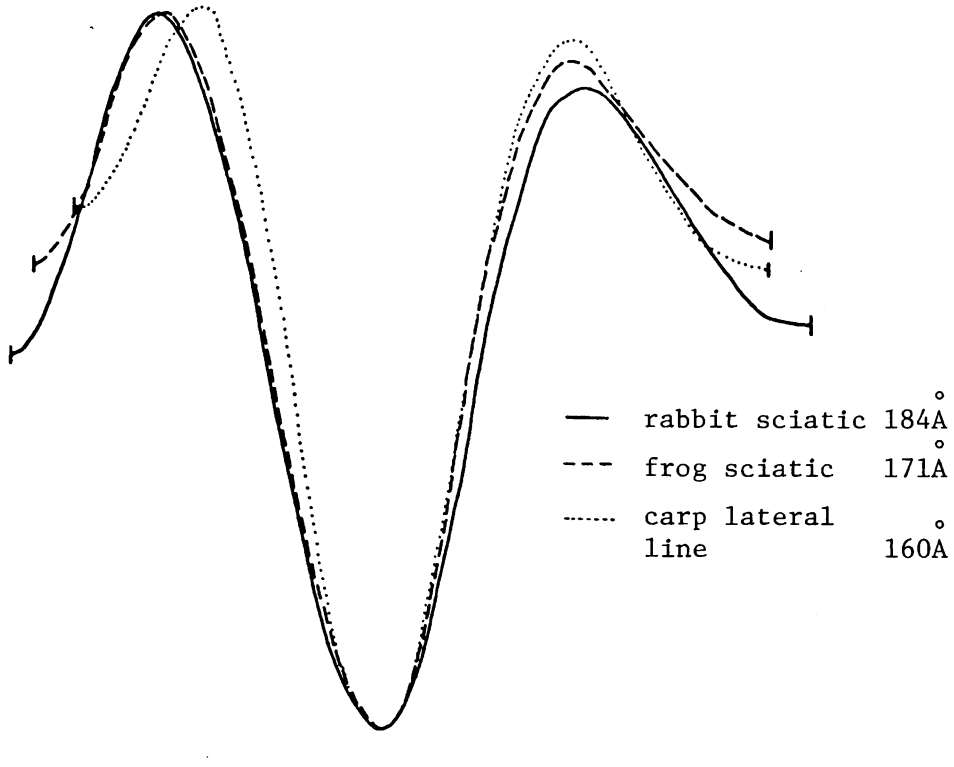

Fig. 5-3 Calculated electron density profiles of myelin membrane units for rabbit sciatic nerve myelin, frog sciatic nerve myelin and the I-phase of carp lateral line myelin.

In CNS nerve myelins for various species, different from PNS nerve myelin, the differences in the periodicity are within, at most, 6Å and the electron density profiles for rabbit optic (Rb.O) , chicken optic (Ch.O) and rat optic (Rt.O) are almost identical each other. It is also shown that frog optic (Fg.O) is not so much changed from them. However, in the I-phase of carp spinal

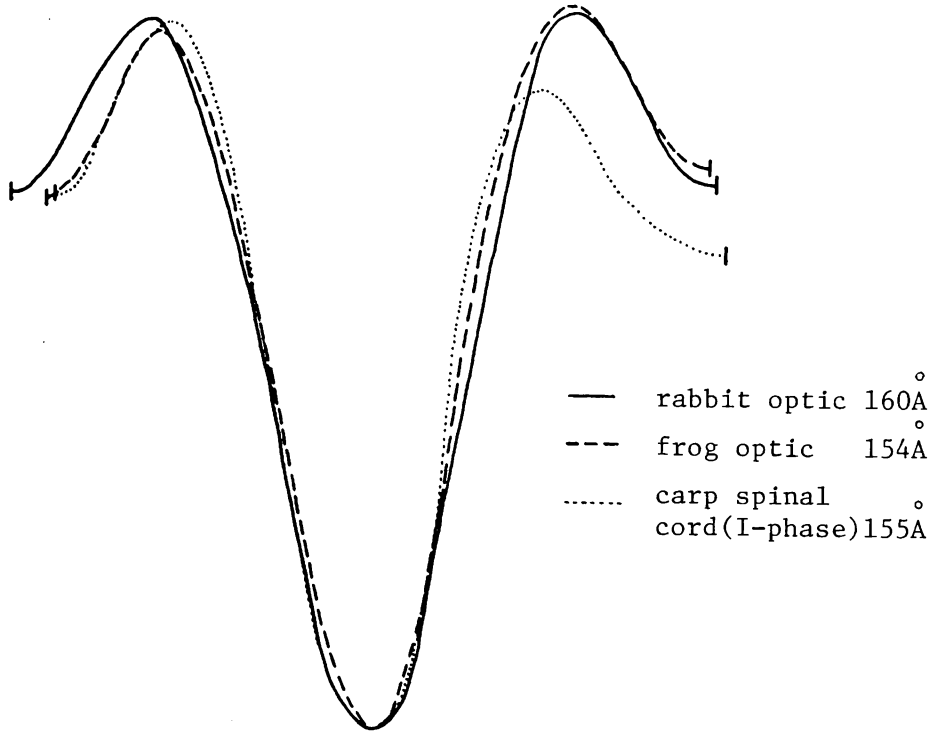

Fig. 5-4 Calculated electron density profiles of myelin membrane units for rabbit optic nerve myelin, frog optic nerve myelin and the I-phase of carp spinal cord myelin.

cord (FSP-I) a shrinkage (6Å) in the lipid bilayer region and anomalous expansion (6Å) in the extracellular space are apparently observed. In Fig. 5-4 are shown the electron density profiles for rabbit optic (Rb.O), frog optic (Fg.O) and I-phase of carp spinal cord (FSP-I), which are depicted in an arbitary unit and superposed at the center of the trough in lipid bilayer region.

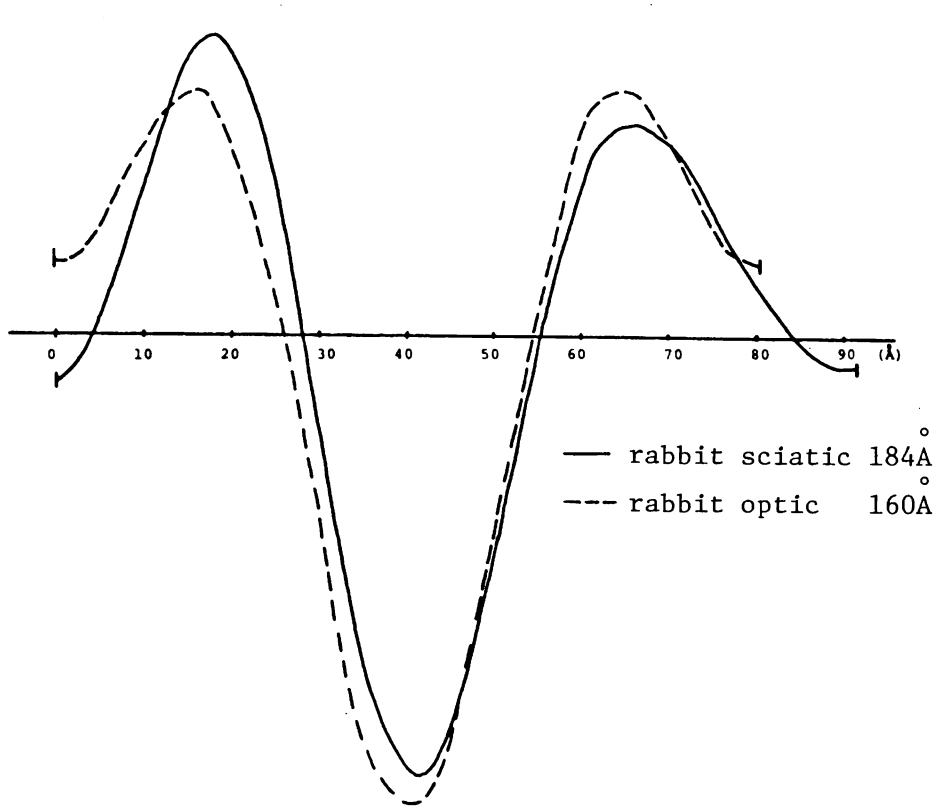

Fig. 5-5 Calculated electron density profiles of myelin membrane units for rabbit sciatic nerve myelin and rabbit optic nerve myelin as a function of distance from the cytoplasmic boundary.

Thus it is concluded that carp nerve myelin, both in PNS and CNS, shows extremely different structure from that of other vertebrate. From the present data no systematic changes from higher taxonomic group to the lower are to be detected.

Next the PNS and CNS nerve myelin are studied in comparison with each other in the same vertebrate. The difference in the

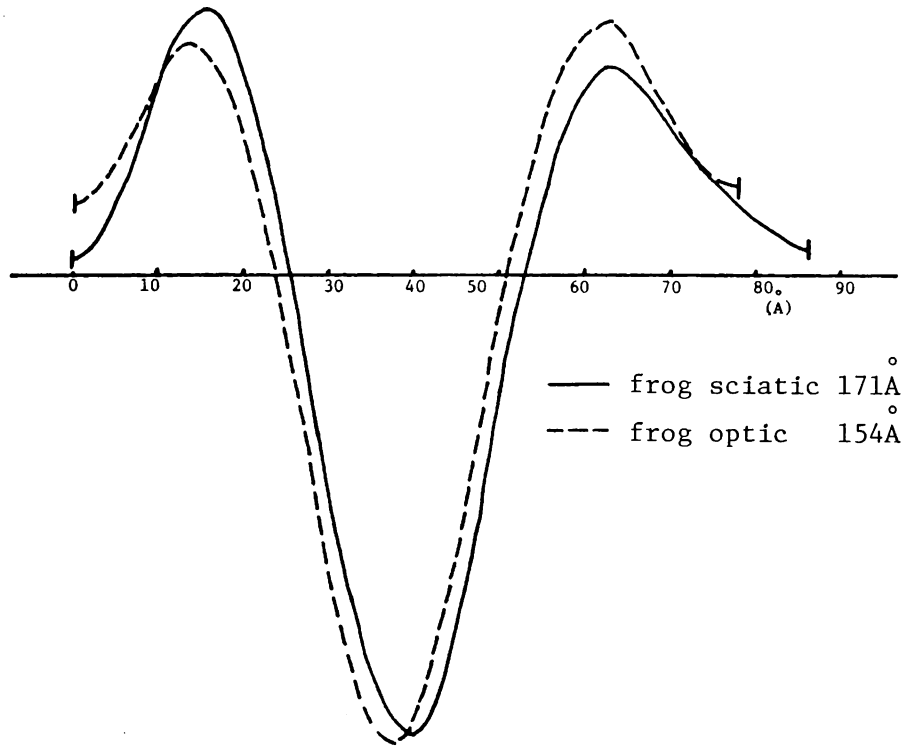

Fig. 5-6 Calculated electron density profiles of myelin membrane units for frog sciatic nerve myelin and frog optic nerve myelin as a function of distance from the cytoplasmic boundary.

periodicity between them becomes larger with the higher taxonomic group, 24Å for rabbit, 17Å for rat, 27Å for chicken, 17Å for frog and 5Å for carp. Of interest is the fact that this difference is mainly due to the separation of the external space. Calculating the ratio of the difference in the extracellular space against the total difference, 44% for rabbit, 41% for frog

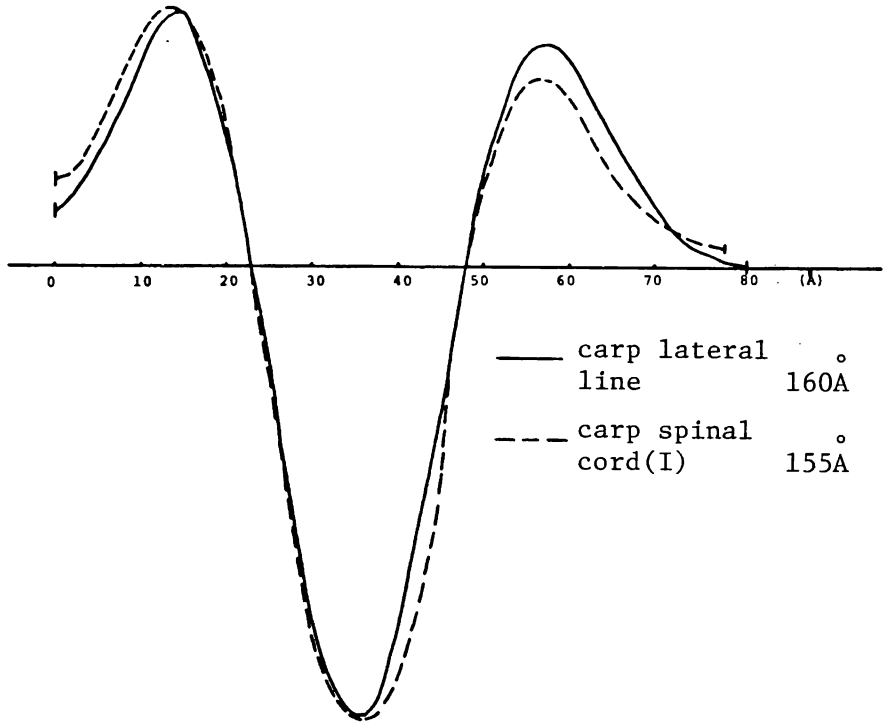

Fig. 5-7 Calculated electron density profiles of myelin membrane units for the I-phase of carp lateral line myelin and the I-phase of carp spinal cord myelin.

and 58% for carp are given. Fig. 5-5, 5-6 and 5-7 show the electron density profiles for PNS and CNS nerve myelin from rabbit , frog and carp, which are superimposed at the basal line.

Thus it is ascertained that, irrespective of the kind of vertebrate, the extracellular space gives the critical factor to lead the structural difference between PNS and CNS. The same

conclution was obtained from frog sciatic and optic nerve myelin by Finean and Burge (1963). Furthermore it is noteworthy that above specimens preserve the same separation across the lipid bilayer region except for carp.

5-3 Studies of the external perturbation

In chapter 3 was shown the difference in the response to DMSO between rabbit optic nerve and rabbit sciatic nerve. Both of them showed the similar collapsed phase, while the other phase was different in such a way that for PNS the expanded phase emerged above 40% DMSO, but for CNS the phase with reduced periodicity was only observed as increasing DMSO concentration. Washing in normal Ringer's solution, rabbit optic nerve gave the native pattern even at a DMSO concentration where rabbit sciatic nerve was irreversibly modified. In carp nerve myelin was also detected the collapsed phase and washing the treated nerve in Ringer's solution the original I-phase faded away and the II-phase increased in intensity. In addition, the above mentioned collapsed phase was also observed in the process of drying, irrespective of the species and nervous system including carp nerve myelin. Above the critical concentration where irreversible change is induced, the fresh phase of rabbit sciatic nerve was modified. On washing the treated nerve the fresh phase changed

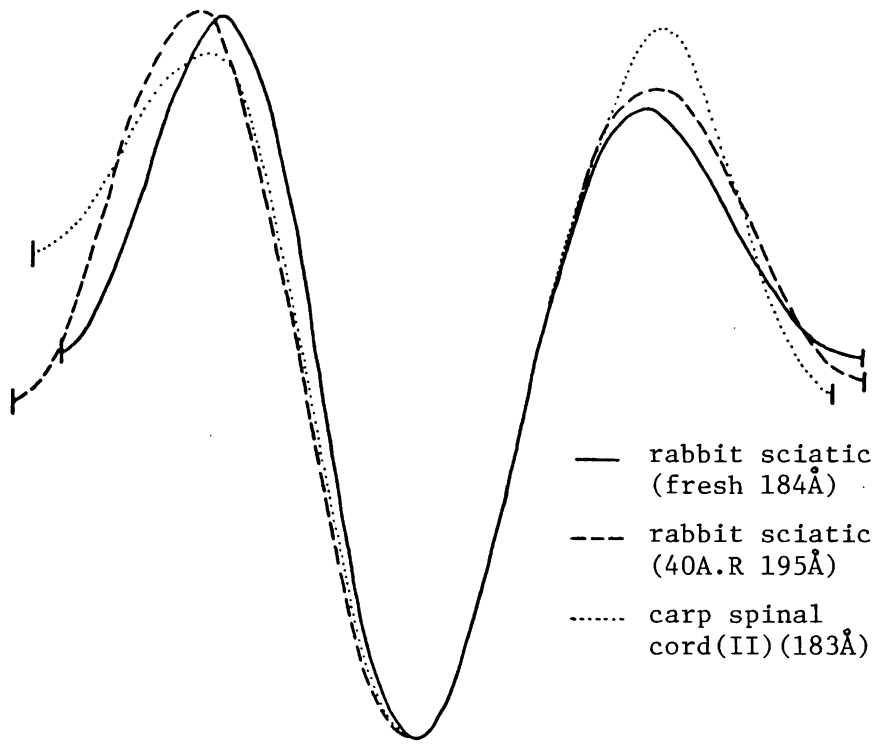

Fig. 5-8 Calculated electron density profiles of myelin membrane units for fresh rabbit sciatic nerve myelin, 40% acetone treated-and-washed rabbit sciatic nerve myelin and the II-phase of carp spinal cord myelin.

to a quasi fresh phase with a slight expansion and with weak odd order reflection. This kind pattern was also observed from carp spinal cord as the II-phase. In this regard the II-phase of carp spinal cord (FSP-II) is structurally correlated with the quasi fresh phase of rabbit sciatic nerve (Rb.S). Fig. 5-8 shows the electron density profiles of them superposed at the center of lipid

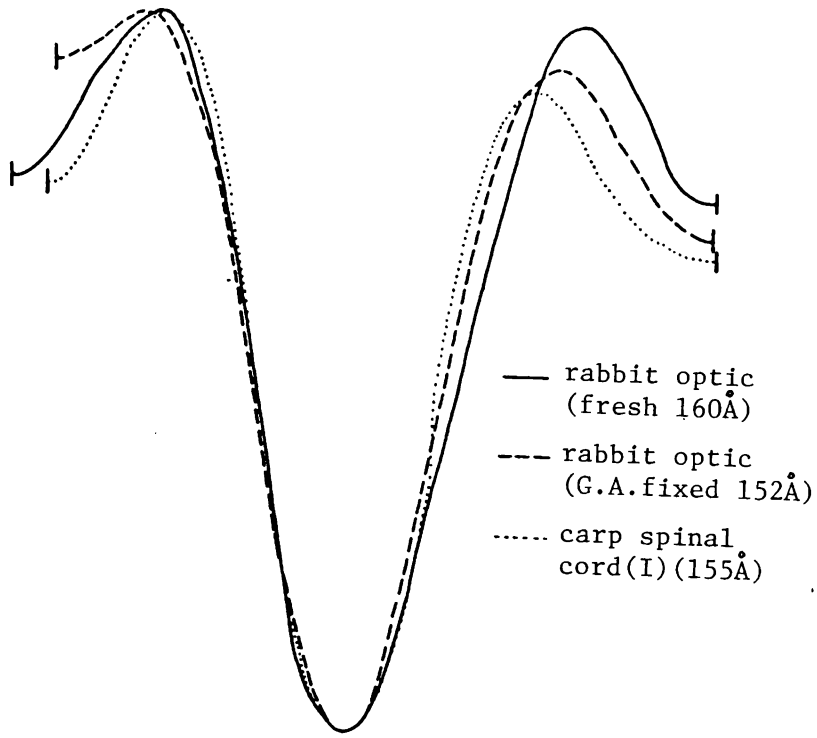

Fig. 5-9 Calculated electron density profiles of myelin membrane units for fresh rabbit optic nerve myelin, glutaraldehyde fixed rabbit optic nerve myelin and the I-phase of carp spinal cord myelin.

bilayer.

Applying glutaraldehyde on rabbit optic nerve the original phase (160Å) discretely changes to the new phase (152Å) with the intense 3rd order reflection which is quite similar to the I-phase of the carp spinal cord. Fig. 5-9 shows the electron density profiles of them superposed at the center of lipid bilayer.

On the treatment of glutaraldehyde to the I-phase of carp spinal cord, no remarkable changes in intensity or periodicity were observed. This suggests that the rearrangement of the membranous constituents presumably residing at the external side lays the difference in the x-ray diffraction pattern between rabbit optic nerve and carp spinal cord (I-phase) and moreover this gives the evidence that those structures are closely related in an unknown way. In contrast, the fixed pattern for rabbit sciatic nerve was quite different from that of rabbit optic nerve, giving 197Å period expanded phase with an asymmetric feature. Their electron density profiles, however, demonstrated a common behaviour that glutaraldehyde shrinks the separation across the cytoplasmic space and expands the separation across the external space, preserving the lipid bilayer region.

The collapsed phase was shown to be the lipid rich phase in former chapter, which shows that the lipid region is not crucial for the structural difference between PNS and CNS. In this connection it may be reminded that glutaraldehyde mainly effects on the protein as a fixing or crosslinking reagent and then gives the fixed pattern to reflect the protein to protein interaction or protein to lipid interaction. DMSO treatment on the glutaraldehyde fixed nerve or glutaraldehyde fixing on the DMSO treated nerve, both of them give the similar collapsed phase and on washing the treated nerve in Ringer's solution, the glutaraldehyde pattern

is restored. These things elucidate the glutaraldehyde effect on the nerve myelin.

Thus it is concluded that the way to organize the proteins in the myelin is essential for the difference involved in the nervous system, PNS or CNS.

The coincidence of the same patterns shared in rabbit optic nerve (glutaraldehyde fixed) and the I-phase of carp spinal cord or rabbit sciatic nerve (quasi fresh) and the II-phase of carp spinal cord (FSP-I) demonstrates that the structural difference between PNS and CNS is not inherent in the difference in each nervous system and species. Such a difference is rather due to the assembly of the membranous components. Fig. 5-10 shows the schematic diagram showing the relationships among rabbit sciatic (Rb.S), rabbit optic (Rb.O), the I-phase of carp spinal cord (FSP-I) and the II-phase of carp spinal cord (FSP-II). Schematic drawings of the x-ray diffraction patterns of them are depicted as well. Fig. 5-11 shows the electron density profiles of these phases, which are superposed in arbitary unit at the center of the low density trough.

From this diagram, the mode of irreversible structural modification is common in the rabbit sciatic nerve and carp spinal cord. The irreversible transformation from fresh rabbit sciatic nerve (184Å) to quasi fresh nerve myelin was shown to be associated with the expansion across the cytoplasmic space and

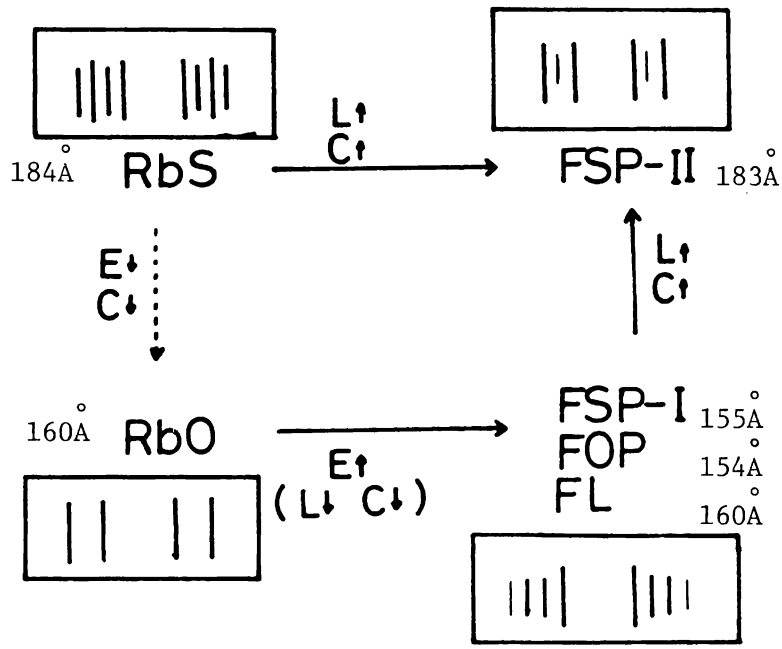

Fig. 5-10 Schematic diagram showing the relationships among different phases for rabbit nerve myelin and carp nerve myelin.

across lipid bilayer region. In the similar way carp spinal cord (I-phase) was irreversibly modified to the II-phase, with extensive expansion in cytoplasmic space. Hence the structural stability to preserve the compact myelin is shown to be involved in the tight apposition at the cytoplasmic side. In this regard the stability exhibited in rabbit optic nerve against the external perturbation

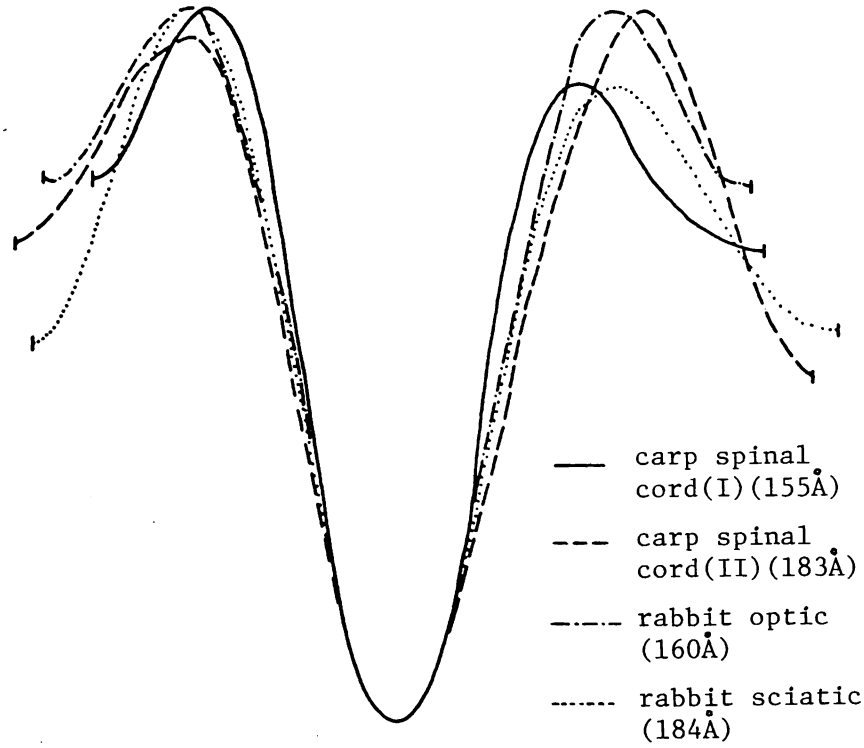

Fig. 5-11 Calculated electron density profiles of myelin membrane units for the I-phase and the II-phase of carp spinal cord myelin , rabbit optic nerve myelin and rabbit sciatic nerve myelin.

can be ascribed to the tightness at the cytoplasmic side. This thought can be supported by the glutaraldehyde treatment experiments. Glutaraldehyde fixed patterns for rabbit optic, rabbit sciatic, carp spinal cord (I-phase) show the common features that the distances across the cytoplasmic space are enormously reduced, which is correlated with the stability of the glutar-

aldehyde fixed nerve myelin against the external perturbation.

Thus it is concluded that, 1) irrespective of the species and nervous system, the irreversible modification in nerve myelin is triggered by the structural rearrangement of the membranous components at the cytoplasmic side and in hydrophobic region, 2) the organization of protein and lipid within membrane is essential for the differences in diffraction pattern between PNS and CNS.

5-4 On the structure of PNS and CNS nerve myelin

Section 5-2 and 5-3 elucidated that the difference in the structure between PNS and CNS is mainly due to the different protein to protein or protein to lipid interactions. Moreover the diffraction pattern of carp nerve myelin was related to that of other animal's nerve myelin. So in this section, as a conclusion, the structural differences between them are discussed in terms of the chemical constituents.

Electron density profiles clearly show that the difference in PNS and CNS in each vertebrate is ascribed to the separation across the external space and cytoplasmic space. Especially in carp spinal cord (I-phase) the width in the half of the membrane

at the cytoplasmic side is considerably reduced. Chemical analysis unanimously nowadays assists that the basic protein peripherally resides in the cytoplasmic side and proteolipid (CNS) or P_0protein (PNS) is embedded in the lipid bilayer matrix. And these proteins amount to be 1 : 1 in stoichiometry. Hence it is assumed that basic protein and hydrophobic protein cooperatively integrate the framework of the compact multilayered membrane. Recently Crang and Rumsby (1977) proposed the similar arrangement of the basic protein in during compaction. (Fig. 5-12) Following this concept the structural difference between PNS and CNS is ascribed to the interaction of these proteins.

Such view is supported by the external perturbation experiments, in which air drying, freezing, hypertonic solution, DMSO and acetone produce almost the same pattern that is characterized by the intense 2nd order reflection of the 120Å period phase. Since the collapsed phase is the lipid rich phase, the essential factor to distinguish PNS from CNS lies in the protein-protein or protein-lipid interactions. Furthermore glutaraldehyde treatment gives the evidence that the above concept is correct, for glutaraldehyde has the property to fix or crosslink the membranous proteins. In fact by applying glutaraldehyde to the rabbit sciatic nerve myelin, the fresh phase (184Å) turns into the expanded phase (197Å) which has the intense odd order reflections. In contrast the fixed pattern from rabbit optic

nerve gives the reduced period phase (152Å) with intense odd order reflections. In addition, DMSO treated nerve is not modified markedly by the following glutaraldehyde treatment, and glutaraldehyde fixed nerve gives the collapsed phase in the DMSO treatment. Both patterns, on restoring to the normal Ringer's solution, change to the glutaraldehyde fixed pattern. Thus it is ascertained that the structural difference between PNS and CNS is ascribed to the protein-protein or protein-lipid interaction. These evidences demonstrate the existence of lipids which are loosely associated with the membrane structure. It is of interest to know the functional role of these lipids in the compact myelin sheath. These aspects have been generalized and extended to other membranes by Finean et al.(1968).

Carp nerve myelins, FSP, FOP and FL, show the curious phenomenon that the original I-phase (155Å for FSP, 154Å for FOP and 160Å for FL) undergoes degeneration and transforms into the II-phase (about 180Å). This curiosity might be due to the protein-protein or protein-lipid interaction, for the several perturbations (drying, freezing, DMSO and acetone treatment) induce the collapsed phase even in this carp nerve myelin. The electron density distribution shows an extremely short separation across the cytoplasmic space so that the half length of the single membrane at the cytoplasmic side (35Å) is comparable to that of the lipid model membrane (30Å) (Franks,1976). On the transformation from the

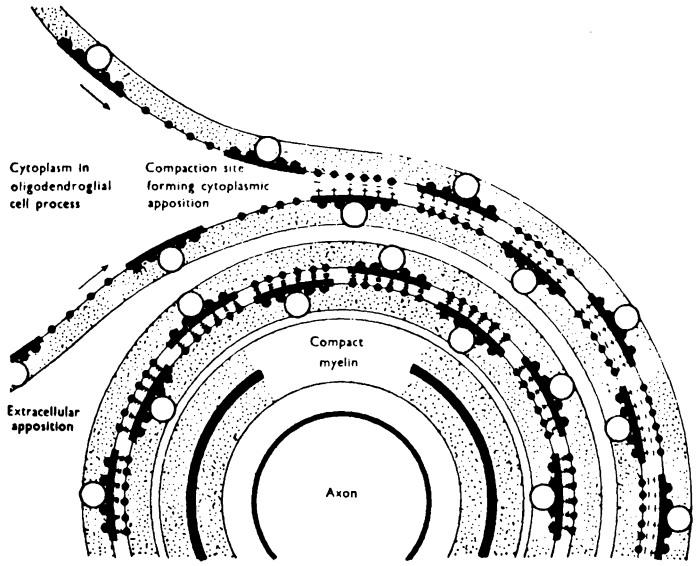

Fig. 5-12 Cross-sectional view of nerve myelin (proposed by Crang and Rumsby, 1977)

I-phase to the II-phase, a marked expansion to 10Å in the cytoplasmic space is observed. Hence the cytoplasmic side must contribute to the special structure and in result respond to the external perturbation.

X-ray diffraction study on the model membrane composed of the basic protein and acidic lipids (Mateu et al.,1973)suggests that the difference in the physico-chemical character of the basic protein between PNS basic protein and CNS basic protein is reflected directly in the long range membrane-to-membrane interaction. Therefore it can be stated that the difference between PNS and CNS lies in the conformational change or assemblage of the basic protein, as far as the periodicity is concerned.

Similar patterns were observed from different nerve myelins, such as 1) glutaraldehyde treated rabbit optic and carp spinal cord (I-phase), 2) rabbit optic and carp spinal cord at pH 3, 3) rabbit sciatic (quasi fresh) and carp spinal cord (II-phase). Such a thing gives evidence that the structural difference between them is not due to the inherent character involved in each nervous system and species, but to the characteristic assembly of the membrane constituents.

At present, however, there is no confirmed explanation about the structural relationship between CNS and PNS. Other proteins might also be essential to determine the structure, so the above demonstration in the case of carp nerve myelin might be

too speculative. In fact from the diagram depicted in the former section, it seems that the hydrophobic protein plays an indispensable role to integrate the multilamllar structure. For example the transformation from rabbit sciatic fresh phase (F phase) to the quasi freah phase (F' phase) was triggered by the disorganization of the hydrophobic interaction and as a result the cytoplasmic expansion was induced. In addition the freeze fracture electromicroscopic studies showed that in optic nerve there were seen the extensive zonulae occludentes in the myelin sheath of medullary rays, though in the sciatic nerve of rabbit zonulae occludents could be identified in limited number and extension (Reale, Luciano and Spitznas,1975). The enormous stability of the rabbit optic nerve against the external perturbation might be associated with this hydrophobic protein. Furthermore the close apposition at the cytoplasmic space will be made by the interaction between the basic protein and the hydrophobic protein.

APPENDIX (I)

DIFFERENCE BETWEEN PERIPHERAL AND CENTRAL NERVE MYELIN SHEATH

In the peripheral nervous system the lamellae are derived from infolded plasma membranes of Schwann cells and in central nervous system the myelin sheath originates from the oligodendroglia cell.

1. Morphology

Myelin periodicity

X-ray diffraction data on fresh myelin sheaths show that the fundamental repeating unit of central myelin is about 10% lower than that of peripheral myelin. The periodicity in higher taxonomic group is longer than that in lower group. (Table A-1)

Amount of cytoplasm outside of sheaths

While the cytoplasm on the outside of peripheral sheaths forms complete covering to the myelin, that of central sheaths is generally confined to a thin ridge extending along the entire internode.

Schmidt-Lanterman clefts

No structures similar in appearance to Schmidt-Lanterman

Table A-1 Periodicities of different vertebrate nerve myelin membranes for central and peripheral nerve.

Species	PNS (Å)	CNS (Å)		PNS (Å)	CNS (Å)
(Mammal)			(Amphibian)		
Human	185(3) (H)	-	Frog	171 (S)	-
	178 (P)	-		171 (F)	-
	184.4(1.40) (Ch.)	160.3-165.8		171(3) (H)	-
Monkey	185(3) (H)	-		171 (B)	154 (B)
Sheep	185(3) (H)	-		171(2.8) (A)	-
Rabbit	185(3) (H)	-		170 (Ca)	-
	180 (Ca)	156 (Ca)	Toad	171(3) (H)	-
	179 (W)	-	(Fish)		
Gunie pig	185(3) (H)	-		160 (F)	150 (F)
Rat	180 (F)	160 (F)	Bream	161(3) (H)	-
	176 (B)	159 (B)	Mackerell	161(3) (H)	-
(Bird)			Pike	161(3) (H)	-
Pigeon	180 (F)	-	Salmon	161(3) (H)	-
Dove	182(3) (H)	-	Trench	161(3) (H)	-
Duck	181(3) (H)	-		159,184 (B)	156,182-183 (B)
Hen	183(3) (H)	-			
Chicken	182 (B)	155 (B)			

S: Schmitt,F.O.(1935) F: Finean,J.B.(1960) H: Hoglund,G.(1961) B: Blaurock,A.E.(1969) 1% accuracy

P: Parsons,D.F.(1969) A: Akers,C.K.(1970) Ca: Caspar,D.L.D.(1971)

W: Worthington,C.R.(1976) Ch: Chandross,R.J.(1978)

clefts, or incisures have been reported within central myelin sheaths.

Radial component

In the transverse section of central myelin sheaths in electron microscopic study, a radial component is prominent. It cannot be considered to be a regular component of peripheral sheaths.

Sheath thickness

For the same diameter of axon, myelin sheaths of peripheral nerves are apparently thicker than those within the central nervous system.

Features described above are shown in Fig. A-1.

2. Chemical composition

Myelin is a lipid rich and dehydrated structure. Finean (1960) determined the water content to be about 40% by x-ray diffraction studies on nerve tissue during drying. The solid part is composed mainly of lipids and proteins, whose content is 70% to 85% and 15% to 30%, respectively.

In Table A-2 is listed the chemical composition of myelin proteins. In central nervous system it is generally agreed that

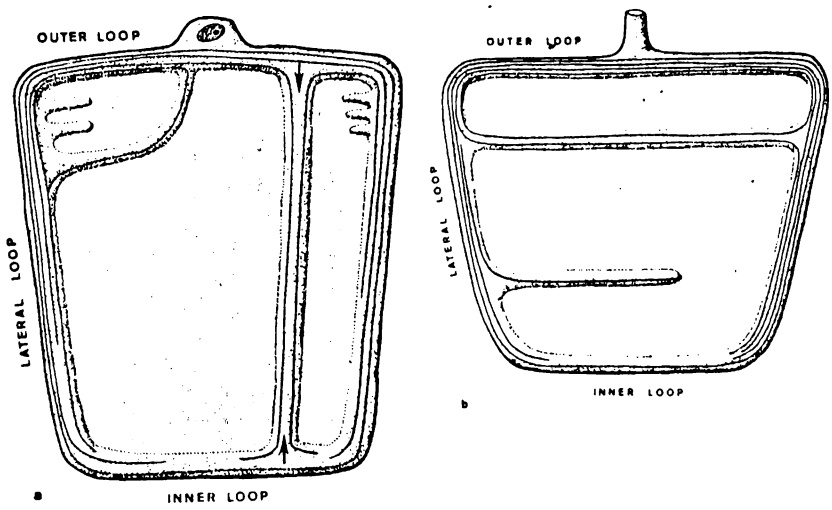

PNS CNS

Fig. A-1 Schematic drawings of peripheral and central nerve myelin. (Schnapp et al., 1975)

there are three major proteins in myelin, 30% to 50% proteolipid , 30% to 35% basic protein and a lower percentage of a higher molecular weight protein (Wolfgram protein). After Singer's defintion proteolipid protein is an integral protein, for it can be extracted with chloroform-methanol (2:1). While basic protein is a peripheral protein which can be readily extracted

from nervous tissue by dilute acid or by salt solutions. Wolfgram protein is assumed to be an integral protein which is soluble in acidified chloroform-methanol. The topology of the above proteins, however, has not yet been established.

Of peripheral nervous system protein, glycoprotein and minor other protein are reported to reside in nerve myelin. P_1 protein , one of the basic proteins, is considered to be the same as the basic protein in central nervous system.

Table A-2 Chemical composition of proteins in nerve myelin (Uyemura and Kitamura, 1977)

	CNS	
30%	BP-Al : M.W. 18,400	
50%	Folch Lees Proteolipid	
	P7-PLP : M.W.23,500	
	P8M-DM20 : M.W. 20,000	
	LMW : M.W. 17,000	
	Wolfgram Protein: 50,000-60,000	
	CNP	
	PNS	
	BP-Al : M.W. 18,000	
	BF-P2 : M.W. 13,000	
50-60%	BR-PO : M.W. 28,000	
	PAS-II : M.W. 13,000	

Table A-3 lists the chemical composition of lipids in nerve myelin. Due to the difficulty of homogenizing peripheral nerve the existing documents on PNS myelin are not yet extensive. Most CNS myelin, so far reported contains cholesterol, phospholipids and galactolipid in molar ratios varying from 4:3:2 to 4:2. Cerebrodide is assumed to be the most typical lipid in nerve myelin

for the direct increase in the cerebroside concentration with the myelination. Some lipids are reported to closely interact with proteins. It was demonstrated for the case of in vitro system that, for example, cerebroside sulfate or other acidic lipids having minus charge could interact with basic protein, in addition to that triphosphoinositides are suggested to bind tightly to the protein.

Table A-3 Chemical composition of lipids in nerve myelin. (O'Brien, 1967)

	Human CNS myelin	Beef PNS myelin
Lipid content(% of dry weight)	78.7	75.9
Molar % of total lipid		
Cholesterol	40.1	39.0
Ethanolamine glycerophosphatides	13.4	12.7
Serine glycerophosphatides	5.0	6.8
Choline glycerophosphatides	10.8	10.2
Inositol glycerophosphaties	2.0	2.0
Cardiolipin	tr	tr
Phosphatidyl glycerol	tr	tr
Sphingomyelin	4.6	13.0
Cerebroside	15.4	11.5
Cerebroside sulfate	4.0	1.8
Other sphingolipids	1.6	-
Galactosyl diglyceride	-	-
Digalactosyl diglyceride	-	-
Sulfoquinovosyl diglyceride	-	-
Other minor lipids	3.1	3.0
Total glycerolipis	34.4	34.7
Total sphingolipis	25.6	26.3

APPENDIX (II)

CALCULATED DISTANCES ACROSS CYTOPLASMIC SPACE, LIPID BILAYER SPACE AND EXTRACELLULAR SPACE FOR DIFFERENT NERVE MYELINS (Table A-4)

Fresh state (rabbit and carp)

	d(Å)	d_c	d_1	d_e
Rb.S	184	17.5	48.8	25.8
Rb.O	160	15.2	49.6	15.2
FSP-I	155	13.2	44.2	20.8
FSP-II	183	18.3	52.2	21.1
FL	160	13.6	42.7	23.7

Collapsed phase in the treated state (rabbit sciatic)

	d(Å)	d_c	d_1	d_e
20D	125	6.9	47.6	8.0
40D	119	5.4	47.9	6.1
20A.20D	126	7.1	48.2	7.5
20A.40D	120	5.9	48.4	5.7
G.A.20D	124	5.9	48.7	7.3
G.A.40D	119	4.9	48.4	6.0
20A	129	8.4	47.7	8.4

Washed state (rabbit sciatic)

	d(Å)	d_c	d_1	d_e
20D.R	184	17.5	49.7	24.8
40D.R	187	18.7	50.5	24.3
70D.R	192	18.2	53.8	24.0
20A.R	192	19.2	52.8	24.0
40A.R	195	20.5	52.7	24.4

Glutaraldehyde fixed (rabbit)

	d(Å)	d_c	d_1	d_e
Rb.S	198	13.9	49.6	35.2
Rb.O	152	10.2	47.6	18.2

REFERENCES

Akers, C. K. and Parsons, D. F. (1970) Biophys. J. 10, 116

Bear, R. S. (1942) J. Amer. Chem. Soc. 64, 727

Becker, D. P., Young, H. F., Nulsen, F. E. and Jane, J. A. (1969) Exp. Neurol. 24, 272

Benson, A. A. (1966) J. Amer. Oil Chemists' Soc. 43, 265

Berg, H. C. (1969) Biochim. Biophys. Acta 183, 65

Blaurock, A. E. and Worthington, C. R. (1966) Biophys. J. 9, 305

Blaurock, A. E. and Worthington, C. R. (1969) Biochim. Biophys. Acta 173, 419

Blobel, G. et al. (1975) J. Cell Biol. 67, 835

Boehm, G. (1931) Z. Biol. 91, 203

Boggs, J. M. and Moscarello, M. A. (1978) Biochim. Biophys. Acta 515, 1

Bolduan, O. E. A. and Bear, R. S. (1949) J. Appl. Phys. 20, 983

Branton, D. (1971) Phil. Trans. R. Soc. B261, 133

Bretscher, M. S. (1971a) Nature New Biol. 231, 229

Bretscher, M. S. (1971b) Science 181, 622

Bretscher, M. S. (1975) Nature 258, 43

Carnegie, P. R. and Dunkley, P. R. (1975) Advances in Neurochemistry (Agranoff, B. W. and Aprison, M. H., eds.) 1, 95, Plenum Press, New York

Caspar, D. L. D. and Kirshner, D. A. (1971) Nature New Biol. 231,

Caspar, D. L. D. and Philips, W. C. (1976) Brookhaven Symposium Biol. 7, 107

Chandross, R. J., Bear, R. S. and Montogomery, R. L. (1978) J. Comparative Neurol. 177, 1

Cherry, R. J. (1976) in Biological Membranes (Chapman, D. and Wallach, D. F. H., eds.) p. 47, Academic Press, New York

Cossins, A. R. (1977) Biochim. Biophys. Acta 470, 395

Crang, A. J. and Rumsby, M. G. (1977) Biochem. Soc. Trans. 5, 1431

Craven, B. M. (1977) Nature 267, 287

Cuzner, M. L., Davison, A. N. and Gregson, N. A. (1965) J. Neurochem. 12, 496

Danielli, J. F. and Davson, H. (1956) J. Cell Physiol. 5, 495

Davis, H. L., Davis, N. L. and Clemons, A. L. (1967) Ann. N. Y. Acad. Sci. 141, 310

Demal, R. A. (1976) Biochim. Biophys. Acta 457, 109

DeWolff, P. M. (1948a) Acta Cryst. 1, 207

DeWolff, P. M. (1948b) Appl. Sci. Res. B1, 119

Edelman, G. M. et al. (1973) Proc. Nat. Acad. Sci. 70, 1442

Einstein, E. R. (1972) Handbook of Neurochemistry 7, 107

Einstein, E. R., Csejtey, J., Dalal, K. B., Adams, C. W. M., Bayliss, O. B. and Hallpike, J. F. (1972) J. Neurochem 19, 653

Ekstein, H. (1949) Acta Cryst. 2, 99

Elkes, J. and Finean, J. B. (1953a) Exptl. Cell Res. 4, 69

Elkes, J. and Finean, J. B. (1953b) Exptl. Cell Res. 4, 82

Elliot, A. (1965) J. Sci. Instrum. 42, 312

Engelman, D. M. (1970) J. Mol. Biol. 47, 115

Finean, J. B. (1957) Acta Neurol. Psychiat. Belg. 5, 462

Finean, J. B. (1960) in Modern Aspects of Neurology (Cumings, J. N. ed.) p. 232, Edward Arnold

Finean, J. B. (1961) Int. Rev. Cytol. 12, 303

Finean, J. B. and Burge, R. E. (1963) J. Mol. Biol. 7, 672

Finean, J. B., Coleman, R., Knutton, S., Limbrick, A. R. and Thompson, J. E. (1968) J. Gen. Physiol. 51, 19s

Finean, J. B. and Millington, P. M. (1957) J. Biophys. Biochem. Cytol. 3, 89

Franks, A. (1955) Proc. Phys. Soc. B68, 1054

Franks, A. (1958) J. Appl. Phys. 9, 349

Franks, N. P. (1976) J. Mol. Biol. 100, 345

Freeman, R. (1975) personal communication

Freeman, R., Inouye, H. and Masaki, N. (1975) unpublished data

Frigerio, N. A. and Shaw, M. J. (1969) J. Histochem. Cytochem. 17, 176

Fruya, K., Yamaguchi, T., Inoko, Y. and Mitsui, T. (1976) Acta Cryst. B32, 1811

Frye, L. D. and Edidin, M. (1970) J. Cell Sci. 7, 319

Gabrieleson, E. (1975) Inter. Review Neuro. Biol. 17, 189

Geren, B. B. (1954) Exp. Cell Res. 7, 558

Gillett, R. and Gull, K. (1972) Histochemie 30, 162

Golay, M. J. E. (1963) Spectro Chim. Acta 19, 1013

Gorter, E. and Grendel, F. (1925) J. exp. Med. 41, 439

Green, D. E. and Perdue, J. F. (1966) Proc. Nat. Acad. Sci. 55, 1295

Guinier, A. (1939) Ann. Phys. Paris 12, 161

Hoglund, G. and Ringertz, H. (1961) Acta Physiol. Scand. 51, 290

Hoseman, R. and Bagchi, S. N. (1962) Direct Analysis of Diffraction by Matter, North-Holland Publishing Company, Amsterdam

Hubbell, W. L. and McConnell, H. M. (1968) Proc. Nat. Acad. Sci. 61, 12

Huxley, H. E. and Brown, W. (1967) J. Mol. Biol. 30, 383

Hybl, A. (1977) J. Appl. Cryst. 10, 141

Iizuka, H. (1977) D. Phil. Thesis, Kyoto University

Kato (1942) Seirigaku, Nankodo

Kirshner, D. A. (1977) in Myelin (Morell, P. ed.) p. 51, Plenum Press, New York

Kirshner, D. A. and Caspar, D. L. D. (1975) Proc. Nat. Acad. Sci. 72, 3513

Klug, H. P. and Alexander, L. E. (1974) in X-ray diffraction procedures, p. 566, John Wiley and Sons

Kornberg, R. D. and McConnell, H. M. (1971a) Biochemistry 10, 1111

Kornberg, R. D. and McConnell, H. M. (1971b) Proc. Nat. Acad. Sci. 68, 2564

Ladbrooke, B. D., Jenkinson, T. J., Kamat, V. B. and Chapman, D. (1968) Biochim. Biophys. Acta 164, 101

Livingston, R. B., Pfenninger, K., Moor, H. and Akert, K. ()973) Brain Res. 58, 1

London, Y. and Vossenberg, F. G. A. (1973) Biochim. Biophys. Acta 307, 478

Luzzati, V. (1968) in Biological Membranes (Chapman, D. ed.) p. 71, Academic Press, New York

Marks, N. and Lajtha, A. (1971) Handbook of Neurochemistry 5A, 49

Mateu, G., Luzzati, V., London, Y., Gould, R. M. and Vossenberg, F. G. A. (1973) J. Mol. Biol. 75, 697

Maturana, H. R. (1960) J. Biophys. Biochem. Cytol. 7, 107

McIntosh, T. J. and Worthington, C. R. (1974) Biophys. J. 14, 363

Mehl, E. and Halaris, A. (1970) J. Neurochem. 17, 659

Melchoir, D. L. et al. (1970) Biochim. Biophys. Acta 219, 114

Miller, N. G. A., Hill, M. W. and Smith, M. W. (1976) Biochim. Biophys. Acta 455, 644

Mokrasch, L. C., Bear, R. S. and Schmitt, F. O. (1971) Neurosciences Research Program Bulletin, vol. 9

Moretz, R. C., Akers, C. K. and Parsons, D. F. (1969) Biochim. Biophys. Acta 193, 12

Nelander, J. C. and Blaurock, A. E. (1978) J. Mol. Biol. 118, 497

Nicolson, G. L. (1976) Biochim. Biophys. Acta 457, 57

Norton, W. T. (1975) in The Basic Neurosciences (Tower, D. B. ed.) p. 467, Raven Press, New York

O'Brien, J. S. (1967) J. Theor. Biol. 15, 307

Papahadjopoulos, D., Moscarello, M., Eylar, E. H. and Isac, T. (1975) Biochim. Biophys. Acta 401, 317

Parrish, W. and Wilson, A. J. C. (1968) International Tables for X-ray crystallography 2, 216

Parsons, D. F. and Akers, C. K. (1969) Science 165, 1016

Peters, A. (1960) J. Biophys. Biochem. Cytol. 8, 431

Pinto da Silva and Miller, R. M. (1975) Proc. Nat. Acad. Sci. 72, 404

Rand, R. P., Papahadjopoulos, D. and Moscarello, M. (1976) Biophys. J. 16, 192a

Rasmussen, K. -E. and Albrechtsen, I. (1974) Histochemistry 38, 19

Reale, E., Luciano, L. and Spitznas, M. (1975) J. Neurocytology 4, 131

Robertson, J. D. (1958) J. Biophys. Biochem. Cytol. 3, 1043

Robertson, J. D. (1959) Biochem. Soc. Symp. 16, 3

Robertson, J. D. (1960) Prog. Biophys. Biochem. 10, 343

Rothman, J. E. and Lenard, J. (1977) Science 195, 743

Saeki, S. (1972) Kagaku no ryoiki 98, 9

Sabatini, D. D., Bensch, K. and Barrnett, R. J. (1963) J. Cell

Biol. 17, 19

Sammeck, R. and Brady, R. O. (1972) Brain Res. 42, 441

Savitzky, A. (1964) Anal. Chem. 36, 1627

Schmitt, F. O., Bear, R. S. and Clark, G. L. (1935) Radiology 25, 131

Schmitt, F. O., Bear, R. S. and Palmer, K. J. (1941) J. Cellular Comp. Physiol. 18, 31

Schnapp, B. and Mugnaini, E. (1975) in Golgi Centennial Symposium Proceedings (Santini, M. ed.) p. 209, Raven Press, New York

Shapiro, A. L. et al. (1967) Biochem. Biophys. Res. Comm. 28, 815

Shieh, H. S. et al. (1976) Nature, 260, 727

Sinensky, M. (1974) Proc. Nat. Acad. Sci. 71, 522

Singer, S. J. (1974) Ann. Rev. Biochem. 43, 805

Singer, S. J. and Nicolson, G. L. (1972) Science 175, 720

Sjostrand, F. S. (1949) J. Cell Comp. Physiol. 33, 383

Sjostrand, F. S. (1953) Experimentia 9, 68

Skoulios, A. et al. (1959) Nature 183, 1310

Steck, T. H. (1972) J. Mol. Biol. 66, 295

Steim, J. M. et al. (1970) Proc. Nat. Acad. Sci. 63, 104

Stoeckenius, W. and Engelman, D. M. (1969) J. Cell Biol. 42, 613

Swanson, H. E. and Fuyat, R. K. (1953) Standard X-ray Diffraction Powder Patterns 2, 43, United States Department of Commerce,

National Bureau of Standards

Swanson, H. E. and Tatge, E. (1953) Standard X-ray Diffraction Powder Patterns 1, 12 United States Department of Commerce, National Bureau of Standards

Tasaki, I. (1953) Nervous Transmission, Springfield, Thomas

Tsukada, Y. (1977) Protein, Nucleic acid and Enzyme 22, 833

Uyemura, K. and Kitamura, K. (1977) Protein, Nucleic acid and Enzyme 22, 642

Vanderheuvel, F. A. (1963) J. Amer. Oil Chem. Soc. 40, 455

Vanderkooi, G. and Green, D. E. (1970) Proc. Nat. Acad. Sci. 66, 615

Vold, R. D. et al. (1952) J. Phys. Chem. 56, 128

Walf, K. and Quimky, M. C. (1969) in Fish Physiology (Hoar, W. S. et al. eds.) p. 253, Academic Press, New York

Wood, J. G. (1973) Biochim. Biophys. Acta 329, 118

Worthington, C. R. (1969) Biophys. J. 9, 222

Worthington, C. R. (1971) in Biophysics and Physiology of excitable membranes (Adelman, W. J. ed.) p. 1, Van Nostrand Reinhold, Princeton

Worthington, C. R. and McIntosh, T. J. (1974) Biophys. J. 14, 703

Worthington, C. R. and McIntosh, T. J. (1976) Biochim. Biophys. Acta 436, 707

Yamamoto (1949) Dobutsu seiri no zikken p. 212, Kawade syobo